Interaction of Surface Energy and Microarchitecture in Determining Cell and Tissue Response to Biomaterials

A Dissertation
Presented to
The Academic Faculty

by

Ge Zhao

In Partial Fulfillment
of the Requirements for the Degree
Doctor of Philosophy in the
School of Engineering

Georgia Institute of Technology
August 2007

Interaction of Surface Energy and Microarchitecture in Determining Cell and Tissue Response to Biomaterials

Approved by:

Dr. Barbara D. Boyan, Advisor
Department of Biomedical Engineering
Georgia Institute of Technology

Dr. Andres Garcia
Department of Mechanical Engineering
Georgia Institute of Technology

Dr. Carson Meredith
Department of Chemical Engineering
Georgia Institute of Technology

Dr. Zvi Schwartz
Department of Biomedical Engineering
Georgia Institute of Technology

Dr. Robert E. Baier
Department of Oral Diagnostic Sciences
State University of New York at Buffalo

Date Approved: June 5th, 2007

ACKNOWLEDGEMENTS

First of all, I would like to thank my advisor Dr. Barbara Boyan. She does not only guide me through specific scientific research, but always encourages me to think big. I really appreciate her tremendous efforts on editing every sentence of all the abstracts, papers and proposals I have written in the last five years. She sets a hard-working example herself and helps me to exert my best potentials. She is also the inspiration for me to pursue the success in career, as well as keep a balanced family life. I also want to thank my thesis committee. Dr. Zvi Schwartz leads me into the research step by step. I am deeply impressed by his endless energy and broad knowledge. When I encountered problems in the research, he is always there to sweep the obstacles. Dr. Andres Garcia has provided valuable advices and guidance all the way through my research. Dr. Robert Baier has exchanged extensive discussions with me and devoted a large amount of time helping me to correct the dissertation. Dr. Carson Meredith has provided many suggestions and recommendations for the data analysis.

Thanks to all Boyan labmates for the support and collaborations. Seyed Safavynia, Gary Seeba, John Douly and Reyhaan Chaudhri have cultured all the cells that I need to finish these studies. Without Reyhaan's excellent management of the lab, I can not perform the research so efficiently. Special thanks to Andrew Raines, who have collaborated with me over two years and assisted a large amount or research work. Through the discussions with Dr. Rene Olivares-Navarrete, Dr. Liping Wang, Dr. Hai Yao and Dr. Jida Chen, I learned a lot in material science, biology and biomechanics. I really appreciate the support from my fellow graduates, Jennifer Hurst-Kennedy, Ming Zhong, Tracy Denison, Kevin Wong and Jessica Mata, as well as the fun activities out of the lab. Thanks to my officemates, Ramsey Kinney and Bryan Bell, who helped me develop critical thinking, communication skills and more understanding of American

iii

culture during frequent discussions. Thanks to every one in the lab for the support and assistance.

Thanks to the love and endless support from my parents and in-laws. Particular appreciation to my husband Chenyu Yan. I will never forget those midnights he drove me to the school for the SEM analysis and waited for me until finish. Thank you so much for your patience and care that help me get over the low time. I weren't be able to finish graduate school without your being there.

TABLE OF CONTENTS

LIST OF TABLES

LIST OF FIGURES

SUMMARY

Biomaterials are widely used in medical practice to help maintain, improve or restore diseased tissues or organs. The successful integration of biomaterials with host tissue depends on substratum surface properties, as well as host tissue quality and its regulatory environment. The overall goal of this dissertation is to incorporate these three factors to achieve better biomaterial-host tissue interactions. Important surface properties include surface topography, surface energy, chemical composition and surface charge. We designed a new titanium (Ti) substratum with modified surface chemical composition by preventing the contamination when in contact with the atmosphere. The new Ti surface has lower carbon contamination and promotes osteoblast differentiation phenotype. The osteogenic effect is synergistic with micrometer and sub-micrometer scale surface structures. To further investigate the effects of bone quality on peri-implant bone formation, we developed a novel mouse femoral medullary bone formation model. This new model will facilitate research evaluating the effects of biomaterial surface treatments in host animals with deficient bone development, including genetically engineered mice. Finally, we studied sexual dimorphism in the response of osteoblasts to systemic regulatory hormones $1\alpha,25$-dihydroxyvitamin D_3 and 17β-estradiol. The results showed intrinsic differences in male and female osteoblasts with respect to their differentiation and their responses to hormones, suggesting that host chromosomal sex should be considered in biomaterial research. Taken together, this research provides fundamental information on biomaterial surface properties and the regulation of host tissue response, which are important in guiding biomaterial design and evaluation.

CHAPTER 1. INTRODUCTION

Bone Structure and Osteoblast Isolation

Bone is one of the hardest tissues in human body. The rigid structure provides mechanical support to frame the body, transfers force for locomotion and protects internal organs. More importantly, the organic and inorganic components together serve physiological functions to regulate homeostasis by maintaining constant calcium levels and producing blood cells through hematopoiesis. Generally, bone is classified into two types: cortical bone (or compact bone), a layered solid structure; and trabecular bone (or cancellous bone), a bony lattice that has a spongy appearance. These two types of bone differ in the spatial arrangement of cells, in the density of mineralized matrix and in the distribution of blood vessels and marrow [2]. Microscopic analysis of compact bone shows a hierarchical arrangement (Fig. 1-1). The basic structures of cortical bone are osteons, which are composed of Haversian canals with surrounding concentric layers of bone matrix (lamellae). These canals are interconnected with each other via Volkmann's canals that contain blood vessels, nerves and lymph vessels. Bone cells
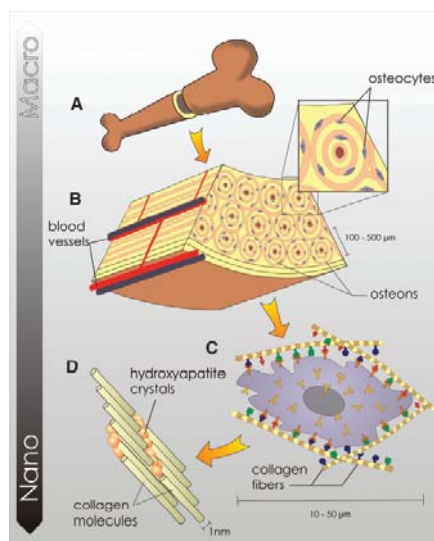
Figure 1-1. Hierarchy arrangement of bone structures [1].

1

together with extracellular matrix containing collagen fibers and various growth factors, constitute the organic components in bone tissue. Type I collagen is the main structural protein in the bone extracellular matrix. The inorganic part of the matrix is crystalline mineral salts and calcium, mostly present in the form of hydroxyapatite.

Bone is an active tissue constantly being remodeled throughout the life. The old bone is removed by tissue-resorbing cells (osteoclasts) and replaced with new bone laid by matrix-producing cells (osteoblasts). Osteoblasts are cuboidal in shape and located at the bone surface to form a tight layer with their precursor cells. Osteoblast viability and functionality highly depend on substratum anchorage and intercellular contacts. The osteoblast lifespan ranges between 3 days in young rabbits to 8 weeks in humans [3].

The bone remodeling processes take place at discrete units throughout the bone and last for about 90 days. This process allows the skeletal system to repair itself without leaving a scar, to adjust its mass and morphology to outside mechanical and chemical stimulation, and to mobilize mineral storage on metabolic demand. It is initiated by osteoclasts eroding the mineralized surface and making resorption pits about 100 μm in diameter, followed by recruitment of osteoblasts to the outer edge of the resorption cavity. The osteoblasts secret new bone matrix (osteoid) at a rate around 0.5 – 1.5 μm per day, which gradually fills in the resorption cavity [3]. Osteoblasts are actively involved in mineralization of surrounding osteoid by secreting matrix vesicles containing alkaline phosphatase, and ultimately become osteocytes when completely embedded in hard bone matrix. Osteocytes remain in fluid-filled cavities within the concentric lamellae, and connect to other similar cells and bone-lining cells (inactive osteoblasts) through canaliculi, creating an extensive network of intercellular communication [4].

As bone forming cells, osteoblasts or osteoblast-like cells are used as standards for *in vitro* studies to evaluate bone responses to various biological, chemical or

2

electrophysical stimulations before any animal study is conducted. To acquire sufficient cells, immortalized cell lines from rat (UMR-106, ROS 17/2.8, ROB-C26), mouse (MC3T3-E1, C3H10T1/2) and human (SaOS-2, MG63, HOS) are widely used [5, 6]. These cells are derived from stroma, bone or other mesenchymal/mesodermal tissues, and retain many markers of the osteoblast phenotype [7]. For example, the well characterized MG63 cell line is originally derived from a male human osteosarcoma and represents a less differentiated stage of osteoblastic maturation. MG63 cells exhibit increased alkaline phosphatase activity and osteocalcin levels in response to $1\alpha,25$ dihydroxyvitamin D_3 $[1\alpha,25\text{-}(OH)_2D_3]$ [8]. However, they do not mineralize the osteoid they synthesize. Thus, MG63 cells are used to assess early differentiation events but not terminal differentiation with respect to matrix calcification.

Although it is convenient to grow osteogenic sarcoma cell lines, the transformed cells differ from normal bone cells in their functional activity, cell membrane receptors and responses to biological regulators. To overcome this limitation, primary osteoblasts from normal mouse, rat or human are isolated from fresh bone samples by using explant or enzymatic methods. Generally, the bone fragments are first cut into small pieces to increase the contact area with media or enzyme, and then washed extensively for the removal of bone marrow cells, fibroblasts, blood cells and other contaminations. For the explant method, the bone pieces are directly cultured in media to allow osteoblasts to grow out from the bone explant. For the enzymatic method, bone pieces are treated with sequential trypsin/collagenase to remove the bone matrix and release the osteoblasts. The properties of isolated osteoblasts depend on the sample species, ages, anatomical sites and the choice of methods [9]. Enzymatically isolated fetal calvarial osteoblasts exhibit higher proliferative capacity and osteogenic potential [10]. For the heavily mineralized bones of adult animals, explant methods with collagenase pretreatment may result in the best osteoblast quantity and quality. To keep osteoblastic

3

characteristics in tissue culture conditions, primary cultures are usually treated with osteogenic media containing β-glycerophosphate or glucocorticoids that stimulate the osteoblastic phenotype.

Osteoblast Development and Differentiation

Osteoclasts are descendants of hematopoietic stem cells, while the osteoblasts are derived from multipotent mesenchymal stem cells capable of differentiating into fibroblast, osteoblast, chondrocyte and adipocyte lineages [7]. In bone, osteoprogenitor cells from the surrounding connective tissue are recruited to the inner periosteum layer, retaining proliferative capacity but expressing osteoblast specific proteins [11]. Osteoblast development is controlled by two genes, Cbfa1 and Indian hedgehog (Ihh) through direct or indirect pathways [7]. The morphological and histological criteria of osteoprogenitors and osteoblasts are reviewed by Aubin and others (Fig. 1-2) [7, 12].

4

Decreasing Proliferation and Increasing Differentiation →

Unlimited self renewal — Limited self renewal / Extensive proliferation — Limited proliferation — Post-mitotic

Multipotential stem cell → Immature osteoprogenitor → Mature osteoprogenitor → Preosteoblast → Mature osteoblast → Lining cells or osteocyte or apoptosis

Myoblasts Adipocytes Chondrocytes

	Unlimited self renewal	Immature osteoprogenitor	Mature osteoprogenitor	Preosteoblast	Mature osteoblast	Lining cells or osteocyte or apoptosis
Transcription Factors						
Cbfa-1	++	?	?	?	++	?
Enzyme						
Alkaline phosphatase	?	-	+	++	+++	-
Phex	?	-	-	-	+++	+++
Collagen and non-collagenous proteins						
Collagen type 1	?	-	++	++	++	-
Osteocalcin	-	-	-	-	- → +++	-
Bone sialoprotein	-	- → ++	++ → -	- → +++	- → +++	- → +++
Osteopontin	-/+?	-/+	-/+	- → +	- → +++	- → +++
Factors and receptors						
PTH/PTHrP-R	?	-	-/+	+++	+++	++
PTHrP	?	-/+	+	++	++	-
PDGF-Rα	?	-/+	-/+	+++	+++	+++
Adhesion molecules						
CD44	?	-/+	-/+	+	++	++
Galectin 3	?	-/+	-/+	- → +	- → +++	- → +++

Figure 1-2. Osteoprogenitor differentiation (Adapted from [7]).

The approaches to identify osteoblast characteristics are through determining specific enzyme activities or cellular products of osteoblasts, which are used as bone formation markers. Alkaline phosphatases are expressed in bone, liver, kidney, intestine and germ cells. The bone specific alkaline phosphatase anchors on the extracellular surface of plasma membranes or matrix vesicles, and is involved with mineralization [13]. Mutations in conserved regions of the protein result in hypophosphatasia, defective mineralization of bones and disorders of osteogenesis [14]. The enzyme cleaves phosphate groups, thereby increasing local inorganic phosphate concentration, resulting

in calcium and phosphate deposition. Matrix vesicles, enriched in alkaline phosphatase, are the centers for crystals to grow [15]. *In vitro*, proliferating osteoblasts produce low levels of alkaline phosphatase. At confluence, the enzyme activity peaks at the initiation stage of mineralization, and then diminishes (Fig. 1-2) [2, 7]. The main clinical methods to detect bone-specific alkaline phosphatase include immunoassay, selective heat inactivation and electrophoretic techniques. In osteoblast culture systems, which are not contaminated by other types of cells, measurement of total alkaline phosphatase activity represents early differentiation of osteoblasts.

Type I collagen is often used as bone formation marker because it constitutes 90% of the protein matrix in bone. Collagen is synthesized by osteoblasts in the precursor form of pre-procollagen. The precursor molecules are characterized by the intact C-terminal propeptide (PICP) and N-terminal propeptide of procollagen I (PINP), both of which are considered quantitative indicators of newly formed type I collagen.

Osteocalcin (or bone γ-carboxyglutamic acid protein, BGP) is a small protein primarily synthesized by mature osteoblasts and is one of most abundant non-collagenous proteins in the bone (20%) [16]. Osteocalcin is considered as the most bone-specific protein [17], although odontoblasts and hypertrophic chondrocytes also produce it. This 49-residue protein is characterized by the presence of three carboxyglutamic residues, a calcium binding amino acid that results from carboxylation of glutamate residues [18]. This reaction is catalyzed by vitamin K-dependent enzymes. The carboxyglutamic residues reside in Ca^{2+}-dependent α-helix and facilitates adsorption of hydroxyapatite. Osteocalcin deficient mice developed higher bone mass and improved bone quality without impairing bone resorption, indicating that osteocalcin may act via a negative feedback mechanism [19]. *In vitro* studies demonstrate that osteocalcin is a marker of late osteoblast differentiation (Fig. 2) [2, 7, 20]. Osteocalcin synthesis increases along with mineralization and remains high during progressive

6

osteoblastic differentiation while alkaline phosphatase activity decreases. Most of the newly synthesized osteocalcin is immediately bound to the extracellular matrix, with only a fraction being released into the culture media. Immunoassays are designed to measure free osteocalcin in the media, the level of which is assumed to be proportional to total synthesized osteocalcin.

Other non-collagenous proteins in bone matrix, such as osteonectin (20%), bone sialoproteins (12%), proteoglycans (10%), osteopontin and bone morphogenetic proteins (BMPs) [16], are also used to evaluate bone cell differentiation.

Regulation of Osteoblast Differentiation

Bone growth is regulated by co-ordinate expression of various growth factors, cytokines and transcription factors. The major bone regulating factors include $1\alpha,25(OH)_2D_3$, parathyroid hormone (PTH), glucocorticoid, BMP, transforming growth factor-β1 (TGF-β1), osteoprotegerin (OPG) and others. The mechanism of osteoblast differentiation is a complicated network; and the effects of these regulators depend on the relative maturation stage of osteogenic cells. For example, glucocorticoid simulates osteoblast differentiation *in vitro* while inducing osteoporosis *in vivo* [21, 22]. It is also reported that dexamethasone, one of the most efficient glucocorticoids, stimulates maturation of osteoprogenitor cells into osteoblasts, while inhibiting expression of collagen type I and osteocalcin in mature osteoblastic cells [7]. These complex effects are explained by the facts that glucocorticoid enhances progenitor cell differentiation, inhibits several molecules synthesized by the mature osteoblast and increases osteoblast apoptosis.

TGF-β belongs to a superfamily of growth factors, including BMPs, that regulates cell proliferation, differentiation and matrix protein production. There are five isoforms of TGF-β (β1 - β5), among which TGF-β1 is the most abundant form. TGF-β1 is stored in

the matrix through non-covalent binding with TGF-β binding protein. It has biphasic effects on osteoblast development *in vitro*, recruiting osteoprogenitor cells to proliferate providing a pool of early osteoblasts, while stimulating matrix production by more mature cells [23]. TGF-β1 increases the steady-state rate of osteoblastic differentiation from osteoprogenitor cell to terminally differentiated osteocyte and regulates bone remodeling, structure and biomechanical properties [24, 25].

Osteoblast proliferation and differentiation are not only regulated by soluble factors, but are also affected by various molecules that are deposited in the matrix during development. These matrix molecules interact with osteoblasts through cellular receptors and initiate signaling cascades that lead to cytoskeleton reorganization and gene expression. These signaling pathways are synergistic with cell responses to other growth factors. For example, it is found that collagen matrix synthesis is required for the expression of osteoblast differentiation markers, such as osteocalcin [26]. The interaction of type I collagen with its receptor integrin α1β1 and α2β1 regulates osteoblast response to BMP at the upstream of early differentiation marker gene expression [27]. Other matrix components, such as fibronectin or its cell-binding domains, also play a complex regulatory role in osteoblast differentiation and bone morphogenesis [28].

Orthopaedic Biomaterials

The five major categories of biomaterials are metals, ceramics, polymers, natural materials and composites of these materials. The worldwide market for all biomaterials exceeded $20 billion in 2000, including $9 billion for the U.S. market [29]. Among them, metals, metallic alloys and metal composites are the most extensively used materials in orthopaedic implants because of their tensile strength, stiffness, fracture toughness, and fatigue resistance. The commonly used materials include Ti, stainless steels and cobalt

alloys.

Commercially pure Ti (cpTi) is widely used in orthopaedic and dental fields and leads to predictable and satisfactory clinical outcomes. Over 300,000 hip/knee joint implants and 100,000-300,000 dental implants are applied annually in the U.S. to restore diseased tissue function [30]. A large amount of scientific research and technical development has been devoted to Ti, which further intensifies the role of Ti as a model substratum for studying biomaterial properties. Ti provides desired mechanical strength, as well as corrosion resistance and biocompatibility because of its spontaneously formed surface oxide layer.

The atomic structure of pure Ti under 882°C is a hexagonal close packed lattice (α-titanium), and is transformed to a cubic face centered structure (β-titanium) at higher temperatures. α+β alloys only exist in the presence of other additives as in Ti-6Al-4V alloy, which exhibits higher tensile strength. Because higher tensile strength is usually in company with lower ductility and impacts the fitness into the shape of bone surface, an optimized tensile strength is desired rather than an extremely high strength. Due to the crystal structure, cpTi has lower elastic modulus and higher flexibility than other metallic biomaterials, preventing bone resorption seen with other stiffer metals due to stress shielding phenomena [31].

Host Tissue-Biomaterial Interaction

Biocompatibility is defined as the ability of a material to support an appropriate host response in a specific application [32], and is evaluated by a series of standards including toxicity, carcinogenicity and local effects after implantation [33]. Biomaterials that have low toxicity and initiate formation of a relatively acellular foreign body capsule are generally accepted as biocompatible. The first stage of reaction to biomaterial insertion is adsorption of organic and inorganic molecules. After implantation, the

9

biomaterial surfaces are immediately covered by the components from hematoma, which initiate a coagulation cascade. The type and amount of adsorbed proteins keep dynamically changing when the surface is in contact with biological solutions. *In vitro* studies show that selective albumin, fibronectin, vitronectin, and other serum protein adsorption depends on surface properties, such as surface chemical composition, topography and surface energy [34-36]. It is often hypothesized that the protein type, amount and orientation adsorbed on Ti surfaces determine cell adhesion and responses; however, the relationship between *in vitro* cell adhesion and *in vivo* tissue response is still uncertain. For example, surfaces coated with the adhesion peptide Arg-Gly-Asp (RGD) significantly increase cell attachment, adhesion and spreading [37]; however, reports of the effects of RGD on osteoblast differentiation and *in vivo* bone formation are not consistent [38-41].

Bone healing following surgical implantation begins with an inflammatory process. The first cells that actually come in contact with the implant are neutrophils and macrophages. These cells approach the implant surface to remove bone debris produced by the surgical operation. Bone may be formed extending from the implant by two sources. The first is the migration of osteoblast progenitors toward the implant from the endosteal surface of the surrounding bone bed; alternatively differentiated progenitor cells may migrate from vasculature and marrow. In addition, osteoblasts at the surface of the healing bone deposit osteoid as they approach implant surface. The speed of bone formation extending away from the implant is approximately 30% faster than from the surrounding bone bed to the implant, which may be related to the osteogenic microenvironment created by the osteoblast on structured implant surfaces [30, 42]. Although most of the osteoblasts will not contact the implants directly, there is abundant evidence indicating that surface morphology does play an important role through autocrine, paracrine and endocrine signaling pathways. Mature peri-implant bone is

10

established at four to six weeks. This process is enhanced by various growth factors and cytokines, or disrupted by interfacial micro-motion.

Ti substrata exhibit a classical foreign body reaction in soft tissue characterized by a thin, acellular and collagenous capsule. When implanted in bone, pure titanium exhibits good healing without an obvious foreign body capsule or chronic inflammation. Similar bone formation processes were also observed around corrosion resistant metals such as zirconia and gold [43]. One hypothesis to explain the unique bone response to these materials is that the collagen capsule around Ti serves as a nucleation template for mineralization in the ionically rich environment in the bone [33].

Biomaterial Surface

Biomaterial surface properties are critical in cell-substratum interactions and biocompatibility, through the regulation of water, ions, lipids and proteins adsorption that further determine cell and tissue responses. The organization and reactivity of atoms that make up the outermost surface of biomaterials are different from those of the bulk. Therefore, the characterization and modification of surface are very important to improve biocompatibility and reactivity of biomaterials.

The binding sites of the atoms at the outmost Ti surface are not filled, resulting in more active properties compared to the atoms in the bulk. When in contact with atmosphere, Ti surfaces spontaneously form an oxidation layer, consisting mainly of TiO_2. The passive oxidation layer ranges from 20 to 200 nm, depending on procedures, aging time and sterilization methods. This reactivity also leads to other surface chemical reactions such as atmospheric contamination [44]. The common contamination molecules include hydrocarbons, carbon dioxide, silicones, thiols and iodine. Under the clinical conditions that all biomedical devices are applied, surface contamination is inevitable. However, it is important to make surfaces with consistent properties, to which

the cell and tissue responses are reproducible and predictable.

Ti maintains a lower corrosion rate in biological media and protein solutions compared to stainless steel or Ti alloy [45]. Ti atoms react with oxygen in the environment immediately to form an oxide layer. Therefore, even under the consistent fretting conditions as in micro-motion movement between the implant and host tissue, the implant is still protected by the spontaneously formed oxide layer [31]. The relatively high dielectric constant of the Ti oxide layer results in stronger van der Waals bonds on Ti compared to other metal oxide layers, and contributes to its biocompatibility. [31]. Although stable, the Ti oxide layer still undergoes electrochemical changes in biological environments, represented by thickening of the oxide layer, releasing of trace metals and deposition of Ca, P and S from physiological solutions [30].

Surface Modification

Because of the significant impact of biomaterial surfaces on biological responses, a wide variety of methods have been applied to modify implant surface properties to achieve the desired tissue-implant integration. The three major approaches in changing surface properties are physicochemical, biochemical and morphological methods [30].

Surface energy, surface charge and surface chemical composition are important in regulating osteoblast differentiation and *in vivo* bone formation. Glow discharge treatment and water storage of calcium phosphate coated implants accelerate integration with bone [46], indicating appropriate sterilization and storage are required to maintain intrinsically high surface energy implant [47].

Various chemical modifications of Ti surfaces have been investigated to achieve better bone formation, including bioactive ceramic coatings, silane treatments, protein/peptide coatings and others [33]. The immobilized proteins, enzymes or peptides on surfaces induce specific cell and tissue response to control tissue implant

interactions. The most widely used molecules on biomimic surfaces are cell attachment ligands and peptides, including RGD [41], GFOGER [48], fibronectin motifs [49], vitronectin and others or combinations . Other approaches include releasing growth factors (TGF-β1) and enzymes (alkaline phosphatase) [30].

It is generally accepted that micrometer scale roughness enhances osseointegration. More studies indicate that sub-micrometer scale textures regulate osteoblast differentiation when combined with micrometer scale roughness [50]. There are more investigations around nano scale structures, although a firm conclusion has not yet been made [51]. Besides the roughness parameter, other surface structure features are important. For instance, a microgrooved structure is important to provide contact guidance for the osteoblast to form specific patterns. The *in vitro* and *in vivo* effects of surface microtopography will be discussed in the next section in detail.

In Vitro Osteoblast Response to Ti Surface Morphology

Osteoblast responses to biomaterials, including attachment, proliferation, extracellular matrix synthesis and differentiation, are sensitive to surface microtopography [52]. On microrough structured Ti surfaces, osteoblasts exhibit a more differentiated phenotype. With the advantage of rapid growth, the human osteosarcoma cell line MG63 has been widely used to study the effects of surface roughness. Attachment is reduced on rough surfaces compared to tissue culture plastic or smooth Ti surfaces. When MG63 cells are cultured on smooth Ti surfaces, they display a flattened morphology, while on rougher surfaces with average center line height (R_a) of 4-7µm, they display a more cuboidal morphology characterized by prominent cytoplasmic extensions [53]. MG63 cells exhibit decreased cell number and [^{3}H]-thymidine incorporation when grown on rough Ti surfaces, indicating reduced proliferation rate. In contrast, those cells show increased markers of osteoblastic differentiation. The cells

exhibit increased alkaline phosphatase activity and osteocalcin, as well as bone regulatory factors including osteoprotegerin (OPG), prostaglandin E_2 (PGE_2) and TGF-β1 when they were grown on rough Ti surfaces [53, 54]. Moreover, osteoblast differentiation marker expression and local factor production are modulated by the vitamin D metabolite 1α,25$(OH)_2D_3$ in a synergistic manner with surface microtopography [55].

To overcome the consideration that MG63 cells are a transformed cell line and may not respond to surface microstructure in the same way as normal osteoblasts, fetal rat calvarial cells (FRC) and normal human osteoblasts (NHOst) were also examined on same Ti substrata and showed a similar response to the surface morphology as MG63 cells did, indicating that MG63 represents general osteoblast properties in response to surface structure. The NHOst cells demonstrated a more mature phenotype on rougher surfaces with increased levels of osteocalcin, PGE_2 and TGF-β1. However, in contrast to MG63 cells, alkaline phosphatase activity decreased with increasing surface roughness [56]. The difference in alkaline phosphatase activity between MG63 cells and NHOst cells in these two studies may reflect the fact that alkaline phosphatase is an early marker of osteoblast differentiation. Activity of this enzyme increases before mineralization and then decreases. The relatively immature MG63 cells may have been at a different state of osteoblastic maturation than the NHOst cells, such that at the time of assay MG63 cell activity was on its way up whereas NHOst cell activity had already peaked and was in its way down [56]. This hypothesis is supported by studies using other cell culture models [57].

Previous reports showed that mature osteoblast-like cells and osteocyte-like cells also respond to surface microtopography [58]. As the surface becomes rougher, all the cells exhibit more differentiated phenotype with decreased cell proliferation, and increased osteocalcin, PGE_2 and TGF-β1. FRC cells, which are also in the early stage

14

of osteoblastic linage like MG63 cellss, exhibit increased alkaline phosphatase activity; OCT-1 cells, a more differentiated osteoblast-like cell line, respond with decreased alkaline phosphatase activity; and the terminally differentiated MLO-Y4 cells exhibit no change in alkaline phosphatase activity. The effect of surface roughness was also examined using rat costochondral cartilage cells [57]. Resting zone cells, which are less mature in terms of endochondral differentiation than growth zone cells, respond to surface roughness like the MG63 cells. However, growth zone chondrocytes exhibited a different response with respect to alkaline phosphatase and collagenase-digestible protein production. These observations indicate that response of cells to surface roughness is dependent on cell maturation state.

The response of osteoblast-like cells to circulating hormones is also affected by surface roughness. Treatment of to MG63 and FRC cells with $1\alpha,25(OH)_2D_3$ caused a synergistic increase in alkaline phosphatase specific activity, osteocalcin levels and local factor levels on rougher Ti surfaces [58]. In contrast, $1\alpha,25(OH)_2D_3$ did not affect proliferation and alkaline phosphatase activity in more mature cells (OCT-1 and MLO-Y4 cells), but it increased osteocalcin levels. The results indicate that the surface roughness promotes osteogenic differentiation of less mature cells and enhances their responsiveness to $1\alpha,25(OH)_2D_3$. Osteoblast response to implant surface morphology is also modulated by estradiol [56]. On smooth surfaces, estradiol affected only alkaline phosphatase in female NHOst cells, but on rough surfaces, estradiol increased levels of osteocalcin, TGF-β1 and PGE$_2$.

The local factors released by osteoblast are important in regulating both bone formation and bone resorption. PGE$_2$ modulates normal osteoblast differentiation in a concentration dependent manner. At low concentrations, PGE$_2$ stimulates alkaline phosphatase activity and osteocalcin production; however, PGE$_2$ inhibits osteoblast function and stimulates osteoclastic activity at high concentrations [59]. The increased

15

level of PGE$_2$ on microrough surfaces appears to be required for osteoblast differentiation, because inhibition of prostaglandin expression inhibits osteoblast phenotypic expression on rough surfaces [60]. Most of TGF-β1 is stored with the extracellular matrix in latent form through association with TGF-β1-binding protein-1. In bone remodeling, osteoclasts resorb bone mineral by decreasing local pH, resulting in activation of latent TGF-β1 [61]. The increase in local concentration of active TGF-β1 causes an inhibition of bone resorption and contributes to bone formation by enhancing production of extracellular matrix, especially type I collagen [62]. OPG is a decoy receptor that binds to RANK ligand, resulting in inhibition of osteoclast maturation [63]. The increased expression of OPG by osteoblasts on microrough surfaces indicates that surface roughness is also important in regulating osteoclast activity [54].

Surface roughness also modulates the cell response to other local or systemic factors including BMP, estradiol and shear force. Ong *et al.* reported that when osteoblast progenitor 2T9 cells were plated on polished and 600 grit Ti surfaces, BMP-2 prolonged alkaline phosphatase specific activity and caused more rapid osteocalcin production on 600 grit Ti surfaces [64]. Estradiol synergistically increases PGE$_2$ and TGF-β1 in osteoblast cultures on rough surfaces [56]. Shear force did not affect cell proliferation and differentiation on smooth surfaces but caused reversal of the increase in osteoblast differentiation seen in cultures on rough surfaces [65].

To understand the effects of specific surface structure features, electrochemical micromachining (EMM) was used to produce Ti surfaces with controlled size and placement of micrometer scale cavities [66]. The 100 µm diameter cavities produced by EMM are comparable to the sizes of osteoclast resorption pits, which is critical in bone development and bone remodeling. The results showed that 100 µm cavities favored osteoblast attachment and growth and PGE$_2$ production. When MG63 cells were cultured on bone wafers with osteoclast resorption pits, they exhibit increased

16

differentiation. This effect is due to specific resorption cavities instead of demineralization, because general demineralization induced by tetracycline had much less effect on osteoblast-like cells [67]. The addition of the sub-micrometer scale etch enhanced differentiation and TGF-β1 production [50].

Mechanisms Mediating Osteoblast Response to Surface Topology

The osteoblasts must first attach to the surface before they produce and mineralize their extracellular matrix. The number of osteoblasts that actually adhere to the Ti surface appears to be less than that on a tissue culture plastic surface [68]. The cell morphologies on Ti surfaces depend on surface roughness. The cells cultured on rough Ti surfaces appear to attach to the surface through multiple cytoplasmic extensions and show a cubical morphology typical of differentiated osteoblasts. The results indicate that the cytoskeleton in the cells cultured on rough surface is rearranged and may have important consequences downstream.

Integrins are important membrane receptors that mediate cell attachment and adhesion to the extracellular matrix and regulate the arrangement of the cytoskeleton, followed by cell function. Integrins are heterodimers that are composed of α and β subunits. The major integrins expressed by osteoblasts are α2β1, α5β1 and αvβ3, whose main binding ligands are type I collagen, fibronectin and vitronectin, respectively. Other integrin subunits, including α1, α3, α4, α6 and β5, are also found in osteoblasts, but the results are not consistent [38]. The differences depend on cell source, development stages, culture system and detection antibodies. The activation of integrin initiates a cascade signaling pathway, resulting in changes of cytoskeleton arrangement, cell morphology, migration, proliferation, and differentiation. Focal adhesion kinase (FAK), protein kinase C (PKC), and phosphalipase C (PLC) are the main enzymes that mediate the integrin signaling pathway [69]. Recent studies indicate that the expression

17

of integrin is regulated by surface roughness, and integrins are actively involved in surface dependent cell behavior. For example, surface roughness induced BMP production by macrophages is mediated through integrin β1 [70]. Integrin α2 and β1 expression is higher on microrough Ti than smooth surfaces; however, α5, αv and β3 levels are not affected by rough Ti surfaces [71].

Prostaglandins may also mediate the initial response of MG63 cells to Ti surfaces [72]. Indomethacin, a general cyclooxygenase (Cox) inhibitor that blocks prostaglandin production, inhibits the response of non-confluent MG63 cells to surface roughness, and the effect vanishes when cells reach confluence. In further studies, both constitutive Cox-1 and inducible Cox-2 were found to be involved in mediating the cell response to surfaces [73]. The results indicate that both forms of the enzymes are involved and cell response to prostaglandins is complex.

In Vivo Bone Formation in Response to Surface Structure

The osteoblast response to implants *in vivo* is more complicated than the *in vitro* response. Previous studies showed that when Ti was implanted into marrow ablated rat tibia, matrix vesicle production was increased [74]. Interestingly, similar effects were also observed in the contralateral limb, suggesting there is a material specific effect both locally and systematically [75]. The cells may interact either directly with the surface, releasing bioactive factors that act both locally and systemically, or indirectly with the surface by responding to factors released by cells at the bone-implant interface.

Over 400 hundred original animal studies have be performed to investigate the effects of implant surface roughness on bone response and implant fixation [76]. Due to differences in surface preparations, animal models and surgical techniques, the results of bone-to-implant contact in response to substrata structure were inconsistent. Meta-analyses with stricter inclusion criteria compare the studies with similar experimental

design and provide accurate data analyses. Shalabi *et al.* has systemically reviewed 16 studies that provided surface roughness parameters, histomorphological quantification and biomechanical tests with healing period of at least 3 months [76]. The results are summarized in Table I. Six of 16 studies reported significantly increased bone-to-implant percentage around implants with rougher surfaces. Among the other 10 studies that failed to show statistical differences, nine of them showed a positive relation and one had negative results. Push-out and removal torque tests are the two techniques used to evaluate biomechanical strength of osseointegration. Totally, six papers reported significantly higher mechanical force around implant with rougher surfaces. The other studies reported no statistical difference.

Table 1-1 In vivo analyses of relation between surface roughness and bone formation. Data summarized from Shalabi et al.'s paper [75].

	Positive relation with statistical difference	Positive relation without statistical difference	Negative result without statistical difference
Bone-to-implant contact	6	9	1
Push-out force	3	2	
Removal torque	3	2	4

There is no consensus yet on the optimized surface roughness for bone implant. Albrektsson and Wennerbergy suggested that moderately rough surfaces with center line average height (S_a or R_a) of 1-2 µm promote stronger bone responses than either smoother or rougher surfaces [77]. Others reported a positive effect of surface roughness on bone formation up to roughness of 8.5 µm [76]. The differences are not only caused by measurement techniques, but also related to general integral design of

implant macrostructure.

Evaluation of clinical data showed that both smooth and rough surfaces achieved predictable high success rates in dental applications. In subgroups of patients with specific indications, implants with rough surfaces had significantly higher success rates than smooth surfaces [78]. The traditional practice of dental implant placement requires 4 to 6-month pre-loading period to allow uneventful wound healing. The rationale of this approach is to prevent micro-movement caused by functional force, to allow the wound healing process to occurr without disturbance, and to promote osseointegration around the implants. A prospective, randomized multi-center clinical study compared 247 dual acid-etched and 185 machined surfaced dental implants and found that the pre-loading integration success rate of dual acid etched implants (95.0%) was statistically higher than machined-surfaced implants (86.7%) [79]. With the application of rough surfaced dental implants, the pre-clinical loading period decreases to less than 3 months.

Objective

The overall goal of this thesis is to understand how surface microtopography and surface chemical composition or surface energy interact to elicit a synergistic osteogenic response, and to explore whether there is the sexual dimorphism in the response of primary osteoblasts to bone regulating hormones. To address this problem, we first a developed modified Ti surface with increased hydrophilicity by preventing contact with atmosphere via production in nitrogen environment and storage in physiological solutions. MG63 cells respond to the modified surface with decreased cell number and enhanced differentiation. The increased osteoblast differentiation is synergistic with respect to surface microtopography and surface hydrophilicity. The effects of surface hydrophilicity also require the presence of both surface micrometer scale and sub-micrometer scale structures. We also developed a novel mouse femur medullary bone

20

formation model. New bone formation was observed around the inserted Ti implant. To explore the intrinsic differences in male and female osteoblasts and their responses to systemic hormones, effects of 17β-estradiol and $1,25(OH)_2D_3$ were examined on primary rat osteoblasts. Results showed that male osteoblasts have higher alkaline phosphatase and osteocalcin, and male osteoblasts respond to $1,25(OH)_2D_3$ in a surface dependent way. Female osteoblast differentiation is regulated by 17β-estradiol and this effect is mediated through a membrane associated signaling pathway. This study is significant because it will provide fundamental information on biomaterial surface properties in regulating host tissue response. The results will be important in guiding biomaterial design and evaluation. The results will also add to our knowledge of the mechanisms that modulate cell responses to their substrata that will improve the use of biomaterials in sites where host bone is compromised.

References

1. Stevens MM, George JH. Exploring and engineering the cell surface interface. Science 2005; 310: 1135-1138.

2. Calvo MS, Eyre DR, Gundberg CM. Molecular basis and clinical application of biological markers of bone turnover. Endocr.Rev. 1996; 17: 333-368.

3. Sommerfeldt DW, Rubin CT. Biology of bone and how it orchestrates the form and function of the skeleton. Eur.Spine J. 2001; 10 Suppl 2: S86-S95.

4. Donahue HJ, McLeod KJ, Rubin CT, Andersen J, Grine EA, Hertzberg EL, Brink PR. Cell-to-cell communication in osteoblastic networks: cell line-dependent hormonal regulation of gap junction function. J.Bone Miner.Res. 1995; 10: 881-889.

5. Sudo H, Kodama HA, Amagai Y, Yamamoto S, Kasai S. In vitro differentiation and calcification in a new clonal osteogenic cell line derived from newborn mouse calvaria. J.Cell Biol. 1983; 96: 191-198.

6. Katagiri T, Yamaguchi A, Ikeda T, Yoshiki S, Wozney JM, Rosen V, Wang EA, Tanaka H, Omura S, Suda T. The non-osteogenic mouse pluripotent cell line, C3H10T1/2, is induced to differentiate into osteoblastic cells by recombinant human bone morphogenetic protein-2. Biochem.Biophys.Res.Commun. 1990; 172: 295-299.

7. Aubin JE. Regulation of osteoblast formation and function. Rev.Endocr.Metab Disord. 2001; 2: 81-94.

8. Franceschi RT, James WM, Zerlauth G. 1 alpha, 25-dihydroxyvitamin D3 specific regulation of growth, morphology, and fibronectin in a human osteosarcoma cell line. J.Cell Physiol 1985; 123: 401-409.

9. Wurtz T, Berdal A. Osteoblast precursors at different anatomic sites. Crit Rev.Eukaryot.Gene Expr. 2003; 13: 147-161.

10. Declercq H, Van dV, De Maeyer E, Verbeeck R, Schacht E, De Ridder L, Cornelissen M. Isolation, proliferation and differentiation of osteoblastic cells to study cell/biomaterial interactions: comparison of different isolation techniques and source. Biomaterials 2004; 25: 757-768.

11. Owen M. The origin of bone cells. Int.Rev.Cytol. 1970; 28: 213-238.

12. Freemont AJ. Basic bone cell biology. Int.J.Exp.Pathol. 1993; 74: 411-416.

13. Whyte MP. Hypophosphatasia and the role of alkaline phosphatase in skeletal mineralization. Endocr.Rev. 1994; 15: 439-461.

14. Khandwala HM, Mumm S, Whyte MP. Low serum alkaline phosphatase activity and pathologic fracture: case report and brief review of hypophosphatasia diagnosed in adulthood. Endocr.Pract. 2006; 12: 676-681.

15. Simon PR, Arnett TR. Biochemical markers of bone turnover. In: Methods in Bone Biology. London: New York Chapman&Hall; 1998.

16. Anselme K. Osteoblast adhesion on biomaterials. Biomaterials 2000; 21: 667-681.

17. Hughes FJ, Turner W, Belibasakis G, Martuscelli G. Effects of growth factors and cytokines on osteoblast differentiation. Periodontol.2000. 2006; 41: 48-72.

18. Gallop PM, Lian JB, Hauschka PV. Carboxylated calcium-binding proteins and vitamin K. N.Engl.J.Med. 1980; 302: 1460-1466.

19. Ducy P, Desbois C, Boyce B, Pinero G, Story B, Dunstan C, Smith E, Bonadio J, Goldstein S, Gundberg C, Bradley A, Karsenty G. Increased bone formation in osteocalcin-deficient mice. Nature 1996; 382: 448-452.

20. Owen TA, Aronow M, Shalhoub V, Barone LM, Wilming L, Tassinari MS, Kennedy MB, Pockwinse S, Lian JB, Stein GS. Progressive development of the rat osteoblast phenotype in vitro: reciprocal relationships in expression of genes associated with osteoblast proliferation and differentiation during formation of the bone extracellular matrix. J.Cell Physiol 1990; 143: 420-430.

21. Lukert BP, Kream BE, Bilezikian JP, Raisz LG, Rodan GA. Clinical and basic aspects of glucocorticoid action in bone. In: Principles of Bone Biology. San Diego: Academic Press; 1996: 533-548.

22. Weinstein RS, Jilka RL, Parfitt AM, Manolagas SC. Inhibition of osteoblastogenesis and promotion of apoptosis of osteoblasts and osteocytes by glucocorticoids. Potential mechanisms of their deleterious effects on bone. J.Clin.Invest 1998; 102: 274-282.

23. Bonewald LF, Bilezikian JP, Raisz LG, Rodan GA. Transforming growth factor-beta. In: Principles of Bone Biology. San Diego: Academic Press; 1996: 647-659.

24. Erlebacher A, Filvaroff EH, Ye JQ, Derynck R. Osteoblastic responses to TGF-beta during bone remodeling. Mol.Biol.Cell 1998; 9: 1903-1918.

25. Filvaroff E, Erlebacher A, Ye J, Gitelman SE, Lotz J, Heillman M, Derynck R. Inhibition of TGF-beta receptor signaling in osteoblasts leads to decreased bone remodeling and increased trabecular bone mass. Development 1999; 126: 4267-4279.

26. Xiao G, Cui Y, Ducy P, Karsenty G, Franceschi RT. Ascorbic acid-dependent activation of the osteocalcin promoter in MC3T3-E1 preosteoblasts: requirement for collagen matrix synthesis and the presence of an intact OSE2 sequence. Mol.Endocrinol. 1997; 11: 1103-1113.

27. Jikko A, Harris SE, Chen D, Mendrick DL, Damsky CH. Collagen integrin receptors regulate early osteoblast differentiation induced by BMP-2. J.Bone Miner.Res. 1999; 14: 1075-1083.

28. Moursi AM, Damsky CH, Lull J, Zimmerman D, Doty SB, Aota S, Globus RK. Fibronectin regulates calvarial osteoblast differentiation. J.Cell Sci. 1996; 109 (Pt 6): 1369-1380.

29. Abramson S, Alexander H, Best S, Bokros JC, Brunski JB, Colas A, Cooper SL, Curtis J, Haubold A, Hench LL, Hergenrother RW, Hoffman AS, Hubbell JA, Jansen JA, King MW, Kohn J, Lamba NMK, Langer R, Migliaresi C, More RB, Peppas NA, Ratner BD, Visser SA, von Recum AF, Weinberg S, Yannas IV, Ratner BD, Hoffman AS, Schoen FJ, Lemons JE. Classes of materials used in medicine. In: Biomaterials Science: An Introduction to Materials in Medicine, vol. 2nd. San Diego: Elsevier Academic Press; 1996: 67-233.

30. Puleo DA, Nanci A. Understanding and controlling the bone-implant interface. Biomaterials 1999; 20: 2311-2321.

31. Pohler OE. Unalloyed titanium for implants in bone surgery. Injury 2000; 31 Suppl 4: 7-13.

32. Williams DF. Definitions in Biomaterials. In: Progress in Biomedical Engineering, vol. 4. Amsterdam: Elsevier; 1987.

33. Ratner BD. A perspective on titanium biocompatibility. In: Brunette DM, Tengvall P, Textor M, Thomsen P (eds.), Titanium in Medicine. Berlin: Springer; 2001: 1-12.

34. Kieswetter K, Schwartz Z, Dean DD, Boyan BD. The role of implant surface characteristics in the healing of bone. Critical Reviews in Oral Biology & Medicine 1996; 7: 329-345.

35. Ellingsen JE. A study on the mechanism of protein adsorption to TiO2. Biomaterials 1991; 12: 593-596.

36. Webster TJ, Schadler LS, Siegel RW, Bizios R. Mechanisms of enhanced osteoblast adhesion on nanophase alumina involve vitronectin. Tissue Eng 2001; 7: 291-301.

37. Hersel U, Dahmen C, Kessler H. RGD modified polymers: biomaterials for stimulated cell adhesion and beyond. Biomaterials 2003; 24: 4385-4415.

38. Siebers MC, ter Brugge PJ, Walboomers XF, Jansen JA. Integrins as linker proteins between osteoblasts and bone replacing materials. A critical review. Biomaterials 2005; 26: 137-146.

39. Kantlehner M, Schaffner P, Finsinger D, Meyer J, Jonczyk A, Diefenbach B, Nies B, Holzemann G, Goodman SL, Kessler H. Surface coating with cyclic RGD

peptides stimulates osteoblast adhesion and proliferation as well as bone formation. Chembiochem 2000; 1: 107-114.

40. Gronowicz GA, Derome ME. Synthetic peptide containing Arg-Gly-Asp inhibits bone formation and resorption in a mineralizing organ culture system of fetal rat parietal bones. J Bone Miner Res 1994; 9: 193-201.

41. Tosatti S, Schwartz Z, Campbell C, Cochran DL, VandeVondele S, Hubbell JA, Denzer A, Simpson J, Wieland M, Lohmann CH, Textor M, Boyan BD. RGD-containing peptide GCRGYGRGDSPG reduces enhancement of osteoblast differentiation by poly(L-lysine)-graft-poly(ethylene glycol)-coated titanium surfaces. J Biomed Mater Res 2004; 68A: 458-472.

42. Boyan BD, Lossdorfer S, Wang L, Zhao G, Lohmann CH, Cochran DL, Schwartz Z. Osteoblasts generate an osteogenic microenvironment when grown on surfaces with rough microtopographies. Eur.Cell Mater. 2003; 6: 22-27.

43. Thomsen P, Larsson C, Ericson LE, Sennerby L, Lausmaa J, Kasemo B. Structure of the interface between rabbit cortical bone and implants of gold, zirconium and titanium. J.Mater Sci.Mater Med. 1997; 8: 653-665.

44. Carew EO, Cooke FW, Lemons JE, Ratner BD, Vesely I, Vogler EA. Surface Properties and Surface Characterization of Materials. In: Biomaterials Science: An Introduction to materials in Medicine: Academic Press; 1996: 40-59.

45. Clark GC, Williams DF. The effects of proteins on metallic corrosion. J.Biomed.Mater Res. 1982; 16: 125-134.

46. Sendax VI, Baier RE. Improved integration potential for calcium-phosphate-coated implants after glow-discharge and water-storage. Dent Clin North Am 1992; 36: 221-224; discussion 225.

47. Baier RE, Meyer AE. Future directions in surface preparation of dental implants. J Dent Educ 1988; 52: 788-791.

48. Reyes CD, Garcia AJ. Alpha2beta1 integrin-specific collagen-mimetic surfaces supporting osteoblastic differentiation. J Biomed Mater Res A 2004; 69: 591-600.

49. Cutler SM, Garcia AJ. Engineering cell adhesive surfaces that direct integrin alpha5beta1 binding using a recombinant fragment of fibronectin. Biomaterials 2003; 24: 1759-1770.

50. Zhao G, Zinger O, Schwartz Z, Wieland M, Landolt D, Boyan BD. Osteoblast-like cells are sensitive to submicron-scale surface structure. Clin.Oral Implants Res. 2006; 17: 258-264.

51. Cai K, Bossert J, Jandt KD. Does the nanometre scale topography of titanium influence protein adsorption and cell proliferation? Colloids Surf.B Biointerfaces. 2006; 49: 136-144.

52. Boyan BD, Hummert TW, Kieswetter K, Schraub D, Dean DD, Schwartz Z. Effect of titanium surface characteristics on chondrocytes and osteoblasts in vitro. Cells and Materials 1995; 5: 323-334.

53. Martin JY, Schwartz Z, Hummert TW, Schraub DM, Simpson J, Lankford J, Dean DD, Cochran DL, Boyan BD. Effect of Titanium Surface-Roughness on Proliferation, Differentiation, and Protein-Synthesis of Human Osteoblast-Like Cells (Mg63). J.Biomed.Mater.Res. 1995; 29: 389-401.

54. Lossdorfer S, Schwartz Z, Wang L, Lohmann CH, Turner JD, Wieland M, Cochran DL, Boyan BD. Microrough implant surface topographies increase osteogenesis by reducing osteoclast formation and activity. J Biomed Mater Res 2004; 70A: 361-369.

55. Boyan BD, Batzer R, Kieswetter K, Liu Y, Cochran DL, Szmuckler-Moncler S, Dean DD, Schwartz Z. Titanium surface roughness alters responsiveness of MG63 osteoblast-like cells to 1 alpha,25-(OH)(2)D-3. J.Biomed.Mater.Res. 1998; 39: 77-85.

56. Lohmann CH, Tandy EM, Sylvia VL, Hell-Vocke AK, Cochran DL, Dean DD, Boyan BD, Schwartz Z. Response of normal female human osteoblasts (NHOst) to 17 beta-estradiol is modulated by implant surface morphology. J.Biomed.Mater.Res. 2002; 62: 204-213.

57. Boyan BD, Lincks J, Lohmann CH, Sylvia VL, Cochran DL, Blanchard CR, Dean DD, Schwartz Z. Effect of surface roughness and composition on costochondral chondrocytes is dependent on cell maturation state. J.Orthop.Res. 1999; 17: 446-457.

58. Lohmann CH, Bonewald LF, Sisk MA, Sylvia VL, Cochran DL, Dean DD, Boyan BD, Schwartz Z. Maturation state determines the response of osteogenic cells to surface roughness and 1,25-dihydroxyvitamin D-3. Journal of Bone and Mineral Research 2000; 15: 1169-1180.

59. Atkin I, Dean DD, Muniz OE, Agundez A, Castiglione G, Cohen G, Howell DS, Ornoy A. Enhancement of osteoinduction by vitamin D metabolites in rachitic host rats. J Bone Miner Res 1992; 7: 863-875.

60. Sisk MA, Lohmann CH, Cochran DL, Sylvia VL, Simpson JP, Dean DD, Boyan BD, Schwartz Z. Inhibition of cyclooxygenase by indomethacin modulates osteoblast response to titanium surface roughness in a time-dependent manner. Clin.Oral Implants.Res 2001; 12: 52-61.

61. Oursler MJ. Osteoclast synthesis and secretion and activation of latent transforming growth factor beta. J.Bone Miner.Res. 1994; 9: 443-452.

62. Bonewald LF. Regulation and regulatory activities of transforming growth factor beta. Crit Rev.Eukaryot.Gene Expr. 1999; 9: 33-44.

63. Khosla S. Minireview: the OPG/RANKL/RANK system. Endocrinology 2001; 142: 5050-5055.

64. Ong JL, Carnes DL, Cardenas HL, Cavin R. Surface roughness of titanium on bone morphogenetic protein-2 treated osteoblast cells in vitro. Implant.Dent. 1997; 6: 19-24.

65. Bannister SR, Lohmann CH, Liu Y, Sylvia VL, Cochran DL, Dean DD, Boyan BD, Schwartz Z. Shear force modulates osteoblast response to surface roughness. J Biomed Mater Res 2002; 60: 167-174.

66. Zinger O, Zhao G, Schwartz Z, Simpson J, Wieland M, Landolt D, Boyan B. Differential regulation of osteoblasts by substrate microstructural features. Biomaterials 2005; 26: 1837-1847.

67. Boyan BD, Schwartz Z, Lohmann CH, Sylvia VL, Cochran DL, Dean DD, Puzas JE. Pretreatment of bone with osteoclasts affects phenotypic expression of osteoblast-like cells. J Orthop.Res 2003; 21: 638-647.

68. Sinha RK, Morris F, Shah SA, Tuan RS. Surface composition of orthopaedic implant metals regulates cell attachment, spreading, and cytoskeletal organization of primary human osteoblasts in vitro. Clin.Orthop.Relat Res. 1994: 258-272.

69. Hynes RO. Integrins: bidirectional, allosteric signaling machines. Cell 2002; 110: 673-687.

70. Takebe J, Champagne CM, Offenbacher S, Ishibashi K, Cooper LF. Titanium surface topography alters cell shape and modulates bone morphogenetic protein 2 expression in the J774A.1 macrophage cell line. J Biomed Mater Res A 2003; 64: 207-216.

71. Raz P, Lohmann CH, Turner J, Wang L, Poythress N, Blanchard C, Boyan BD, Schwartz Z. 1alpha,25(OH)2D3 regulation of integrin expression is substrate dependent. J Biomed Mater Res A 2004; 71A: 217-225.

72. Batzer R, Liu Y, Cochran DL, Szmuckler-Moncler S, Dean DD, Boyan BD, Schwartz Z. Prostaglandins mediate the effects of titanium surface roughness on MG63 osteoblast-like cells and alter cell responsiveness to 1 alpha,25-(OH)(2)D-3. J.Biomed.Mater.Res. 1998; 41: 489-496.

73. Boyan BD, Lohmann CH, Sisk M, Liu Y, Sylvia VL, Cochran DL, Dean DD, Schwartz Z. Both cyclooxygenase-1 and cyclooxygenase-2 mediate osteoblast response to titanium surface roughness. J.Biomed.Mater.Res. 2001; 55: 350-359.

74. Schwartz Z, Amir D, Boyan BD, Cochavy D, Mai CM, Swain LD, Gross U, Sela J. Effect of Glass Ceramic and Titanium Implants on Primary Calcification During Rat Tibial Bone Healing. Calcified Tissue International 1991; 49: 359-364.

75. Schwartz Z, Swain L, Sela J, Gross U, Amir D, Kohavi D, Muller-Mai C, Boyan B. In vivo regulation of matrix vesicle concentration and enzyme activity during primary bone formation. Bone Miner 1992; 17: 134-138.

76. Shalabi MM, Gortemaker A, Van't Hof MA, Jansen JA, Creugers NH. Implant surface roughness and bone healing: a systematic review. J.Dent.Res. 2006; 85: 496-500.

77. Wennerberg A, Albrektsson T. Suggested guidelines for the topographic evaluation of implant surfaces. Int J Oral Maxillofac Implants 2000; 15: 331-344.

78. Cochran DL. A comparison of endosseous dental implant surfaces. J.Periodontol. 1999; 70: 1523-1539.

79. Khang W, Feldman S, Hawley CE, Gunsolley J. A multi-center study comparing dual acid-etched and machined-surfaced implants in various bone qualities. J.Periodontol. 2001; 72: 1384-1390.

CHAPTER 2. HIGH SURFACE ENERGY ENHANCES CELL RESPONSE TO TITANIUM SUBSTRATUM MICROSTRUCTURE

Introduction

Titanium (Ti) is widely used clinically as an implant material, and the properties of the Ti surface are important variables in implant design. Upon implantation, the implant surface is conditioned by proteins, ions, sugars, and lipids present in the blood and tissue fluids. Important surface properties affecting this process include topography, chemistry, surface charge and hydrophilicity. Studies comparing the effects of surface properties on peri-implant bone formation show that they can modulate tissue response. For example, titanium implants with greater roughness enhance bone-to-implant contact [1-3] and increase removal torque forces [4-6].

To understand the specific contributions of surface design features, investigators have used a variety of cell culture models. These studies have shown that surface-dependent adsorption can modulate cell response. Differences in surface topography, including roughness and texture, affect adsorption of fibronectin and albumin *in vitro* [7-9], influencing cell attachment and adhesion [10-12]. Proliferation and differentiation of osteoblastic cells have been shown to be sensitive to surface microarchitecture [13]. When osteoblast-like osteosarcoma MG63 cells or normal human osteoblasts (NHOst cells) are grown on titanium surfaces with different microtopographies, cell number is reduced and differentiation, represented by osteocalcin production, is increased on microrough surfaces [14, 15]. On rough Ti surfaces, osteoblasts also generate an osteogenic microenvironment to regulate bone remodeling through autocrine and paracrine pathways [16]. MG63 cells on rough surfaces secrete more prostaglandin E_2 (PGE_2) and transforming growth factor-β1 (TGF-β1) to promote osteoblastic activity [17], and produce osteoprotegerin to decrease osteoclast formation and activity [18]. The

27

effects of 17β-estradiol and 1α,25$(OH)_2D_3$ on differentiation and local factor levels are increased in a synergistic manner on microrough surfaces [15, 19].

In the studies above, numerous additive and subtractive surface modification techniques have been applied to alter the surface topography of Ti implants. We used Ti surfaces with a complex microtopography as the model substrata for the present study. These surfaces were prepared by sand blasting and acid etching (SLA) of chemically polished (PT) Ti disks [14]. *In vitro* studies indicate that the osteogenic effect of the SLA surface is due to its micrometer-scale and sub-micrometer scale structure [20], which is similar to osteoclast resorption pits on bone wafers [21].

Because surface analysis indicated SLA and PT were comparable, the effects of SLA on enhanced bone response were attributed to surface texture rather than to their specific surface composition [22]. However, surface energy can also be affected by roughness [23, 24]. Higher surface energy has been hypothesized to be desirable for bone implants because increased wettability enhances interaction between the implant surface and the biologic environment [25]. Cell spreading increases on substratum with higher surface energy in both the presence and absence of serum proteins [26]. The cell layer appears to be increased around hydrophilic Ti implants, attributed to the tightly adhered conditioning film [27]. Surface hydrophilicity is another factor that determines biocompatibility of biomaterials and is largely dependent on surface energy [28, 29]. When implants with increased hydrophilicity are implanted in bone, the rate and extent of bone formation are increased [30]. This suggests that surface energy modulates bone cell maturation and differentiation.

Theoretically, pure Ti surfaces exhibit high surface energy due to the oxide layer that grows spontaneously at the room temperature [31, 32]. The oxide surface is hydrophilic, binding structural water and forming -OH and -O^{2-} groups in its outermost layer. Oxide surfaces are known to spontaneously nucleate calcium phosphate layers

28

(apatite) when in contact with physiologically-related fluid solutions [33-35]. A surface film made of a complex of phosphate, titanium and calcium and containing hydroxyl groups and hydrates, is formed when the specimen is immersed in an electrolytic solution. Both the amount of hydroxyl groups and negative charge of Ti surfaces are important for hydroxyapatite formation, and may enhance osseointegration.

However, surfaces with high energy also adsorb inorganic anions or organic hydrocarbon contaminants from the atmosphere within seconds to one minute, resulting in altered surface chemical composition and decreased hydrophilicity [36-38]. Moreover, cleaning processes such as alcohol treatment [39, 40] and autoclave sterilization [41, 42] will further increase hydrophobicity. As a result, existing Ti surfaces tend to have low surface energy and are very hydrophobic [43-45]. The enhanced hydrophobicity of microrough Ti surfaces compared to smooth Ti surfaces might be induced by roughness and topographical surface characteristics [24].

Studies using self assembled monolayers have modified surface chemistry to regulate osteoblast differentiation by changing surface charge [46]. These experiments, while interesting, have not addressed surface microarchitecture, nor have they assessed whether the hydrophilic properties of uncontaminated TiO_2 would be similar. To overcome this deficiency, we took advantage of a novel methodology for producing Ti substrata with identical microstructure to the SLA substrata, but with increased surface energy. Continuous submersion of modified SLA (modSLA, also referred as SLActive®) surfaces in isotonic solution appears to protect the modSLA surface from contamination with hydrocarbons and carbonates naturally occurring in the atmosphere, thus producing a chemically clean and reactive surface. The resulting hydroxylated/hydrated modSLA surface was shown to have an initial advancing water contact angle of 0°, indicating its immediate wettability and extreme hydrophilic character. This result is consistent with the general understanding that the perfectly clean Ti surface with unsaturated chemical

29

bonds represents a higher energy state and thus exhibits more hydrophilic properties than contaminated surfaces [38]. Our results, described below, indicate that osteoblast-like cells grown on modSLA surfaces exhibit a more differentiated phenotype and produce higher levels of local factors. Moreover, these surface effects were synergistic with the effects of the osteotropic hormone, 1α,25-dihydroxyvitamin D_3 [1α,25$(OH)_2D_3$].

Materials and Methods

Preparation and Characterization of Ti Disks

Ti disks were prepared from 1 mm thick sheets of grade 2 unalloyed Ti (ASTM F67 "Unalloyed titanium for surgical implant applications") and supplied by Institut Straumann AG (Walderburg, Switzerland). The disks were punched to be 15 mm in diameter so as to fit into the well of a 24-well tissue culture plate. Disks were degreased by washing in acetone, processing through 2% ammonium fluoride / 2% hydrofluoric acid / 10% nitric acid solution at 55°C for 30 s to produce pretreatment Ti disks (PT). To produce SLA surfaces, PT disks were further coarse grit-blasted with 0.25-0.50 mm corundum grit at 5 bar until the surface became a uniform gray, followed by acid etching as described previously [14]. After preparation, PT and SLA disks were rinsed in deionized water and dried under nitrogen. Prior to cell culture, the disks were sterilized by steam autoclaving at 121ºC for 15 min. ModSLA surfaces were produced with same sandblasting and acid-etching procedure as SLA surfaces. The modSLA surfaces were rinsed under nitrogen protection to prevent exposure to air, and then stored in a sealed glass tube containing isotonic NaCl solution. These sealed disks were sterilized by gamma irradiation at 25 kGy over night.

Surface topography was qualitatively examined using scanning electron microscopy (SEM) and quantitatively measured by confocal three dimensional (3D) white light microscopy (γSurf, NanoFocus AG, Oberhausen, Germany) to calculate

three-dimensional roughness parameters (S_a, S_q, S_t and S_k). Water contact angles of each surface type were tensiometrically determined by dynamic contact angle analysis (DCA) (Tensiometer Sigma 70, KSV Instruments Ltd., Helsinki, Finland) after being dried under nitrogen. DCA has been previously described in detail [24, 47]. The chemical composition of the surfaces was examined by X-ray photoelectron spectroscopy (XPS, VG/SSI 2803 S-Probe, Kratos Analytical Ltd., Hofheim, Germany).

Cell Culture

MG63 osteoblast-like osteosarcoma cells were obtained from the American Type Culture Collection (Rockville, MD). The cells were cultured in Dulbecco's modified Eagle medium (DMEM) containing 10% fetal bovine serum (FBS) and 1% penicillin/streptomycin at 37°C in an atmosphere of 5% CO_2 and 100% humidity. Cells were plated at the same density of 10,000 cells/cm^2 tissue culture plastic for all surfaces. Media were exchanged at 24 hours and then every 48 hours until the cells reached confluence on plastic. At confluence, the media were replaced with experimental media containing vehicle or 1α,25$(OH)_2D_3$ at 10^{-9} and 10^{-8} M.

Analysis of Cell Response

Cell morphology on the test surfaces was examined by scanning electron microscopy (Hitachi S800 FEG, Pleasanton, CA). 7 days after plating, cells were fixed with 1% osmium tetroxide, dehydrated in a sequential series using *tert*-butyl alcohol, and then coated with gold. Cell number was determined in all cultures 24 hours after cells on tissue culture plastic reached confluence. Cells were released from the surfaces by two sequential incubations in 0.25% trypsin for 10 min at 37°C, in order to assure that any remaining cells were removed from rough Ti surfaces, and counted using an automatic cell counter (Z1 cell and particle counter, Beckman Coulter, Fullerton, CA). To measure alkaline phosphatase specific activity [orthophosphoric monoester phosphohydrolase, alkaline; E.C. 3.1.3.1], cell layers were collected by scraping off confluent cells and

extracellular matrix using micropipette tips; and cellular samples were centrifuged from cell counting vials. Enzyme activity was assayed by measuring the release of *p*-nitrophenol from *p*-nitrophenylphosphate at pH 10.2 and results were normalized to protein [48]. Osteocalcin levels in the conditioned media were measured using a commercially available radioimmunoassay kit (Human Osteocalcin RIA Kit, Biomedical Technologies, Stoughton, MA) as described previously [19]. PGE_2 was assessed using a commercially available competitive binding radioimmunoassay kit (NEK020A Prostaglandin E_2 RIA kit, Perkin Elmer, Wellesley, MA) [17]. Active TGF-β1 was measured prior to acidification of the conditioned media, using an enzyme-linked immunoassay (ELISA) kit specific for human TGF-β1 (G7591 TGF-β1 E_{max} Immunoassay System, Promega Corp., Mandison, WI) (17). Total TGF-β1 was measured after acidifying the media and latent TGF-β1 was defined as total TGF-β1 minus active TGF-β1.

<u>Statistical Analysis</u>

The data presented here are from one of two separate experiments. Both experiments yielded comparable observations. For any given experiment, each data point represents the mean ± standard error of six individual cultures. Data were first analyzed by analysis of variance; when statistical differences were detected, the Student's *t*-test for multiple comparisons using Bonferroni's modification was used. *P*-values < 0.05 were considered to be significant.

Results

<u>Surface Characterization</u>

DCA measurements indicated that PT and SLA have hydrophobic surfaces, with average advancing water contact angles of 96°±4° and 138°±4° respectively. In contrast,

modSLA surface indicated a water contact angle of 0°, which represented an extremely hydrophilic surface.

The complex microstructure of the SLA surface results from the large grit sandblasting process, which produces cavities with an average diameter of 20 to 40 µm, and the acid etch, which produces micropits approximately 0.5-3 µm in diameter [49]. Scanning electron microscopy of the SLA and modSLA surfaces indicated no morphological differences between the two surfaces as a result of storage method (Figure 2-1A,B). Quantitative measurements of surface roughness performed using confocal 3D white light microscopy showed no differences for any of the calculated 3D roughness parameters (S_a, S_q, S_t and S_k) (Table 2-1) between SLA and modSLA surfaces. On PT surfaces, all 3D parameters were less than 50% of those on SLA and modSLA surfaces, indicating that PT was much smoother than microstructured Ti surfaces. The results are proved by SEM image of PT surface (Figure 2-1E).

X-ray photoelectron spectroscopy (XPS) indicated signals of Ti, C and O and traces of N on all SLA, modSLA and PT surfaces. The oxide layer consisted mostly of TiO_2 and suboxides TiO and Ti_2O_3 at the metal/oxide interface of all surfaces. ModSLA surface had higher O and Ti surface concentrations (60.1% and 23%, respectively) in comparison with SLA (50.2% and 14.3%, respectively), and less C (14.9%) than SLA (34.2%), indicating less adsorption of CO_2 and other organic molecules from the atmosphere (Table 2-2). Processing under N_2 protection and storage in sealed containers, thereby insulating modSLA surfaces from the ambient environment explains many of these differences. Taken together, these data showed that novel production protocol increased Ti surface energy without altering surface topography.

Cell Response

When MG63 cells were grown on tissue culture plastic or PT surfaces, they formed a continuous monolayer and individual cells were flat in appearance. On SLA or
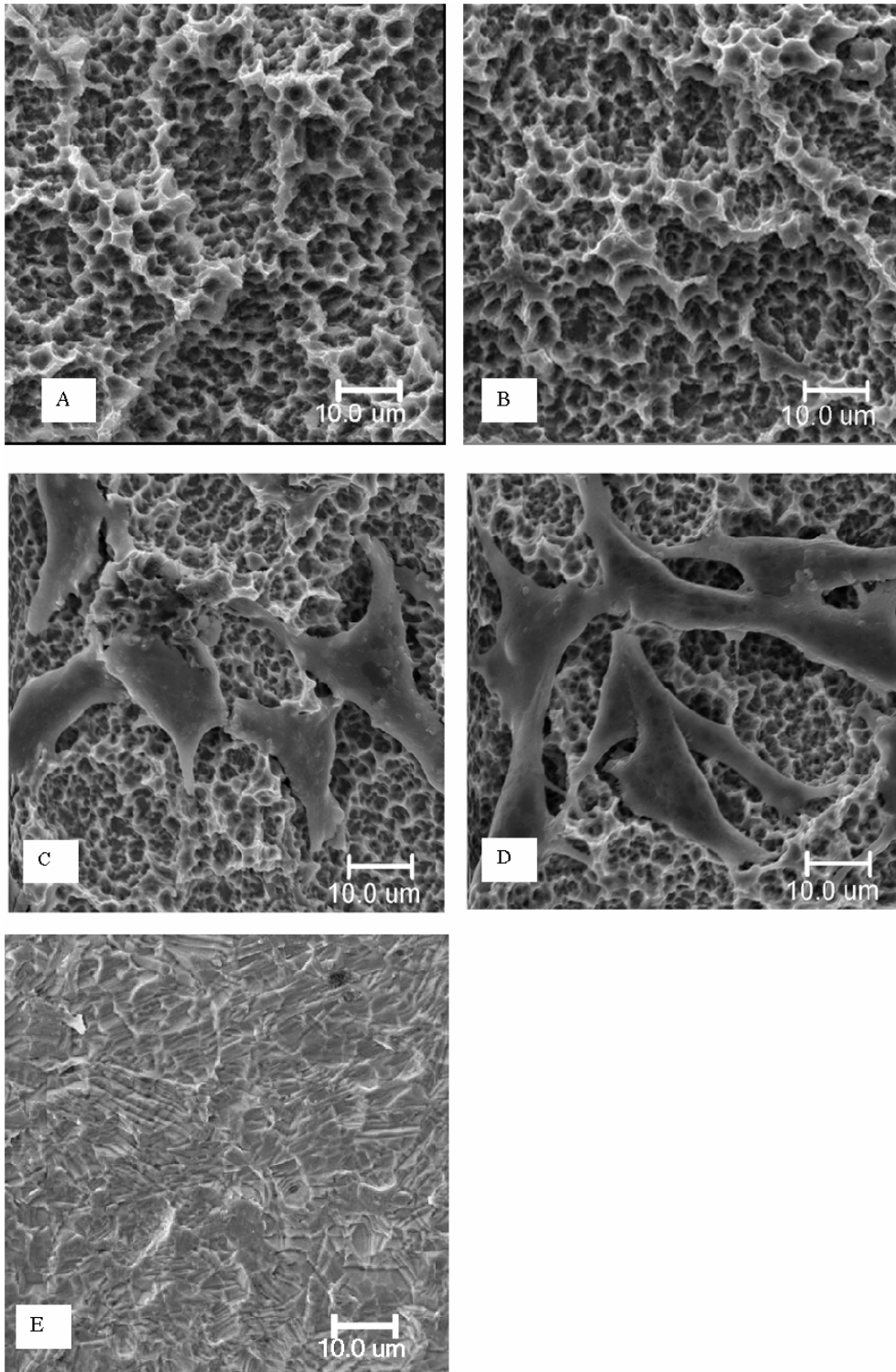
33

Figure 2-1. Morphology of MG63 osteoblast-like cells cultured on SLA and modSLA surfaces. (A) SLA surface. (B) modSLA surface. (C) MG63 cells on SLA. (D) MG63 cells on modSLA. (E) PT surface.

Table 2-1. Characterization of surface roughness. Surface roughness was measured by confocal 3-D white light microscope and parameters were calculated with the use of a Gaussian filter with a cut-off wavelength of 31μm. S_a, arithmetic mean deviation of the surface; S_q, root-mean-square deviation of the surface; S_t, maximum peak-to-valley height of the surface; S_k, amplitude distribution skew. Values are means ± SEM of 10 independent cultures. *$p < 0.05$, v. SLA and modSLA;

Roughness Parameter (μm)	SLA	ModSLA	PT
S_a	1.2 ± 0.04	1.2 ± 0.03	0.6 ± 0.1*
S_q	1.5 ± 0.05	1.5 ± 0.03	0.7 ± 0.1*
S_t	7.9 ± 0.5	7.8 ± 0.3	3.9 ± 0.6*
S_k	4.5 ± 2.3	4.6 ± 2.2	1.8 ± 0.5

Table 2-2. Characterization of surface chemical composition. Surface chemical composition was measured by X-ray photoelectron spectroscopy. Values are means ± SEM of 10 independent cultures. *$p < 0.05$, v. SLA and modSLA; [†]$p < 0.05$, v. SLA; [‡]$p < 0.05$ v. mod SLA.

Chemistry Composition (%)	SLA	modSLA	PT
O	50.2 ± 2.6	60.1 ± 0.7[†]	47.6 ± 1.2[‡]
Ti	14.3 ± 1.4	23.0 ± 1.1[†]	17.9 ± 1.0*
N	1.3 ± 0.3	0.7 ± 0.2[†]	1.2 ± 0.4
C	34.2 ± 2.0	14.9 ± 0.9[†]	29.2 ± 1.5*

Figure 2-2. Effect of surface microstructure and surface energy on differentiation of MG63 osteoblast-like cells regulated by 1α,25(OH)$_2$D$_3$. MG63 cells were cultured on tissue culture plastic (plastic), chemically polished Ti (PT), grit blasted and acid etched Ti (SLA), and modified SLA (modSLA) surfaces. 1α,25(OH)$_2$D$_3$ (10^{-8} and 10^{-9} *M*) or vehicle (Control) were added at confluence and cells were incubated for an additional 24 hours. (A) Cell number was determined 24-hours after cells reached confluence on plastic surfaces. (B) Osteocalcin levels were measured in conditioned media of confluent cultures. (C) Alkaline phosphatase specific activity was measured in cell layer lysates. (D) Alkaline phosphatase specific activity was measured only in isolated cells. Values are means $\pm$ SEM of six independent cultures. Data are from one of two separate experiments, both with comparable results. Data were analyzed by ANOVA and significant differences between groups determined using the Bonferroni's modification of Student's t-test. *$p<0.05$, Ti surfaces v. plastic; #$p<0.05$, 1α,25(OH)$_2$D$_3$ treatment v. control; •$p<0.05$, 10^{-8} *M* 1α,25(OH)$_2$D$_3$ v. 10^{-9} *M* 1α,25(OH)$_2$D$_3$; \$$p<0.05$, modSLA v. SLA surface.
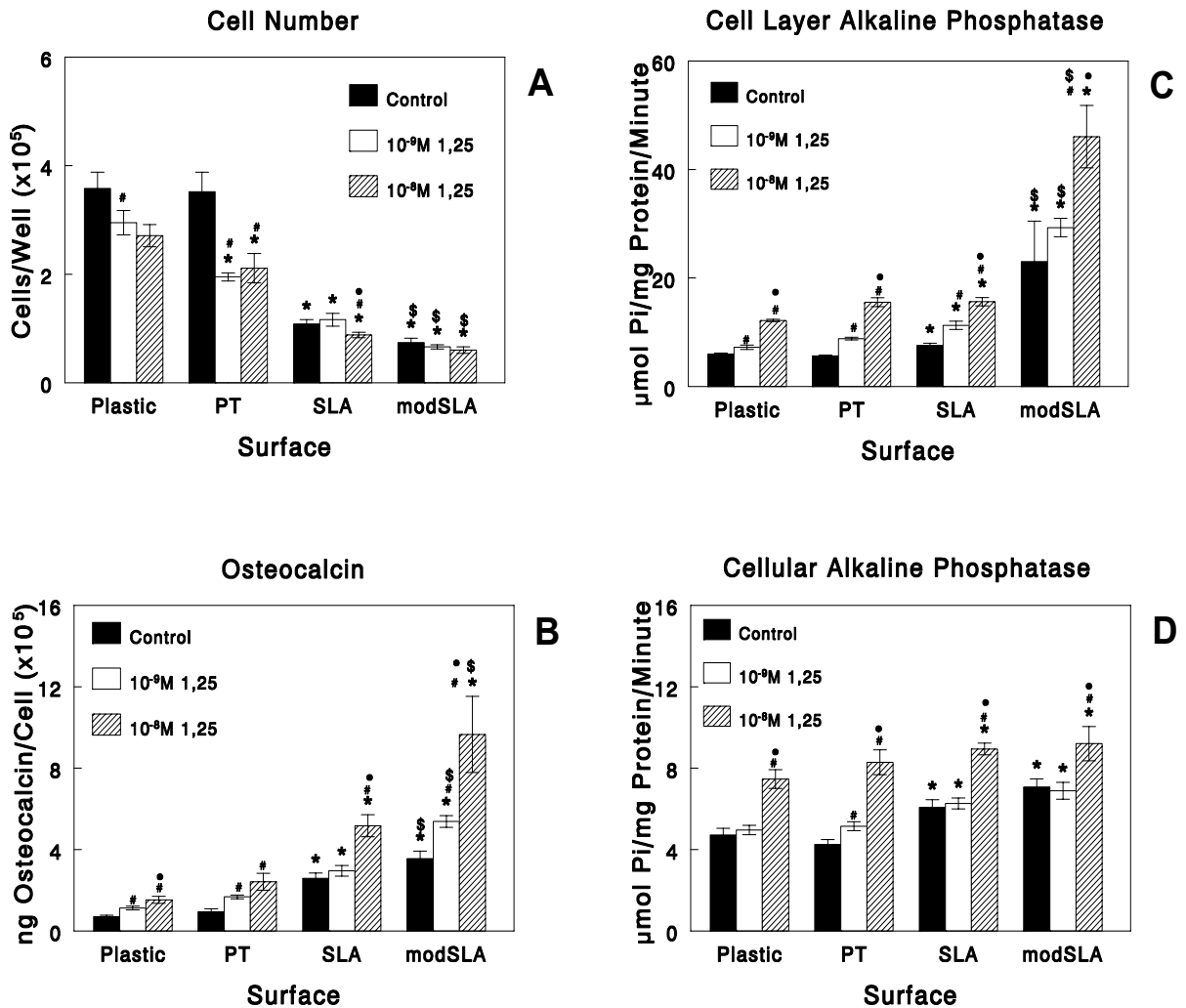
Figure 2-3. Effect of surface microstructure and surface energy on local factor levels of MG63 osteoblast-like cells regulated by $1\alpha,25(OH)_2D_3$. MG63 cells were cultured on tissue culture plastic (plastic), chemically polished Ti (PT), grit blasted and acid etched Ti (SLA), and modified SLA (modSLA) surfaces. $1\alpha,25(OH)_2D_3$ (10^{-8} and 10^{-9} M) or vehicle (Control) were added at confluence and cells were incubated for an additional 24 hours. (A) PGE_2 contents of the conditioned media were determined by RIA. Active TGF-β1 (B) and latent TGF-β1 (C) in the conditioned media were measured using an ELISA kit. Values are means $\pm$ SEM of six independent cultures. Data are from one of two separate experiments, both with comparable results. Data were analyzed by ANOVA and significant differences between groups determined using the Bonferroni's modification of Student's t-test. *$p < 0.05$, Ti surfaces v. plastic; #$p < 0.05$, $1\alpha,25(OH)_2D_3$ treatment v. control; •$p < 0.05$, 10^{-8} M $1\alpha,25(OH)_2D_3$ v. 10^{-9} M $1\alpha,25(OH)_2D_3$; \$$p < 0.05$, modSLA v. SLA surface.

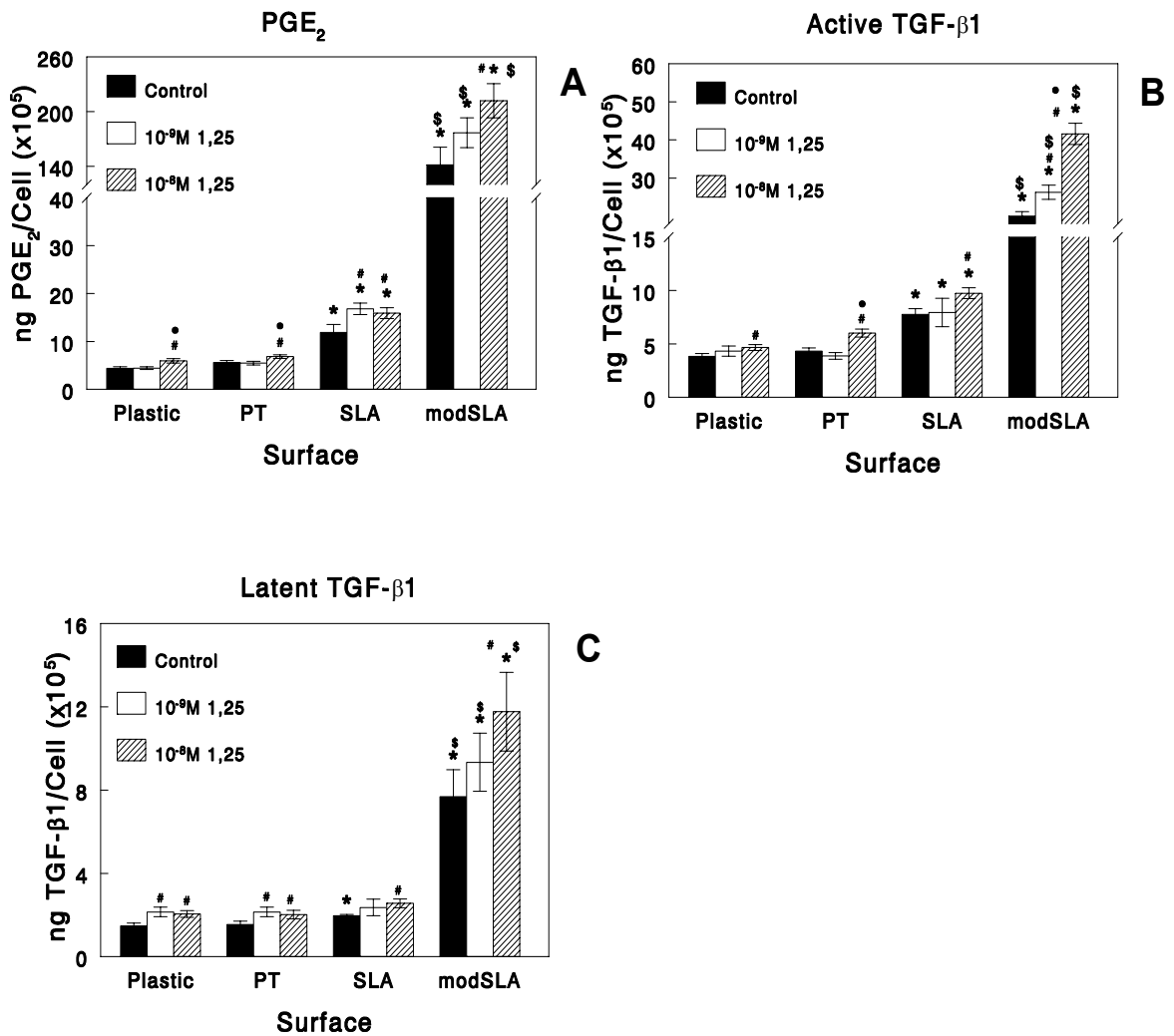modSLA surfaces, they exhibited cuboidal and elongated morphology and cells appeared grow preferentially into the cavities on the surfaces created by sandblasting, forming attachments in the micropits (Fig 2-1C,D). No significant morphological difference was observed between cells grown on SLA or modSLA.

Cell numbers on SLA and modSLA were lower than those on tissue culture plastic or the smooth PT surface and the number of cells on modSLA was 30% less than on SLA (Fig 2-2A). $1\alpha,25(OH)_2D_3$ decreased cell number on smooth surfaces in a dose-dependent manner, significant at 10^{-9} M. The inhibitory effect of $1\alpha,25(OH)_2D_3$ was only evident at 10^{-8} M in cultures grown on SLA and no effect was seen on modSLA.

Increased alkaline phosphatase activity is an early marker of osteoblast differentiation that peaks just before matrix mineralization begins. Activity in cell layer lysates was increased on rough Ti surfaces compared to plastic and PT surfaces, as noted previously [14]. When cells were cultured on modSLA, alkaline phosphatase increased more then 100% over that in cultures grown on SLA (Fig 2-2C). $1\alpha,25(OH)_2D_3$ increased enzyme activity in a dose-dependent manner on all surfaces, and on modSLA, the effect of the hormone was synergistic with the effect of the surface. Enzyme activity in lysates of isolated cells was higher on SLA and modSLA compared to plastic and PT surfaces, indicating that it was sensitive to surface microtopography, but no difference in activity was observed as a function of SLA surface energy (Fig 2-2D). Moreover, $1\alpha,25(OH)_2D_3$ increased activity on all surfaces to a comparable extent.

Surface energy and $1\alpha,25(OH)_2D_3$ treatment also synergistically increased osteocalcin, a late osteoblast differentiation marker (Fig 2-2B). Osteocalcin levels in the conditioned media of control cultures grown on modSLA surfaces were 40% higher than on SLA surfaces. When treated with 10^{-8} M $1\alpha,25(OH)_2D_3$, osteocalcin increased 170% on modSLA compared to 100% increase on SLA.

38

Local factor production was affected as well. In cultures on modSLA, PGE_2 levels in the conditioned media were increased more than 10-fold over those seen in cultures grown on SLA (Fig 2-3A). Treatment with $1\alpha,25(OH)_2D_3$ further increased PGE_2 levels in a synergistic manner.

When MG63 cells were cultured on SLA, we observed an increase in TGF-β1 in the conditioned media as well as in the matrix [50], but we did not discriminate between active and latent growth factor. The present study showed that the amount of active TGF-β1 is specifically increased in the media of cells grown on SLA (Fig 2-3B). Moreover, on modSLA surfaces, active TGF-β1 levels increased 2.5 times compared to those on SLA disks and treatment with $1\alpha,25(OH)_2D_3$ increased active TGF-β1 level in a synergistic manner with surface energy.

Levels of latent TGF-β1 were also affected by the surface energy of the substratum (Fig. 2-3C). The amount of latent growth factor in the conditioned media of MG63 cells grown on modSLA was three times greater than the amount in media from cells grown on SLA. Latent TGF-β1 was regulated by $1\alpha,25(OH)_2D_3$ in a dose-dependent manner but the effect of the hormone was less robust than on active growth factor.

Discussion

The results of this study showed that prevention of rough Ti surfaces from contact with air reduced hydrocarbon contamination and increased hydrophilicity extensively on rough Ti surfaces without changing surface topography. Osteoblast-cells cultured on these cleaner and hydrophilic surfaces produced more differentiation markers represented by increased cell layer alkaline phosphatase specific activity and osteocalcin; and created an osteogenic microenvironment by increasing local factors such as PGE_2, and active and latent TGF-β1 levels.

39

A perfectly clean Ti surface is considered to be composed of only Ti and oxygen, which form a 2-5 nm oxide monolayer on outmost surface, and to be free of any other foreign chemicals. However, these pure surfaces are not available in medical device production or even in the laboratory, because it only takes a few seconds to one minute in atmosphere before the surface is contaminated by a monolayer of hydrocarbons and inorganic impurities [38]. Therefore, protection of Ti surfaces from contact with air is necessary to produce cleaner and well defined surfaces.

In this study, after sandblasting and acid-etching to fabricate rough Ti surfaces, modSLA was rinsed under N_2 protection to be insulated from the surrounding environment, which contains CO_2 and hydrocarbons. This process explains the differences in the chemical composition of SLA and modSLA. A higher carbon contamination was observed on SLA surfaces (34.2%) compared to modSLA surfaces (14.9%), indicating a higher adsorption of CO_2 and other organic molecules from the air. The carbon concentration measured on the SLA surface is consistent with results reported by Massaro [51] on well-cleaned surfaces that were exposed to air for some time. The higher oxygen content of the modSLA surface can be attributed to higher Ti content, which binds oxygen to form the oxide layer (TiO_2 and Ti_2O_3), as well as to the increased hydroxylated/hydrated groups bound to the surface. There was a slight increase in carbon on SLA compared to PT, but overall chemical composition was similar, indicating that contamination but not surface topography is the dominant variable in determining surface chemistry.

Surface topographies were determined both by qualitative SEM imaging and quantitative 3D measurement. Both SLA and modSLA surfaces exhibit wavy macropits of 20-40 μm diameter produced by sandblasting and micropits less than 3 μm produced by acid-etching. Contact profilometry showed that the 2-dimensional (2D) parameter R_a (arithmetic average of center line height) on SLA was approximately 4 μm, and 0.60 μm

40

on PT [19]. The R_a is 3 times higher than corresponding 3D parameter S_a (1.2 µm) on SLA, due to differences in the measurement methods and different resolution as well as scan length and area. The profilometer scanned the whole disk so that the waviness of SLA produced by sandblasting was superimposed on microroughness. In contrast, S_a was calculated from a small area (0.798mm x 0.770mm) and a Gaussian filter with a cut-off wavelength of 31 µm was used to reduce the effect of waviness. Without the interference of waviness, R_a and S_a were the same on the smooth PT surface. Therefore, 3D roughness parameters are more accurate in representing the microtopography sensed by cells.

Sterilizing procedures can also modify surface chemical composition. Steam autoclaving and gamma irradiation decrease surface energy because environmental hydrocarbons react with surface chemical groups activated by these sterilization methods. Plasma cleaning removes contaminants and increases surface energy significantly [38, 42]. However, plasma cleaned surfaces are very active and will react with even trace amounts of environmental impurities. As a result, the purity of gas used for the plasma and interval time between cleaning and storage may bring uncertainties to surface properties. In this study, modSLA surfaces were sterilized by gamma irradiation after storage in a sealed solution in order to prevent further variances generated by sterilization, but SLA surfaces were sterilized by steam autoclaving due to experimental limitations. The difference in sterilizing procedures may also contribute to differences in surface composition thus leading to differences in surface energy between SLA and modSLA.

As reported earlier, cell number decreased on rough Ti surfaces [14] and $1\alpha,25(OH)_2D_3$ inhibited cell proliferation further on smooth surfaces [19]. Compared to SLA, surface hydrophilicity of modSLA decreased cell number by 30%. Cell number reflects cell attachment, adhesion, spreading and proliferation. Cell adhesion is

modulated by a number of variables. On metals, adhesion increases linearly with surface hydrophilicity [52], but polymer enhancement of cell adhesion has been related to hydrophobicity [53]. In these experiments, surfaces were made using different materials and production techniques, and therefore the effect of surface energy could not be separated from surface microarchitecture and chemical composition. Our results showed that with same topography and material, cell number was reversely related to surface energy.

Cell layer alkaline phosphatase activity, which includes enzyme in the cell membrane as well as in alkaline phosphatase enriched extracellular matrix vesicles, was increased 3 times on modSLA compared to SLA. In contrast, cellular alkaline phosphatase activity on modSLA is only 16% higher than that on SLA. These results suggest that enhancement of alkaline phosphatase activity on hydrophilic Ti surfaces is due to production of matrix vesicles, indicating an enhancement of osteoblastic differentiation. Matrix vesicles are extracellular organelles enriched in alkaline phosphatase specific activity and are associated with initial calcification *in vivo* [54]. Therefore, surface hydrophilicity may promote bone mineralization, potentially contributing to more rapid osseointegration in early bone loading [55]. Osteocalcin is the most abundant non-collagenous matrix protein in bone and is associated with bone mineral [56]. Increased osteocalcin together with increased cell layer alkaline phosphatase activity indicates a more differentiated phenotype of osteoblasts cultured on Ti surfaces with higher surface energy.

This study demonstrates for the first time that local factor production is sensitive to surface energy. Prostaglandin produced via cyclooxygenase-1 (Cox-1) and Cox-2, mediates effects of surface topography on MG63 cells [57]. The marked increase in PGE_2 production when cells are grown on substrata with higher surface energy suggests that PGE_2 may play a specific role in the process. A possible mechanism is that

42

increased surface energy alters serum proteins adsorbed on Ti surface, activates certain cell membrane receptors and enhances differentiation.

TGF-β1 is a growth factor that enhances the production of extracellular matrix. It is produced by osteoblasts in latent form and stored in the extracellular matrix as part of a macromolecular complex [17]. We did not measure TGF-β1 in the cell layer, but our previous observations showing increased levels of TGF-β1 in the matrix of MG63 cells grown on SLA [17] suggests the possibility that latent TGF-β1 was differentially stored in the matrix rather than released into the media. $1\alpha,25(OH)_2D_3$ has been shown to regulate expression of latent TGF-β1 binding protein (LTBP1) and the coordinated deposition of the growth factor, its latency associated peptide, and LTBP1 in the extracellular matrix [58, 59]. An alternative explanation is that $1\alpha,25(OH)_2D_3$ regulated the activation of latent TGF-β1 as has been seen in growth plate chondrocyte cultures [59]. The increases in active and latent TGF-β1 on modSLA not only promote matrix production immediately, but also regulate later bone remodeling [16]. This suggests that higher surface energy may result in local production of factors that promote an osteogenic microenvironment.

$1\alpha,25(OH)_2D_3$ has been shown to increase osteoblast differentiation and local factor production synergistically with surface roughness [19] and the effects of surface roughness and $1\alpha,25(OH)_2D_3$ vary with the maturation state of the cells within the osteoblast lineage [60]. The present study shows that growth on a hydroxylated/hydrated TiO_2 substratum with increased surface energy further changes the response of osteoblasts to surface microarchitecture and to regulatory factors like $1\alpha,25(OH)_2D_3$. The results suggest that the hydrophilic surface elicited a more differentiated cellular phenotype that is more sensitive to $1\alpha,25(OH)_2D_3$.

In conclusion, the novel process to protect Ti surface from the surrounding environment during production diminishes hydrocarbon contamination and enhances

surface energy. Osteoblast-cells cultured on these chemically purer and hydrophilic surfaces produced more differentiation markers represented by increased cell layer alkaline phosphatase specific activity and osteocalcin; and created an osteogenic microenvironment by increasing local factors such as PGE_2, and active and latent TGF-$\beta 1$ levels.

References

1. Goldberg VM, Jinno T. The bone-implant interface: a dynamic surface. J Long Term Eff Med Implants 1999; 9: 11-21.

2. Buser D, Schenk RK, Steinemann S, Fiorellini JP, Fox CH, Stich H. Influence of surface characteristics on bone integration of titanium implants. A histomorphometric study in miniature pigs. J.Biomed.Mater.Res. 1991; 25: 889-902.

3. Cooper LF. A role for surface topography in creating and maintaining bone at titanium endosseous implants. J Prosthet Dent 2000; 84: 522-534.

4. Li D, Ferguson SJ, Beutler T, Cochran DL, Sittig C, Hirt HP, Buser D. Biomechanical comparison of the sandblasted and acid-etched and the machined and acid-etched titanium surface for dental implants. J Biomed Mater Res 2002; 60: 325-332.

5. Wennerberg A, Ektessabi A, Albrektsson T, Johansson C, Andersson B. A 1-year follow-up of implants of differing surface roughness placed in rabbit bone. Int.J.Oral Maxillofac.Implants. 1997; 12: 486-494.

6. Klokkevold PR, Nishimura RD, Adachi M, Caputo A. Osseointegration enhanced by chemical etching of the titanium surface. A torque removal study in the rabbit. Clin.Oral Implants.Res 1997; 8: 442-447.

7. Francois P, Vaudaux P, Taborelli M, Tonetti M, Lew DP, Descouts P. Influence of surface treatments developed for oral implants on the physical and biological properties of titanium. (II) Adsorption isotherms and biological activity of immobilized fibronectin. Clin.Oral Implants.Res 1997; 8: 217-225.

8. Deligianni DD, Katsala N, Ladas S, Sotiropoulou D, Amedee J, Missirlis YF. Effect of surface roughness of the titanium alloy Ti-6Al-4V on human bone marrow cell response and on protein adsorption. Biomaterials 2001; 22: 1241-1251.

9. Park JY, Davies JE. Red blood cell and platelet interactions with titanium implant surfaces. Clin.Oral Implants.Res 2000; 11: 530-539.

10. Bowers KT, Keller JC, Randolph BA, Wick DG, Michaels CM. Optimization of surface micromorphology for enhanced osteoblast responses in vitro. Int.J Oral Maxillofac.Implants. 1992; 7: 302-310.

11. Keller JC, Schneider GB, Stanford CM, Kellogg B. Effects of implant microtopography on osteoblast cell attachment. Implant.Dent. 2003; 12: 175-181.

12. Deligianni DD, Katsala ND, Koutsoukos PG, Missirlis YF. Effect of surface roughness of hydroxyapatite on human bone marrow cell adhesion, proliferation, differentiation and detachment strength. Biomaterials 2001; 22: 87-96.

13. Brunette DM. The effects of implant surface topography on the behavior of cells. Int.J Oral Maxillofac.Implants. 1988; 3: 231-246.

14. Martin JY, Schwartz Z, Hummert TW, Schraub DM, Simpson J, Lankford J, Dean DD, Cochran DL, Boyan BD. Effect of Titanium Surface-Roughness on Proliferation, Differentiation, and Protein-Synthesis of Human Osteoblast-Like Cells (Mg63). J.Biomed.Mater.Res. 1995; 29: 389-401.

15. Lohmann CH, Tandy EM, Sylvia VL, Hell-Vocke AK, Cochran DL, Dean DD, Boyan BD, Schwartz Z. Response of normal female human osteoblasts (NHOst) to 17 beta-estradiol is modulated by implant surface morphology. J.Biomed.Mater.Res. 2002; 62: 204-213.

16. Boyan BD, Lossdorfer S, Wang L, Zhao G, Lohmann CH, Cochran DL, Schwartz Z. Osteoblasts generate an osteogenic microenvironment when grown on surfaces with rough microtopographies. Eur.Cell Mater. 2003; 6: 22-27.

17. Kieswetter K, Schwartz Z, Hummert TW, Cochran DL, Simpson J, Dean DD, Boyan BD. Surface roughness modulates the local production of growth factors and cytokines by osteoblast-like MG-63 cells. J.Biomed.Mater.Res. 1996; 32: 55-63.

18. Lossdorfer S, Schwartz Z, Wang L, Lohmann CH, Turner JD, Wieland M, Cochran DL, Boyan BD. Microrough implant surface topographies increase osteogenesis by reducing osteoclast formation and activity. J Biomed Mater Res 2004; 70A: 361-369.

19. Boyan BD, Batzer R, Kieswetter K, Liu Y, Cochran DL, Szmuckler-Moncler S, Dean DD, Schwartz Z. Titanium surface roughness alters responsiveness of MG63 osteoblast-like cells to 1 alpha,25-(OH)(2)D-3. J.Biomed.Mater.Res. 1998; 39: 77-85.

20. Zinger O, Zhao G, Schwartz Z, Simpson J, Wieland M, Landolt D, Boyan B. Differential regulation of osteoblasts by substratum microstructural features. Biomaterials 2005; 26: 1837-1847.

21. Boyan BD, Schwartz Z, Lohmann CH, Sylvia VL, Cochran DL, Dean DD, Puzas JE. Pretreatment of bone with osteoclasts affects phenotypic expression of osteoblast-like cells. J Orthop.Res 2003; 21: 638-647.

22. Perrin D, Szmukler-Moncler S, Echikou C, Pointaire P, Bernard JP. Bone response to alteration of surface topography and surface composition of sandblasted and acid etched (SLA) implants. Clin.Oral Implants.Res. 2002; 13: 465-469.

23. Lim YJ, Oshida Y, Andres CJ, Barco MT. Surface characterizations of variously treated titanium materials. Int.J Oral Maxillofac.Implants. 2001; 16: 333-342.

24. Rupp F, Scheideler L, Rehbein D, Axmann D, Geis-Gerstorfer J. Roughness induced dynamic changes of wettability of acid etched titanium implant modifications. Biomaterials 2004; 25: 1429-1438.

25. Schrader ME. On Adhesion of Biological Substances to Low-Energy Solid-Surfaces. Journal of Colloid and Interface Science 1982; 88: 296-297.

26. Schakenraad JM, Busscher HJ, Wildevuur CR, Arends J. The influence of substratum surface free energy on growth and spreading of human fibroblasts in the presence and absence of serum proteins. J Biomed Mater Res 1986; 20: 773-784.

27. Baier RE, Meyer AE, Natiella JR, Natiella RR, Carter JM. Surface properties determine bioadhesive outcomes: methods and results. J Biomed Mater Res 1984; 18: 327-355.

28. Carew EO, Cooke FW, Lemons JE, Ratner BD, Vesely I, Vogler EA. Surface Properties and Surface Characterization of Materials. In: Biomaterials Science: An Introduction to materials in Medicine: Academic Press; 1996: 40-59.

29. Kilpadi DV, Lemons JE. Surface energy characterization of unalloyed titanium implants. J Biomed Mater Res 1994; 28: 1419-1425.

30. Eriksson C, Nygren H, Ohlson K. Implantation of hydrophilic and hydrophobic titanium discs in rat tibia: cellular reactions on the surfaces during the first 3 weeks in bone. Biomaterials 2004; 25: 4759-4766.

31. Tengvall P, Lundstrom I. Physico-chemical considerations of titanium as a biomaterial. Clin.Mater. 1992; 9: 115-134.

32. Ask M, Lausmaa J, Kasemo B. Preparation and Surface Spectroscopic Characterization of Oxide-Films on Ti6A14V. Applied Surface Science 1989; 35: 283-301.

33. Sundgren JE, Bodo P, Lundstrom I, Berggren A, Hellem S. Auger electron spectroscopic studies of stainless-steel implants. J Biomed Mater Res 1985; 19: 663-671.

34. Hanawa T. [Characterization of surface films formed on titanium in electrolytic solutions]. Shika.Zairyo Kikai 1989; 8: 832-844.

35. Li P, Ohtsuki C, Kokubo T, Nakanishi K, Soga N, de Groot K. The role of hydrated silica, titania, and alumina in inducing apatite on implants. J Biomed Mater Res 1994; 28: 7-15.

36. Brunette DM. Principles of cell behavior on titanium surface and their application to implanted devices. In: Brunette DM, Tengvall P, Textor M, Thomsen P (eds.), Titanium in Medicine. Berlin: Springer; 2001: 485-512.

37. Bumgardner JD, Wiser R, Elder SH, Jouett R, Yang Y, Ong JL. Contact angle, protein adsorption and osteoblast precursor cell attachment to chitosan coatings bonded to titanium. J Biomater.Sci.Polym.Ed 2003; 14: 1401-1409.

38. Kasemo B, Lausmaa J. Biomaterial and implant surfaces: on the role of cleanliness, contamination, and preparation procedures. J Biomed Mater Res 1988; 22: 145-158.

39. MacDonald DE, Deo N, Markovic B, Stranick M, Somasundaran P. Adsorption and dissolution behavior of human plasma fibronectin on thermally and chemically modified titanium dioxide particles. Biomaterials 2002; 23: 1269-1279.

40. Kilpadi DV, Lemons JE, Liu J, Raikar GN, Weimer JJ, Vohra Y. Cleaning and heat-treatment effects on unalloyed titanium implant surfaces. Int.J Oral Maxillofac.Implants. 2000; 15: 219-230.

41. Vezeau PJ, Keller JC, Wightman JP. Reuse of healing abutments: an in vitro model of plasma cleaning and common sterilization techniques. Implant.Dent. 2000; 9: 236-246.

42. Serro AP, Saramago B. Influence of sterilization on the mineralization of titanium implants induced by incubation in various biological model fluids. Biomaterials 2003; 24: 4749-4760.

43. Serro AP, Fernandes AC, Saramago B, Lima J, Barbosa MA. Apatite deposition on titanium surfaces--the role of albumin adsorption. Biomaterials 1997; 18: 963-968.

44. Taborelli M, Jobin M, Francois P, Vaudaux P, Tonetti M, Szmukler-Moncler S, Simpson JP, Descouts P. Influence of surface treatments developed for oral implants on the physical and biological properties of titanium. (I) Surface characterization. Clin.Oral Implants.Res 1997; 8: 208-216.

45. Valagao Amadeu do Serro AP, Fernandes AC, de JV, Norde W. Bovine serum albumin adsorption on titania surfaces and its relation to wettability aspects. J.Biomed.Mater.Res. 1999; 46: 376-381.

46. Garcia AJ, Keselowsky BG. Biomimetic surfaces for control of cell adhesion to facilitate bone formation. Crit Rev.Eukaryot.Gene Expr. 2002; 12: 151-162.

47. Rupp F, Axmann D, Ziegler C, Geis-Gerstorfer J. Adsorption/desorption phenomena on pure and Teflon AF-coated titania surfaces studied by dynamic contact angle analysis. J Biomed Mater Res 2002; 62: 567-578.

48. Martin JY, Dean DD, Cochran DL, Simpson J, Boyan BD, Schwartz Z. Proliferation, differentiation, and protein synthesis of human osteoblast-like cells (MG63) cultured on previously used titanium surfaces. Clinical Oral Implants Research 1996; 7: 27-37.

49. Wieland M, Sittig C, Brunette DM, Textor M, Spencer ND, Davies JE. Measurement and evaluation of the chemical composition and topography of titanium implant surfaces. In: Bone Engineering. Toronto: em squared Inc.; 2004: 163-182.

50. Schwartz Z, Lohmann CH, Sisk M, Cochran DL, Sylvia VL, Simpson J, Dean DD, Boyan BD. Local factor production by MG63 osteoblast-like cells in response to surface roughness and 1,25-(OH)(2)D-3 is mediated via protein kinase C- and protein kinase A-dependent pathways. Biomaterials 2001; 22: 731-741.

51. Massaro C, Baker MA, Cosentino F, Ramires PA, Klose S, Milella E. Surface and biological evaluation of hydroxyapatite-based coatings on titanium deposited by different techniques. J Biomed Mater Res 2001; 58: 651-657.

52. Hallab NJ, Bundy KJ, O'Connor K, Moses RL, Jacobs JJ. Evaluation of metallic and polymeric biomaterial surface energy and surface roughness characteristics for directed cell adhesion. Tissue Eng 2001; 7: 55-71.

53. Lampin M, Warocquier C, Legris C, Degrange M, Sigot-Luizard MF. Correlation between substratum roughness and wettability, cell adhesion, and cell migration. J Biomed Mater Res 1997; 36: 99-108.

54. Boyan BD, Schwartz Z, Swain LD. Matrix vesicles as a marker of endochondral ossification. Connect.Tissue Res 1990; 24: 67-75.

55. Buser D, Broggini N, Wieland M, Schenk RK, Denzer AJ, Cochran DL, Hoffmann B, Lussi A, Steinemann SG. Enhanced Bone Apposition to a Chemically Modified SLA Titanium Surface. J Dent.Res 2004; 83: 529-533.

56. Boskey AL, Gadaleta S, Gundberg C, Doty SB, Ducy P, Karsenty G. Fourier transform infrared microspectroscopic analysis of bones of osteocalcin-deficient mice provides insight into the function of osteocalcin. Bone 1998; 23: 187-196.

57. Boyan BD, Lohmann CH, Sisk M, Liu Y, Sylvia VL, Cochran DL, Dean DD, Schwartz Z. Both cyclooxygenase-1 and cyclooxygenase-2 mediate osteoblast response to titanium surface roughness. J.Biomed.Mater.Res. 2001; 55: 350-359.

58. Bonewald LF. Regulation and regulatory activities of transforming growth factor beta. Crit Rev.Eukaryot.Gene Expr. 1999; 9: 33-44.

59. Pedrozo HA, Schwartz Z, Mokeyev T, Ornoy A, Xin-Sheng W, Bonewald LF, Dean DD, Boyan BD. Vitamin D 3 metabolites regulate LTBP1 and latent TGF-? expression and latent TGF-? incorporation in the extracellular matrix of chondrocytes. J Cell Biochem 1999; 72: 151-165.

60. Lohmann CH, Bonewald LF, Sisk MA, Sylvia VL, Cochran DL, Dean DD, Boyan BD, Schwartz Z. Maturation state determines the response of osteogenic cells to surface roughness and 1,25-dihydroxyvitamin D-3. Journal of Bone and Mineral Research 2000; 15: 1169-1180.

CHAPTER 3. REQUIREMENT FOR BOTH MICROMETER AND SUBMICROMETER SCALE STRUCTURE FOR SYNERGISTIC RESPONSES OF OSTEOBLASTS TO SUBSTRATUM SURFACE ENERGY AND TOPOGRAPHY

Introduction

The surface properties of biomaterials determine the outcome of interactions between biomedical devices and the surrounding host tissue. The important surface properties involved in the process are chemical composition, topography, and energy. We and others have used titanium (Ti) as a model substratum for studying cell and tissue responses to biomaterials because of its clinical relevance, good biocompatibility and adaptability to diverse surface modifications [1-4]. Studies examining the contribution of surface micro-roughness show that differences in surface topography, including roughness, affect fibronectin and albumin adsorption *in vitro* [5], and growth of fibroblasts and osteoblast-like cells in culture [6]. Sandblasted Ti supports stronger osteoblast adhesion [7, 8], related at least in part to altered integrin expression, higher focal contact density and reorganized cytoskeleton of cells on the rough surface [9]. Cells cultured on microrough Ti surfaces also exhibit decreased proliferation and increased differentiation [8, 10]. Moreover, rough Ti surfaces increase osteoblast response to hormones and growth factors, including 1,25-dihydroxyvitamin D_3 [$1\alpha,25(OH)_2D_3$], 17β-estradiol and bone morphogenetic protein [11-13]. On rough Ti surfaces, osteoblasts also generate an osteogenic microenvironment to regulate bone remodeling, represented by releasing local factors to promote osteoblast differentiation and inhibit osteoclast activation [1]. These results are consistent with animal studies showing that Ti implants with greater roughness enhance bone-to-implant contact [14] and increase removal torque forces [15, 16]. Clinical studies demonstrate that the pre-loading integration success rate of acid etched implants is significantly higher than seen

with machined smooth implants [17].

Different surface modifications result in various surface roughness and topographies. For example, sandblasting produces micrometer scale roughness, but acid etching produces sub-micrometer scale roughness. The combination of these two methods results in a complicated three dimensional topography, which is similar to osteoclast resorption pits on bone wafers [18]. Studies using electron micro-machined surfaces show that micrometer scale roughness contributes to cell attachment, spreading and differentiation, and superposition of sub-micrometer scale enhances local factor production [19]. Moreover, osteoblasts are sensitive to the specific structural features of the superimposed roughness, exhibiting a more differentiated phenotype when the surface is created via acid etching rather than by anodic oxidation [20].

Surface energy is another important factor that regulates cell response to biomaterials. Pure Ti spontaneously grows an oxide layer with high surface energy. This oxide surface is hydrophilic because of binding structural water and forming -OH and -O^{2-} groups in its outermost layer. When in contact with electrolyte solutions, a surface film made of phosphate, titanium, calcium and hydroxyl groups spontaneously forms and nucleates an apatitic calcium phosphate layer [21]. Surface energy modulates protein adsorption, which further regulates cell adhesion, cell spreading and proliferation [22]. This can have consequences for the in vivo response to a material. Higher surface energy and increased wettability have been shown to enhance interaction between an implant surface and its biologic environment [23]. When implants with increased hydrophilicity are implanted in bone, the rate and extent of bone formation are increased, supporting the hypothesis that surface energy promotes bone cell maturation and differentiation [24].

While a biomaterial with higher surface energy is bioactive because of its reactive surface, a consequence is that it adsorbs inorganic anions or organic hydrocarbon

50

contaminants from the atmosphere within seconds to one minute. This results in an altered surface chemical composition and decreased hydrophilicity, potentially reducing the biological response. To solve this problem, a new processing method has been developed that retains the high surface energy of the uncontaminated TiO_2 surface by isolating it from contact with atmosphere. This modified sandblasted and acid etched TiO_2 (modSLA) is produced under the continuous protection of nitrogen, stored in isotonic solution and sterilized by gamma irradiation. Studies show that modSLA significantly increases human plasma fibronectin adsorption [25] and promotes osteoblast differentiation and activity in comparison with sandblasted and acid etched surfaces (SLA) produced under standard conditions [26]. In vivo studies show significantly increased bone-to-implant contact and enhanced angiogenesis on modSLA surfaces [27]. In addition, implants with modSLA surfaces provide high removal torque, indicating a higher stability during early stage of osseointegration [28].

The SLA surface has a complex topography consisting of craters varying in diameter from 30 to 100 μm overlaid with micropits varying in diameter from 1-3 μm. The micropits overlay results in an irregular distribution of sharply pointed projections approximately 700 nm in height, but because of the craters, the overall roughness is approximately 4 μm. Surface energy can be affected by roughness [29], but it is not known how surface energy regulates cell responses to different surface roughnesses if chemistry is held constant. To address this, we developed a model in which surface energy was held constant, but we varied surface microstructure. To do this, we prepared acid etched surfaces (A, modA) by the same protocols as are used to produce the acid etch on the SLA and modSLA substrata. These surfaces lacked the morphology generated by grit blasting, but had the same surface chemistry as the SLA and modSLA surfaces. The results of this study show that synergy between surface microtopography and surface energy requires both micrometer and sub-micrometer

51

scale structural features.

Materials and Methods

<u>Substrata</u>

Ti disks were prepared from 1 mm thick sheets of grade 2 unalloyed Ti (ASTM F67 "Unalloyed titanium for surgical implant applications") and supplied to us by Institut Straumann AG (Basel, Switzerland). The disks were punched to be 15 mm in diameter so as to fit snugly into the well of a 24-well tissue culture plate. The methods used to produce the pretreatment (PT), SLA and modSLA surfaces have been reported previously [26]. PT is a smooth Ti surface with arithmetic average of center line heigh (R_a) of 0.2 μm. Sub-micrometer rough A surfaces were produced by treating PT with heated concentrated acid, resulting in an R_a of 830 nm, based on surface profilometry. PT surfaces were also sand blasted and acid etched to produce SLA surfaces with an R_a of 3.2 μm. Prior to use, PT, A, and SLA surfaces were washed in ultrasonic cleaner and sterilized in an oxygen plasma cleaner (PDC-32G, Harrick Plasma, Ithaca, NY). ModA and modSLA surfaces were produced with same mechanical or chemical treatments as A and SLA surfaces, respectively. However, the modA and modSLA surfaces were rinsed under nitrogen protection to prevent exposure to air during procedure, and then stored in a sealed glass tube containing isotonic NaCl solution. These sealed disks were sterilized by gamma irradiation at 25 kGy over night and ready for use.

Previous study showed that this treatment did not alter surface topography and roughness [26, 30]. Instead this modification process changes surface chemical composition by decreasing carbon contamination by more than 50%, thereby retaining a higher surface energy. Rupp et al. [30] have published a detailed analysis of the A, modA, SLA, and modSLA surfaces. Advancing water contact angles were used as an indicator for calculating surface free energy. Both A and SLA are very hydrophobic with

52

water contact angles of 122° and 140°; in contrast, contact angles of modA and modSLA are close to 0°, indicating very hydrophilic surfaces.

<u>Cell Culture</u>

To compare cell responses to different surfaces properties, human osteoblast-like MG63 cells on tissue culture treated polystyrene (plastic) were compared to their morphology on the Ti substrata. MG63 cells were obtained from the American Type Culture Collection (Rockville, MD). The cells were cultured in Dulbecco's modified Eagle medium (DMEM) containing 10% fetal bovine serum (FBS) and 1% penicillin/streptomycin at 37°C in an atmosphere of 5% CO_2 and 100% humidity. Cells were plated at the same density of 10,000 cells/cm^2 tissue culture plastic for all surfaces. Media were exchanged at 24 hours and then every 48 hours until the cells reached confluence on plastic at day 6.

<u>Cell Morphology</u>

Cell morphology on the test surfaces was examined by LEO 1530 scanning electron microscopy (LEO Electron Microscopy, Oberkochen, Germany) at different time points (2, 4, 8 and 24 hours post-seeding and at 3 and 6 days). The cells were fixed with 2.5% glutaraldehyde in cacodylate buffer, dehydrated in a sequential series of ethanol followed by hexamethyl-disilazane, and then coated with gold.

Cell attachment on tissue culture polystyrene (TCPS) and Ti surfaces was evaluated by immunofluorescence staining. Cells were rinsed twice with phosphate buffered saline (PBS), and then fixed for 20 min in 4% paraformaldehyde followed by two PBS rinses. Cells were permeabilized with 0.1% Triton-X100 for 5 min at room temperature followed by two PBS rinses. Non-specific binding sites were blocked with 1% BSA in PBS (BSA/PBS) for 1 h. Cells were first incubated with mouse monoclonal anti-human vinculin antibody (MAB1674, Chemicon, Temecula, CA) (1:100 v/v) for 1 h at room temperature followed by a 1% BSA/PBS wash. The cells were then incubated with

PBS containing rhodamine Red-X goat anti-mouse IgG (1:200 v/v), Alexa Fluor 488 Phalloidin (1:40 v/v) and Hoechst 33342 (1:10,000 v/v) (all from Molecular Probes, Eugene, Oregon) for 30 min, followed by three rinses with 0.05% Tween20/PBS. The Ti disks were mounted on a microscope slide under glass cover slips. The images were taken using a Nikon Eclipse E400 (Nikon Inc., Tokyo, Japan).

Cell Response

Cell number was determined in all cultures 24 hours after cells on tissue culture plastic reached confluence. Cells were released from the surfaces by two sequential incubations in 0.25% trypsin for 10 min at 37°C, in order to assure that any remaining cells were removed from rough TiO_2 surfaces. Released cells were counted using an automatic cell counter (Z1 cell and particle counter, Beckman Coulter, Fullerton, CA). Fewer than 1,000 cells were attached to the plastic surface underlying the Ti disks; therefore, these cells were not separated from total cells released from the disks, nor were they subtracted from the final cell numbers.

We used two determinants of osteoblast differentiation: alkaline phosphatase specific activity [orthophosphoric monoester phosphohydrolase, alkaline; E.C. 3.1.3.1] of cell lysates, and osteocalcin content of the conditioned media. Alkaline phosphatase is an early marker of differentiation and reaches its highest levels as mineralization is initiated. Osteocalcin is a late marker of differentiation and increases as mineral is deposited. Cell lysates were collected by centrifuging the cells after counting. Enzyme activity was assayed by measuring the release of *p*-nitrophenol from *p*-nitrophenylphosphate at pH 10.2 and results were normalized to protein content of the cell lysates [31]. The levels of osteocalcin in the conditioned media were measured using a commercially available radioimmunoassay kit (Human Osteocalcin RIA Kit, Biomedical Technologies, Stoughton, MA) and normalized to cell number, as described previously [11].

54

The conditioned media were also assayed for growth factors and cytokines. Osteoprotegerin (OPG) was measured using enzyme-linked immunosorbent assay (ELISA) kit (DY805 Osteoprotegerin DuoSet, R&D System, Minneapolis, MN). PGE_2 was assessed using a commercially available competitive binding radioimmunoassay kit (NEK020A Prostaglandin E_2 RIA kit, Perkin Elmer, Wellesley, MA). Active TGF-β1 was measured prior to acidification of the conditioned media, using an ELISA kit specific for human TGF-β1 (G7591 TGF-β1 E_{max} Immunoassay System, Promega Corp., Madison, WI). Total TGF-β1 was measured after acidifying the media and latent TGF-β1 was defined as total TGF-β1 minus active TGF-β1 [11].

<u>Statistical Analysis</u>

The data presented here are from one of two separate sets of experiments. Both sets of experiments yielded comparable observations. For any given experiment, each data point represents the mean ± standard error of six individual cultures. Data were first analyzed by analysis of variance; when statistical differences were detected, Student's *t*-test for multiple comparisons using Bonferroni's modification was used. *P*-values < 0.05 were considered to be significant.

Results

The cells exhibited different shapes on PT, A and SLA surfaces. Scanning electron micrographs of the cells on the Ti substrata showed that at two hours after seeding, MG63 cells had become attached with a spherical morphology less than 10μm diameter (Fig. 3-1). Four hours after seeding, cells started to form extensions to explore the surface and the peripheral area of the cells flattened. By eight hours, the cells had become spread and had morphologies similar to those reaching confluence on plastic.

Kinetic immunofluorescence micrographs (Fig. 3-2) confirmed these observations and provided information concerning the cytoskeleton of the cells during attachment and

spreading. Cells changed shape as a function of time following attachment in a surface dependent manner. Two hours after seeding, the cells had a round morphology on all surfaces except PT. Most cells exhibited one or two red spots with strong intensity, representing vinculin accumulations at the beginning of cell attachment. Actin was not distributed evenly in the cells; instead most of the actin was assembled at one side of the nucleus. At four hours after seeding, the cells on relatively smooth surfaces (TCPS, PT and A) had begun to spread. Cells on the rough SLA surfaces were beginning to form lamellipodia, but not to the same extent as seen on smooth surfaces. In contrast, MG63 cells on high energy surfaces (modA and modSLA) did not exhibit significant shape changes at 4 h. At 8 hours
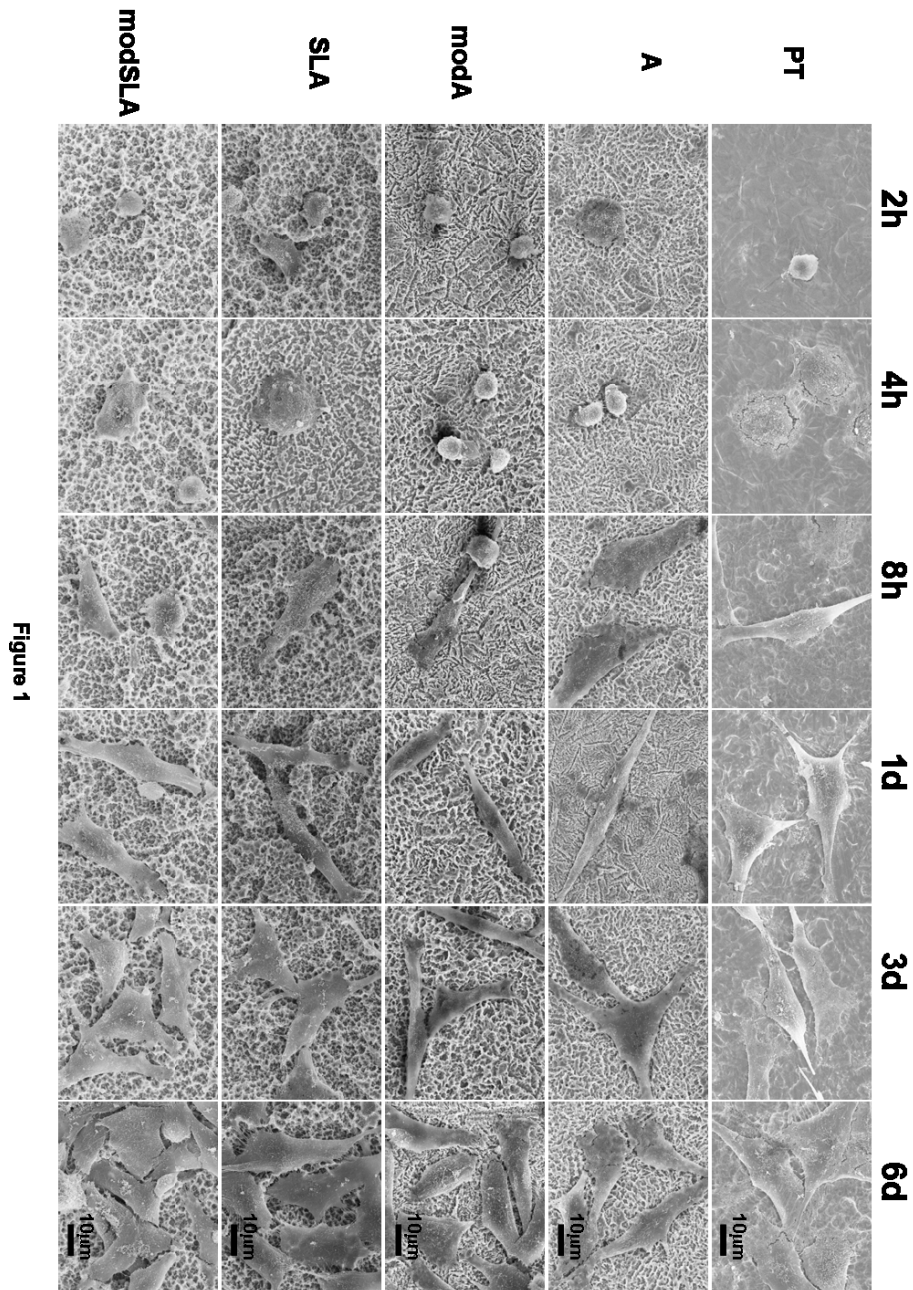
Figure 3-1. Morphology of MG63 osteoblast-like cells cultured on Ti surfaces. MG63 cells were grown on PT, A, modA, SLA and modSLA surfaces for 2 h, 4 h, 8 h, 1 d, 3 d and 6 d and their morphology imaged by scanning electron microscopy. Areas of lower cell density were selected to facilitate observation of individual cell shapes. The images of the cells shown in the selected micrographs are typical of cells throughout the culture.

Figure 3-2. Immunofluorescent staining of MG63 cells cultured on tissue culture

polystyrene (TCPS) and Ti surfaces. MG63 cells were seeded on TCPS, PT, A, modA, SLA and modSLA surfaces for 2, 4, 8, and 24 hours. Cells were stained for vinculin (red), actin (green) and nucleus (blue). The yellow color represents the co-localization of vinculin and actin. Scale bar = 20µm.
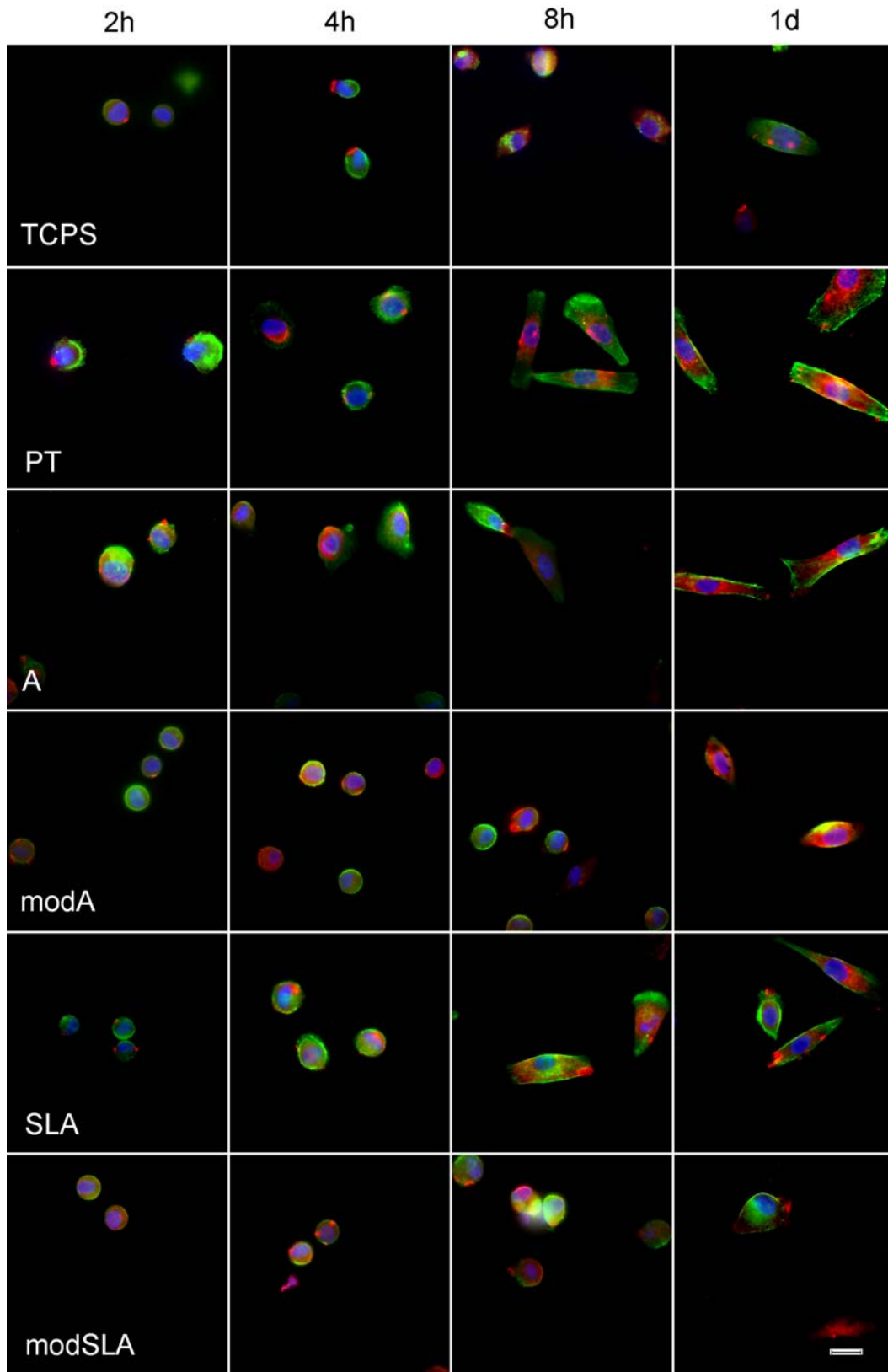
Figure 3-3. Effect of surface microstructure and surface energy on cell number. MG63 cells were cultured on tissue culture polystyrene (plastic), PT, A, mod A, SLA and modSLA surfaces. Cell number was determined 24-hours after cells reached confluence on plastic surfaces. Values are means $\pm$ SEM of six independent cultures. Data are from one of two separate experiments, both with comparable results. Data were analyzed by ANOVA and significant differences between groups determined using the Bonferroni modification of Student's t-test. *$p<0.05$, Ti surfaces v. plastic; #$p<0.05$, v. PT; •$p<0.05$, v. SLA surface.

A

Alkaline Phosphatase Activity

B

Osteocalcin
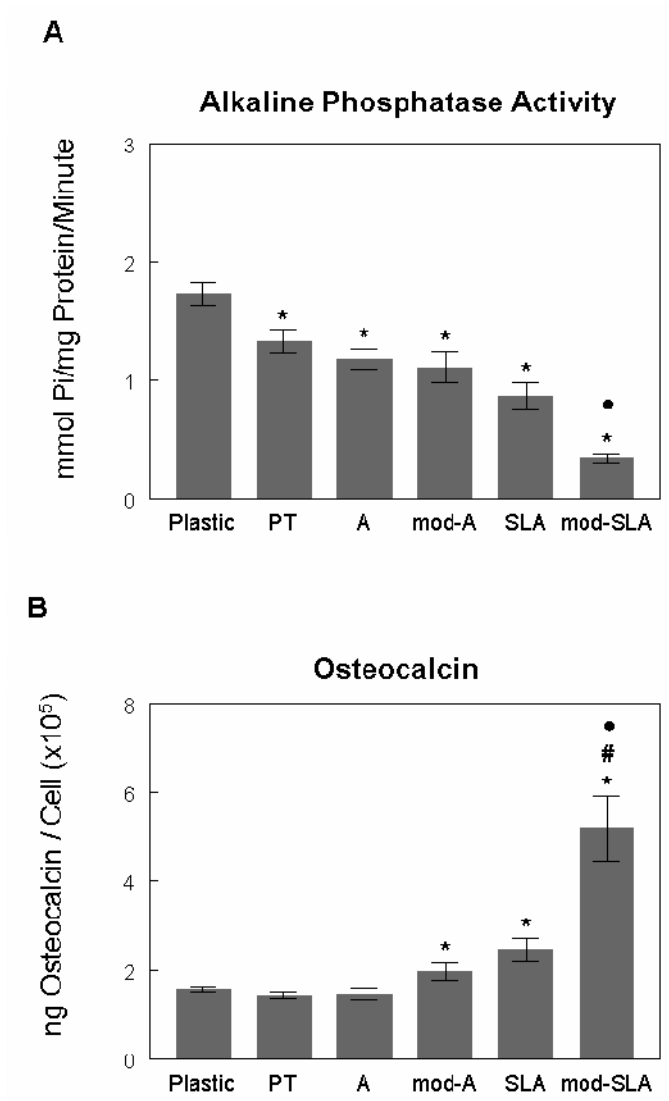
Figure 3-4. Effect of surface microstructure and surface energy on cell differentiation. MG63 cells were cultured on tissue culture polystyrene (plastic), PT, A, mod A, SLA and modSLA surfaces. (A) Alkaline phosphatase specific activity was measured in isolated cells. (B) Osteocalcin levels were measured in conditioned media of confluent cultures. Values are means $\pm$ SEM of six independent cultures. Data are from one of two separate experiments, both with comparable results. Data were analyzed by ANOVA and significant differences between groups determined using the Bonferroni modification of Student's t-test. *$p<0.05$, Ti surfaces v. plastic; #$p<0.05$, v. A; •$p<0.05$, v. SLA surface.
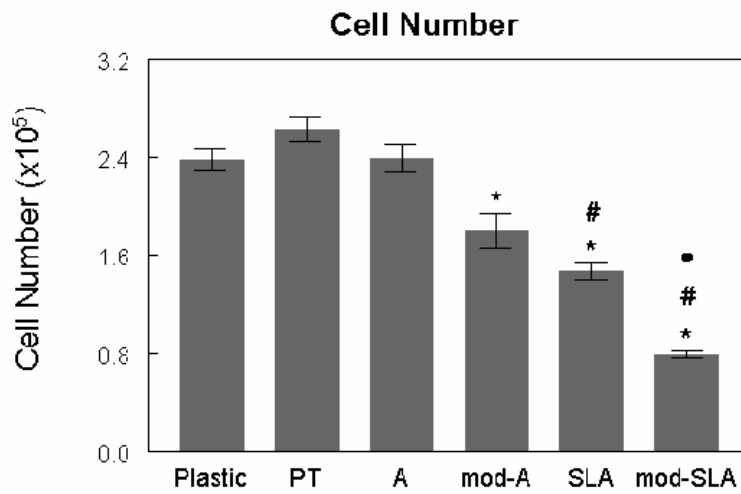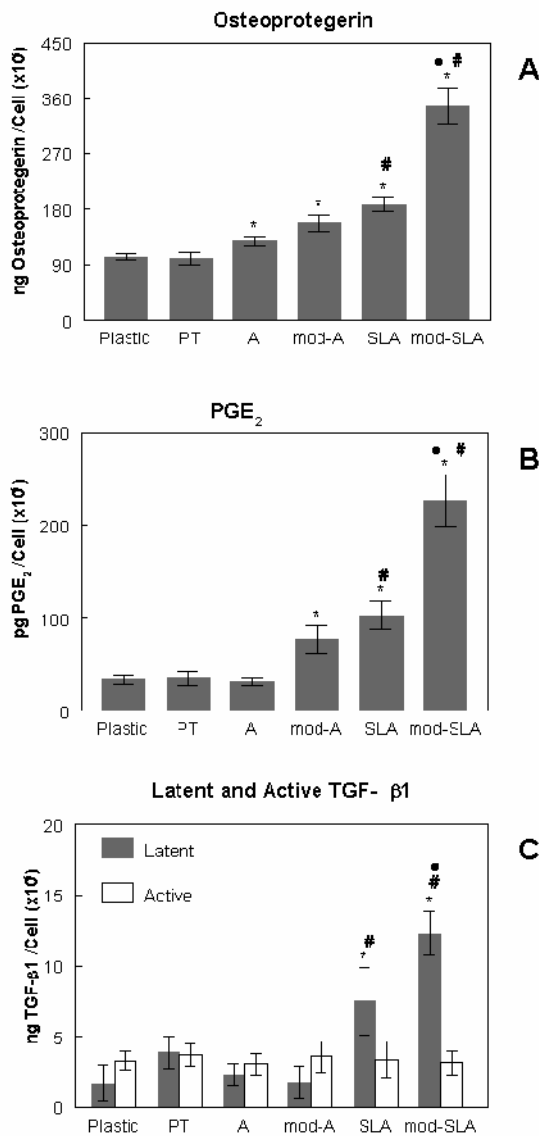
Figure 3-5. Effect of surface microstructure and surface energy on local factor levels. MG63 cells were cultured on tissue culture polystyrene (plastic), PT, A, mod A, SLA and modSLA surfaces. (A) Osteoprotegerin levels of conditioned media were determined by ELISA kit. (B) PGE_2 contents of the conditioned media were determined by RIA. Active TGF-β1 and latent TGF-β1 (C) in the conditioned media were measured using an ELISA kit. Values are means ± SEM of six independent cultures. Data are from one of two separate experiments, both with comparable results. Data were analyzed by ANOVA and significant differences between groups determined using the Bonferroni modification of Student's t-test. *$p < 0.05$, Ti surfaces v. plastic; #$p < 0.05$, v. A; •$p < 0.05$, v. SLA surface.

after seeding, cells on PT, A and SLA continued to spread and exhibited a bi-polar or spindle-like shape through the first 24 hours. The spreading of cells on high energy surfaces (modA and modSLA) was slower than seen on hydrophobic surfaces. Because of surface roughness, part of the image on the SLA and modSLA surfaces were out of the plane of focus.

Scanning electron microscopy was also able to discern substratum-dependent differences in the shape of individual cells in higher density cultures (Fig. 3-1), which could not be resolved using immunofluorescence. Cells increased in number on all surfaces between days 1 to 6. MG63 cells on PT surfaces in general were flat and had two or three major extensions. On A and modA, the cells were elongated and formed spindle-like shapes. On SLA and modSLA, the cells were polygonal in shape with many thin filopodia attached to the surfaces.

After 6 days of in vitro culture, the MG63 cells reached confluence on plastic surfaces. Cell number on PT and A surfaces were the same as those on tissue culture plastic, indicating that sub-micrometer roughness on flat Ti surface had no effect on cell number (Fig. 3-3). Cell number on the SLA surface, which presents a combination of micrometer and sub-micrometer structures, decreased by 44% compared to smooth PT. By comparing modA and A surfaces, high surface energy decreased cell number by 25%. However, in the presence of a complicated three dimensional topography like SLA, higher surface energy decreased cell number by almost 50%.

Cells cultured on all Ti surfaces exhibited decreased alkaline phosphatase activity compared to those on plastic (Fig. 3-4A). Although the enzyme activity of cells on SLA was 30% less than that on PT, there was no statistical difference among PT, A, modA and SLA surfaces. With higher surface energy on modSLA, enzyme activity was 60% lower than on SLA.

Osteocalcin levels in cultures grown on PT and A were the same as on plastic (Fig. 3-4B). With high surface energy on sub-micrometer scale roughness, osteocalcin levels in cultures grown on modA increased by 30% compared with cultures grown on A. The micrometer roughness of SLA increased osteocalcin by 70% compared to A. There was as strong synergistic effect between surface energy and roughness. The combination of high surface energy and micrometer scale roughness enhanced osteocalcin by more than 250%.

Local factors were also regulated by surface properties. OPG levels increased on all Ti surfaces except smooth PT (Fig. 3-5A). OPG in the conditioned media of cells grown on modA was slightly higher (20%) than on A, but the difference is not statistically significant. Compared with cultures grown on A, OPG on SLA increased 50% with statistic significance. The amount of OPG was almost doubled on modSLA surfaces, showing a synergistic effect of surface high energy and micrometer structure on osteoprotegerin production. PGE_2 was affected in a similar manner (Fig. 3-5B). The degree of PGE_2 enhancement on modSLA (600%) was more than the combination of the increase on modA (100%) and SLA (200%). Active TGF-β1 was unaffected by the surface. However, latent TGF-β1 was modulated in a surface-specific manner, with a 120% increase on SLA and a 330% increase on modSLA. Moreover, latent TGF-β1 levels in conditioned media of cells cultured on modSLA was 65% greater than in the media of cells grown on SLA.

Discussion

The results of this study show that high surface energy is an important variable but by itself it is insufficient to cause marked increases in osteoblast responses to Ti substrata with low surface roughness. In contrast, when substrata with complex micrometer scale and sub-micrometer scale roughness are fabricated to retain the high

64

surface energy of uncontaminated TiO_2, the cells exhibit synergistic enhancement of their response to the surface topography alone. This includes reduced cell number together with increased differentiation and release of factors into the media that stimulate osteogenesis and reduce osteoclastic activity.

Scanning electron microscopic analysis and immunofluorescence of cell morphology identified significant differences in cell shape as a function of both surface chemistry and surface topography, confirming our previous work and the work of others [32, 33]. Immunofluorescence images of MG63 cells over the first 24 hours after seeding demonstrated that osteoblasts on smooth and low energy surfaces spread faster than those on rough and higher energy surfaces. Scanning electron micrographs showed that differences in cell shape were retained even after cell density increased. MG63 cells on PT surfaces, like those on plastic, in general were flat and had two or three major extensions. On A and modA, the cells were elongated and formed spindle like shape; on SLA and modSLA, the cells were polygonal in shape with many thin filopodia to attach to the surfaces.

The observation that osteoblasts grown on smooth Ti surface had fewer cytoplasmic extensions than cells grown on micrometer and sub-micrometer structured surfaces, is consistent with previous findings [8, 34]. Although both A and SLA surfaces had similar 1-2 μm pits produced by acid etching, the MG63 cells grown on SLA extended many more filopodia to attach themselves to the substrata. This suggests that the cells not only sense direct focal contacts with the substratum, but they also respond to the broader waviness created by sand blasting. Others have reported comparable effects of surface topography on epithelial cells [35], suggesting that this is a general property of cell interactions with surface microarchitecture.

Our results confirmed our previous findings that sub-micrometer scale roughness, while contributing to the overall response of the cells, is not a major determinant of cell

behavior in the absence of the larger craters [20]. In the present study, with the exception of OPG production, growth on A did not alter osteoblast number, differentiation or local factor levels to any great extent in comparison with growth on the PT surface. However, in combination with micrometer scale roughness, typified by SLA, there were significant increases in local factor levels to produce an osteogenic environment [20]. This phenomenon may be due to interference between surface topography and surface energy. The potential effect of sub-micrometer scale roughness is counteracted by lower surface energy. Other researchers have observed that osteoblasts grown on nano-textured surfaces express higher osteopontin and bone sialoprotein [36]. Full characterization of surface energy along with surface roughness is necessary to understand cell/substratum interactions.

Our results show a strong synergistic effect between micrometer scale roughness and surface energy. When MG63 cells were grown on A and modA substrata, the increase in surface energy had no effect on alkaline phosphatase activity or latent TGF-β1 levels, and only a small increase in osteocalcin or PGE$_2$. In contrast, when the surface presented a complicated micrometer scale roughness, increased surface energy greatly decreased cell number and enhanced cell differentiation by more than 100%. Both modA and modSLA were produced using the same acid etching procedure to ensure the same surface chemistry. Therefore the differences observed in the cell response were only dependent on micrometer scale roughness. We did not include modified PT substrata to examine the effect of high surface energy on a relatively smooth surface because PT surfaces were mechanically machined and chemically degreased, resulting in a final modified PT surface chemistry that would be different from modA or modSLA.

It is likely that the differential response of MG63 cells to surface roughness and topography reflects differences in integrin mediated signaling. Cells respond to

biomaterial surfaces through interaction between plasma membrane receptor integrins and adsorbed extracellular matrix proteins including fibronectin [37]. Protein adsorption is highly influenced by surface chemistry, hydrophilicity and topography; small proteins tend to adsorb on hydrophobic surfaces, but large proteins are less affected by surface wettability [38]. In addition, proteins adsorbed onto hydrophobic surfaces are more sensitive to unfolding and denaturing processes due to electrostatic forces between the surface and cells. Thus, fibronectin fragments adsorb faster on hydrophobic $-CH_3$ surfaces, but lack cell adhesion activity [39]. Protein adsorption also depends on the scale of surface roughness. Nano scale surface texture seems have little to no effect on protein adsorption and cell proliferation [40]. However, microrough surfaces adsorb more fibronectin and the protein orientation is different from that on machined smooth Ti, which further alters integrin adhesion. In addition, the profile of integrin expression in osteoblasts is sensitive to surface roughness [9]. These findings indicate cell behavior is not determined by a single surface feature, but is in response to combinations of different surface properties as a whole.

Previous studies show that osteoblasts grown on microrough surfaces produce an osteogenic environment to promote osteoblast differentiation by paracrine and autocrine pathways [1]. Our results suggest that the increase in the rate and extent of peri-implant bone formation seen with modSLA implants *in vivo* [27] reflects enhanced osteogenesis as well. Osteocalcin levels were increased whereas alkaline phosphatase specific activity was decreased, indicative of mature secretory osteoblasts [41]. PGE_2, which is necessary for osteoblastic differentiation [1], was also increased. Interestingly, levels of OPG, a local factor produced by osteoblasts that reduces osteoblast-dependent activation of osteoclasts [42], were higher as well. These results indicate that the increase of OPG on modSLA surfaces plays an important role in controlling osteoclast

67

differentiation in bone remodeling cycle, and contributes to early upregulation of bone to implant contact [27].

TGF-β1 also reduces osteoclast activity [43] and increases osteoblast differentiation [44]. We previously showed that cells grown on SLA deposit more TGF-β1 in their extracellular matrix than do cells grown on smooth Ti [45], and cells grown on modSLA release increased levels of latent TGF-β1 into their media than do cells grown on SLA. In the present study, we also found higher levels of latent growth factor in the conditioned media of cells grown on SLA and this was further increased when cells were cultured on modSLA. This suggests that cells on the more reactive surface are producing a larger reservoir of growth factors on high energy surfaces that can be used downstream to control osteoclast formation and activity.

In summary, this study examined the independent effect of surface roughness and surface energy by applying a modification technique to eliminate hydrophobic surface contamination and retain a high surface energy. Osteoblast-like cells cultured on higher energy surfaces exhibit a more differentiated phenotype and produce more local factors to regulate osteoblast and osteoclast activity. The combination of micrometer scale roughness and high surface energy synergistically promotes osteoblast responses. The results suggest that surface energy is an important factor in mediating cell-substratum interactions, and higher surface energy should be incorporated in biomaterial design to improve the host tissue response.

References

1. Boyan BD, Lossdorfer S, Wang L, Zhao G, Lohmann CH, Cochran DL, Schwartz Z. Osteoblasts generate an osteogenic microenvironment when grown on surfaces with rough microtopographies. Eur.Cell Mater. 2003; 6: 22-27.
2. Pohler OE. Unalloyed titanium for implants in bone surgery. Injury 2000; 31 Suppl 4: 7-13.

3. Cooper LF. A role for surface topography in creating and maintaining bone at titanium endosseous implants. J Prosthet Dent 2000; 84: 522-534.

4. Puleo DA, Nanci A. Understanding and controlling the bone-implant interface. Biomaterials 1999; 20: 2311-2321.

5. Francois P, Vaudaux P, Taborelli M, Tonetti M, Lew DP, Descouts P. Influence of surface treatments developed for oral implants on the physical and biological properties of titanium. (II) Adsorption isotherms and biological activity of immobilized fibronectin. Clin.Oral Implants.Res 1997; 8: 217-225.

6. Harris LG, Patterson LM, Bacon C, Gwynn I, Richards RG. Assessment of the cytocompatibility of different coated titanium surfaces to fibroblasts and osteoblasts. J.Biomed.Mater Res.A 2005; 73: 12-20.

7. Keller JC, Schneider GB, Stanford CM, Kellogg B. Effects of implant microtopography on osteoblast cell attachment. Implant.Dent. 2003; 12: 175-181.

8. Martin JY, Schwartz Z, Hummert TW, Schraub DM, Simpson J, Lankford J, Dean DD, Cochran DL, Boyan BD. Effect of Titanium Surface-Roughness on Proliferation, Differentiation, and Protein-Synthesis of Human Osteoblast-Like Cells (Mg63). J.Biomed.Mater.Res. 1995; 29: 389-401.

9. Raz P, Lohmann CH, Turner J, Wang L, Poythress N, Blanchard C, Boyan BD, Schwartz Z. 1alpha,25(OH)2D3 regulation of integrin expression is substrate dependent. J Biomed Mater Res A 2004; 71A: 217-225.

10. Brunette DM. The effects of implant surface topography on the behavior of cells. Int.J Oral Maxillofac.Implants. 1988; 3: 231-246.

11. Boyan BD, Batzer R, Kieswetter K, Liu Y, Cochran DL, Szmuckler-Moncler S, Dean DD, Schwartz Z. Titanium surface roughness alters responsiveness of MG63 osteoblast-like cells to 1 alpha,25-(OH)(2)D-3. J.Biomed.Mater.Res. 1998; 39: 77-85.

12. Ong JL, Carnes DL, Cardenas HL, Cavin R. Surface roughness of titanium on bone morphogenetic protein-2 treated osteoblast cells in vitro. Implant.Dent. 1997; 6: 19-24.

13. Lohmann CH, Tandy EM, Sylvia VL, Hell-Vocke AK, Cochran DL, Dean DD, Boyan BD, Schwartz Z. Response of normal female human osteoblasts (NHOst) to 17 beta-estradiol is modulated by implant surface morphology. J.Biomed.Mater.Res. 2002; 62: 204-213.

14. Buser D, Schenk RK, Steinemann S, Fiorellini JP, Fox CH, Stich H. Influence of surface characteristics on bone integration of titanium implants. A histomorphometric study in miniature pigs. J.Biomed.Mater.Res. 1991; 25: 889-902.

15. Wennerberg A, Ektessabi A, Albrektsson T, Johansson C, Andersson B. A 1-year follow-up of implants of differing surface roughness placed in rabbit bone. Int.J.Oral Maxillofac.Implants. 1997; 12: 486-494.

16. Klokkevold PR, Nishimura RD, Adachi M, Caputo A. Osseointegration enhanced by chemical etching of the titanium surface. A torque removal study in the rabbit. Clin.Oral Implants.Res 1997; 8: 442-447.

17. Khang W, Feldman S, Hawley CE, Gunsolley J. A multi-center study comparing dual acid-etched and machined-surfaced implants in various bone qualities. J.Periodontol. 2001; 72: 1384-1390.

18. Boyan BD, Schwartz Z, Lohmann CH, Sylvia VL, Cochran DL, Dean DD, Puzas JE. Pretreatment of bone with osteoclasts affects phenotypic expression of osteoblast-like cells. J Orthop.Res 2003; 21: 638-647.

19. Zinger O, Zhao G, Schwartz Z, Simpson J, Wieland M, Landolt D, Boyan B. Differential regulation of osteoblasts by substrate microstructural features. Biomaterials 2005; 26: 1837-1847.

20. Zhao G, Zinger O, Schwartz Z, Wieland M, Landolt D, Boyan BD. Osteoblast-like cells are sensitive to submicron-scale surface structure. Clin.Oral Implants Res. 2006; 17: 258-264.

21. Li P, Ohtsuki C, Kokubo T, Nakanishi K, Soga N, de Groot K. The role of hydrated silica, titania, and alumina in inducing apatite on implants. J Biomed Mater Res 1994; 28: 7-15.

22. Kennedy SB, Washburn NR, Simon CG, Jr., Amis EJ. Combinatorial screen of the effect of surface energy on fibronectin-mediated osteoblast adhesion, spreading and proliferation. Biomaterials 2006; 27: 3817-3824.

23. Baier RE, Meyer AE, Natiella JR, Natiella RR, Carter JM. Surface properties determine bioadhesive outcomes: methods and results. J Biomed Mater Res 1984; 18: 327-355.

24. Eriksson C, Nygren H, Ohlson K. Implantation of hydrophilic and hydrophobic titanium discs in rat tibia: cellular reactions on the surfaces during the first 3 weeks in bone. Biomaterials 2004; 25: 4759-4766.

25. Scheideler L, Rupp F, Wieland M, Geis-Gerstorfer J. Storage Conditions of Titanium Implants Influence Molecular and Cellular Interactions. In: 83rd General Session and Exhibition of the International Association for Dental Research; Baltimore, MD.

26. Zhao G, Schwartz Z, Wieland M, Rupp F, Geis-Gerstorfer J, Cochran DL, Boyan BD. High surface energy enhances cell response to titanium substrate microstructure. J.Biomed.Mater Res.A 2005; 74: 49-58.

27. Buser D, Broggini N, Wieland M, Schenk RK, Denzer AJ, Cochran DL, Hoffmann B, Lussi A, Steinemann SG. Enhanced Bone Apposition to a Chemically Modified SLA Titanium Surface. J Dent.Res 2004; 83: 529-533.

28. Ferguson SJ, Broggini N, Wieland M, de WM, Rupp F, Geis-Gerstorfer J, Cochran DL, Buser D. Biomechanical evaluation of the interfacial strength of a chemically modified sandblasted and acid-etched titanium surface. J.Biomed.Mater Res.A 2006; 78: 291-297.

29. Rupp F, Scheideler L, Rehbein D, Axmann D, Geis-Gerstorfer J. Roughness induced dynamic changes of wettability of acid etched titanium implant modifications. Biomaterials 2004; 25: 1429-1438.

30. Rupp F, Scheideler L, Olshanska N, de Wild M, Wieland M, Geis-Gerstorfer J. Enhancing surface free energy and hydrophilicity through chemical modification of microstructured titanium implant surfaces. J.Biomed.Mater Res.A 2006; 76: 323-334.

31. Bretaudiere JP, Spillman T, Bergmeyer HU. Alkaline phosphatases. In: Methods of Enzymatic Analysis. Weinheim, Germany: Verlag Chemica; 1984: 75-92.

32. Ismail FS, Rohanizadeh R, Atwa S, Mason RS, Ruys AJ, Martin PJ, Bendavid A. The influence of surface chemistry and topography on the contact guidance of MG63 osteoblast cells. J.Mater Sci.Mater Med. 2006.

70

33. Goto T, Yoshinari M, Kobayashi S, Tanaka T. The initial attachment and subsequent behavior of osteoblastic cells and oral epithelial cells on titanium. Biomed.Mater Eng 2004; 14: 537-544.

34. Zhu X, Chen J, Scheideler L, Altebaeumer T, Geis-Gerstorfer J, Kern D. Cellular reactions of osteoblasts to micron- and submicron-scale porous structures of titanium surfaces. Cells Tissues.Organs 2004; 178: 13-22.

35. Di CM, Toto P, Feliciani C, Scarano A, Tulli A, Strocchi R, Piattelli A. Spreading of epithelial cells on machined and sandblasted titanium surfaces: an in vitro study. J.Periodontol. 2003; 74: 289-295.

36. de Oliveira PT, Nanci A. Nanotexturing of titanium-based surfaces upregulates expression of bone sialoprotein and osteopontin by cultured osteogenic cells. Biomaterials 2004; 25: 403-413.

37. Degasne I, Basle MF, Demais V, Hure G, Lesourd M, Grolleau B, Mercier L, Chappard D. Effects of roughness, fibronectin and vitronectin on attachment, spreading, and proliferation of human osteoblast-like cells (Saos-2) on titanium surfaces. Calcif Tissue Int 1999; 64: 499-507.

38. Sigal GB, Mrksich M, Whitesides GM. Effect of surface wettability on the adsorption of proteins and detergents. Journal of the American Chemical Society 1998; 120: 3464-3473.

39. Michael KE, Vernekar VN, Keselowsky BG, Meredith JC, Latour RA, Garcia AJ. Adsorption-induced conformational changes in fibronectin due to interactions with well-defined surface chemistries. Langmuir 2003; 19: 8033-8040.

40. Cai K, Bossert J, Jandt KD. Does the nanometre scale topography of titanium influence protein adsorption and cell proliferation? Colloids Surf.B Biointerfaces. 2006; 49: 136-144.

41. Stein GS, Lian JB, Owen TA. Relationship of cell growth to the regulation of tissue-specific gene expression during osteoblast differentiation. FASEB J. 1990; 4: 3111-3123.

42. Lacey DL, Timms E, Tan HL, Kelley MJ, Dunstan CR, Burgess T, Elliott R, Colombero A, Elliott G, Scully S, Hsu H, Sullivan J, Hawkins N, Davy E, Capparelli C, Eli A, Qian YX, Kaufman S, Sarosi I, Shalhoub V, Senaldi G, Guo J, Delaney J, Boyle WJ. Osteoprotegerin ligand is a cytokine that regulates osteoclast differentiation and activation. Cell 1998; 93: 165-176.

43. Bonewald LF, Mundy GR. Role of transforming growth factor-beta in bone remodeling. Clin.Orthop.Relat Res. 1990: 261-276.

44. Bonewald LF, Kester MB, Schwartz Z, Swain LD, Khare A, Johnson TL, Leach RJ, Boyan BD. Effects of combining transforming growth factor beta and 1,25-dihydroxyvitamin D3 on differentiation of a human osteosarcoma (MG-63). J Biol.Chem. 1992; 267: 8943-8949.

45. Kieswetter K, Schwartz Z, Hummert TW, Cochran DL, Simpson J, Dean DD, Boyan BD. Surface roughness modulates the local production of growth factors and cytokines by osteoblast-like MG-63 cells. J.Biomed.Mater.Res. 1996; 32: 55-63.

CHAPTER 4. EVALUATION OF OSSEOINTEGRATION BY IN VIVO MOUSE INTRAMEDULLARY BONE FORMATION MODEL

Introduction

Integration of bone with an implant surface depends on both bone physiology and surface design. The major surface properties that regulate bone response include surface structure, chemical composition, surface charge and energy. Titanium (Ti) is a widely used biomaterial in orthopaedic and dental application. Bone tissue directly deposits along the Ti surface and forms a tight interface between substratum and bone, referred to as osseointegration. Surface roughness is important in determining bone responses to implant fixation. A systemic review of *in vivo* animal studies on the effects of Ti implants with rough surfaces demonstrated a positive relationship between surface roughness and osseointegration after 3-months of implantation, represented by higher percentage of bone-to-implant contact and increased mechanical force [1]. Similar results were reported in other animal models and experimental designs [2]. Most *in vivo* peri-implant studies were performed in rat, rabbit, sheep, dog or other larger animals. Albrektsson and Wennerbergy suggested that moderately rough surfaces with arithmetic average of center line height (S_a or R_a) of 1-2 μm promote stronger bone responses than either smoother or rougher surfaces [3]. Others reported a positive effect of surface roughness on bone formation up to roughness of 8.5 μm [1]. The differences are not only caused by measurement techniques, but also related to general integral design of implant macrostructure. The osteogenic effects of rough surfaces were also confirmed in clinical studies, which demonstrate that the pre-loading integration success rate of acid etched implants is significantly higher than that with machined smooth implants [4]. The healing period of dental implants with microrough structure was reduced from 3 months to 6 weeks; and the success rate exceeded 90% at 3-year follow up [5-7].

Surface chemical composition is another critical factor that regulates peri-implant bone formation. The change of surface chemical composition is also associated with surface hydrophilicity and surface energy. When in contact with the atmosphere, regular Ti surfaces are contaminated with a layer of carbon dioxide or hydrocarbon molecules adsorbed from the air. Previous study found that if the Ti substratum was prevented from contact with air and stored in physiologic solutions, the carbon contamination decreased by more than 50%, and the surface hydrophilicity increased [8]. This modified surface promotes osteoblast differentiation and faster bone apposition along the interface [9, 10]. This is consistent with Sendax and Baier's earlier finding that radio-frequency-glow-discharge treatment and water storage of calcium phosphate coated implants benefit bone response to host tissue, suggesting the important role of higher surface free energy in regulating bone-biomaterial interactions [11].

Besides biomaterial surface properties, bone quality also affects osseointegration. Bone formation is regulated by various local or systemic conditions. For example, inhibition of cyclooxygenase decreases bone growth *in vivo* and blocks osteoblast responses to surface structure *in vitro* by interfering with prostaglandin production [12, 13]. Therefore, patients who are in need of orthopaedic/dental implantation while taking cyclooxygenase inhibitor treatments for chronic pain may suffer from poor osseointegration or even failure of the implantation. Lack of vitamin D also impairs bone development and bone to implant growth [14].

Knock-out mice models have been widely used to explore the effects of these specific conditions on bone development. However, there is no available intramedullary mouse peri-implant bone formation model because of the small size of mouse bone and the difficulty in surgery. The objective of this pilot study was to develop a novel peri-implant bone formation mouse model, which has the potential to be applied in knock-out mice in the future. To achieve this goal, we designed small Ti implants with different

www.manaraa.com

surface structures and chemical compositions, inserted the implants into the mouse femur and observed the medullary bone formation at 9, 18 and 35 days. Results showed that the success rate of the mouse intramedullary bone formation model is highly dependent on surgical technique. Bone formation in the femur bone marrow starts before 9 days, and remodels extensively at 18 days. Surface structure and chemical composition regulate bone morphology. The results suggest that a formal study using more samples for each group should be performed and bone formation should be examined at an earlier time point.

Materials and Methods

Implants

Ti implants were prepared from grade 2 unalloyed Ti (ASTM F67 "Unalloyed titanium for surgical implant applications") and supplied by Institut Straumann AG (Basel, Switzerland). The implant device was made of two components: the handling device and the implant rod (Fig. 4-1b). The implant rod was 5 mm in length with 0.9 mm in diameter. The implant surfaces were produced to present three different structures and chemistry. The pretreatment (PT) Ti has a smooth Ti surface produced by machining and chemical degreasing. The PT surface was further sand blasted and acid etched to produce SLA surfaces with an R_a around 3-4 μm. To prevent contamination, modSLA surfaces were manufactured under same grit-blasting and acid etching conditions as SLA, but protected from contact with atmosphere by nitrogen gas. The modSLA implants were stored in 0.9% NaCl to preserve isolation from air. All the devices were sterilized by gamma irradiation at 25 kGy over night and ready for use.

In vivo mouse bone formation model and histology

The Ti rod implants were inserted into mouse femur via a medial parapatellar arthrotomy. Nine 6-week old male C57BL/6 mice were anesthetized with 5% isoflurane inhalation and placed in a resupine position. For surgical convenience, the right leg was selected for operation and fixed under light microscope. An 8 mm incision was made on the distal side over the knee. The ligament and patella were moved to expose the intercondylar notch of the distal femur. The position and orientation of the femur were determined by pressing the leg to sense the bony structure. After the femoral cartilage was exposed, the distal end of the femur was penetrated by a dental drill with 0.8 mm diameter tip through the intercondylar notch to access the medullary cavity. The direction of the drill tip was in alignment with the femur. 22G needle was used to confirm the penetration of the femur condyle. The Ti rod was then inserted into the marrow cavity and broken from the handling device. The periosteal tissue and the skin were closed with sutures and wound clips, respectively. Three mice were implanted with each type of Ti implant and were euthanized at day 9, 18 and 35 after the surgery. Both right and left femurs were collected and stored in 10% formalin for histological analyses. The non-surgical contralateral femur was analyzed as control. Tissue sections were ground to a final thickness of 10 to 20 μm. Sections were stained with haematoxylin and eosin for qualitative histology.

Results

To design Ti rod implant with appropriate size, we measured the intramedullary dimension of the middle segment of 6-week male mouse femur by using microCT. The scanning picture showed that the mouse femur has an elliptic morphology, with major axis of 1.5 mm and minor axis of 1.0 mm (Fig. 4-1A). Considering the variance in mouse size, we manufactured Ti rod implants with 0.9 mm diameter. The complete implant device (Fig. 4-1B,C, Fig. 4-2A) is composed of a handling part to facilitate surgery

75

operation (Fig. 4-2B) and the rod implant part. The rod is 5 mm in length, which is half of the length of mouse femur (Fig. 4-2C).

The preliminary study showed that appropriate drilling at the femoral condyle created a direct channel for insertion of Ti rod implant without destroying the cortical bone in the femur (Fig. 4-3A,B).

Extensive trabecular bone formation appeared in the femur bone marrow canal at 9 days after implantation (Fig. 4-4). Compared to the bone marrow in the contralateral tibia, there was greatly increased short, non-continuous new bone formed in the femur medullary canal. A thin layer of separation was present around the Ti rod with the PT surface, indicating most trabecular bone did not directly deposit on the PT implant surface. In contrast, there is no gap between bone and SLA surface. The modSLA implant was misplaced and broke the middle section of the femur.

At 18 days after implantation, the bone quantity around PT was much less compared that at 9 days (Fig. 4-5). At one end of the PT implant that is close to the femur condyle, bone laid directly to the implant surface. The other area of the PT implant surface was separated from the bone with a thin gap as seen at 9 days. The SLA implant was misplaced and only a small part of the implant left in contact with bone. The whole implant was covered by fibrous tissue. The trabecular bone around the modSLA implant was resorbed as around the PT surface. However, there was still continuous bone connecting the cortical bone and the implant surface at several positions.

Thirty-five days after implantation, a continuous layer of cortical bone formed around the PT surface (Fig. 4-6). The SLA implant penetrated the middle section of the femur. Little trabecular bone was left in the medullary canal. However, bone bridges connecting the femur cortical bone and implant surface were left around SLA and modSLA surfaces. The phenomenon was more obvious around modSLA implant.
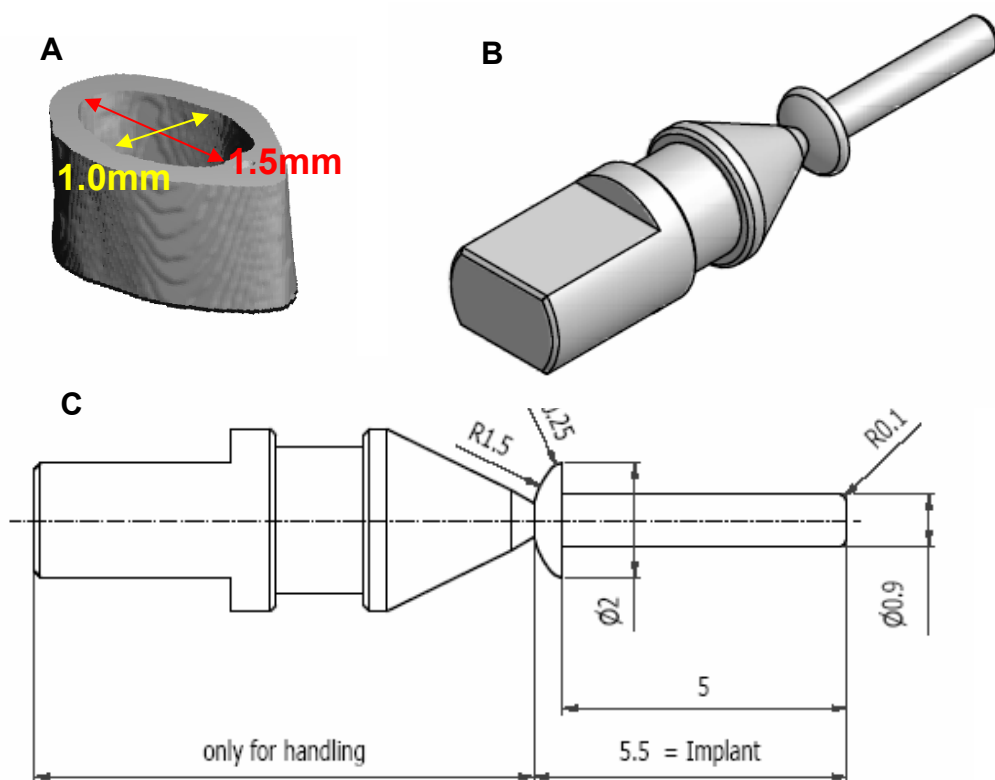
www.manaraa.com

Figure 4-1. Design of Ti rod implant. A) measurement of intramural chamber size of mouse femur by microCT; B) Ti rod implant model; C) mechanical drawing of implant design.
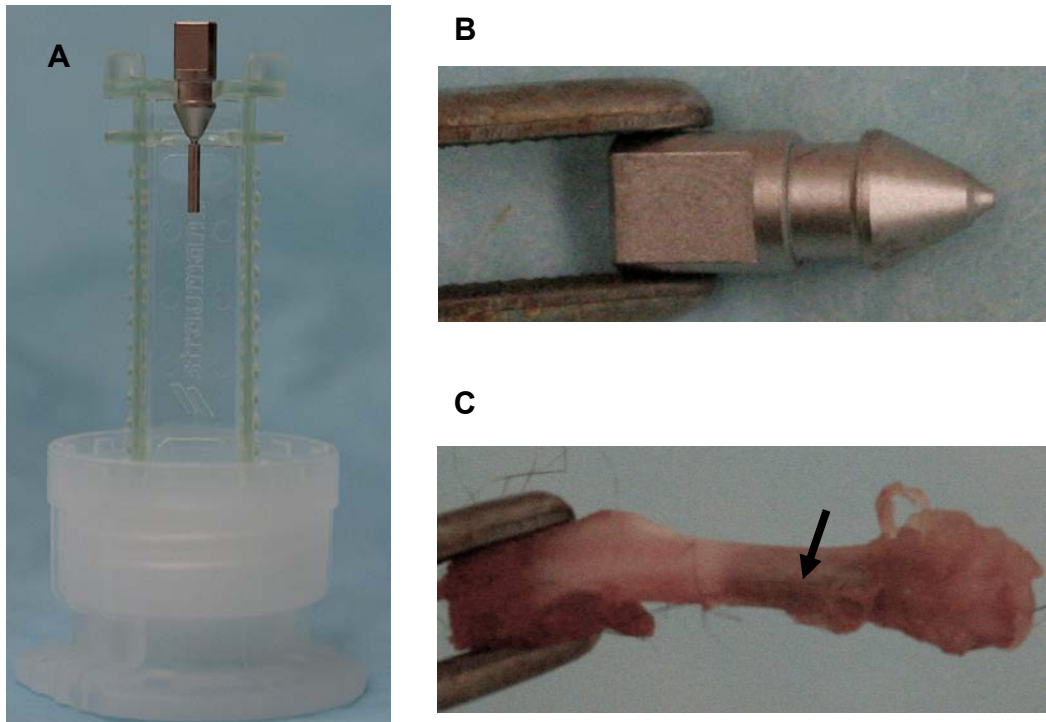
Figure 4-2. Components of Ti rod implants. A) the complete Ti rod implant morphology; B) the handling device which had been broken from the Ti rod; C) mouse femur with inserted rod implant. The implant was completely inserted into mouse femur without break bone (arrow indicates the implant).

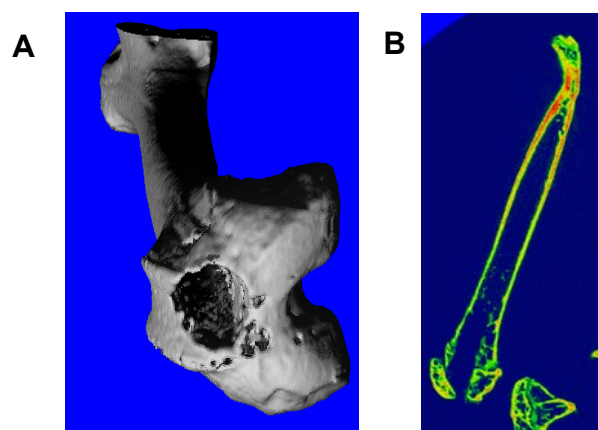Figure 4-3. Bone structure after drilling process. The mouse femur condyle was penetrated by dental drill in a pilot study. MicroCT scanning showed that modeled 3D structure of femur (A) and longitudinal section (B).

Figure 4-4. Histology of bone-to-implant at 9 days after implantation. The pictures from the top to bottom rows are histology images at low, medium, high magnification and the tibia at the contralateral side.

Figure 4-5. Histology of bone-to-implant at 18 days after implantation. The pictures from the top to bottom rows are histology images at low, medium, high magnification and the tibia at the contralateral side.
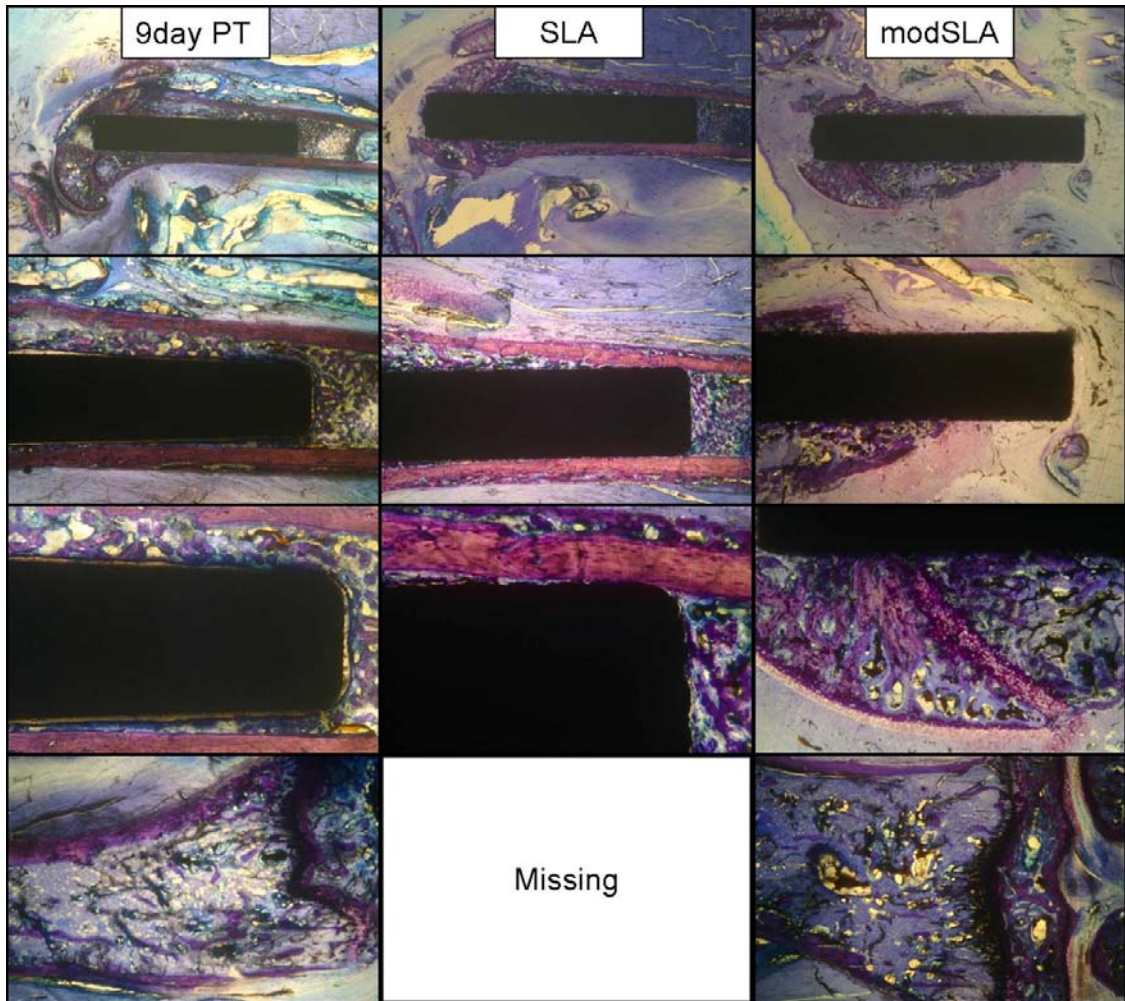
Figure 4-6. Histology of bone-to-implant at 35 days after implantation. The pictures from the top to bottom rows are histology images at low, medium, high magnification and the tibia at the contralateral side.
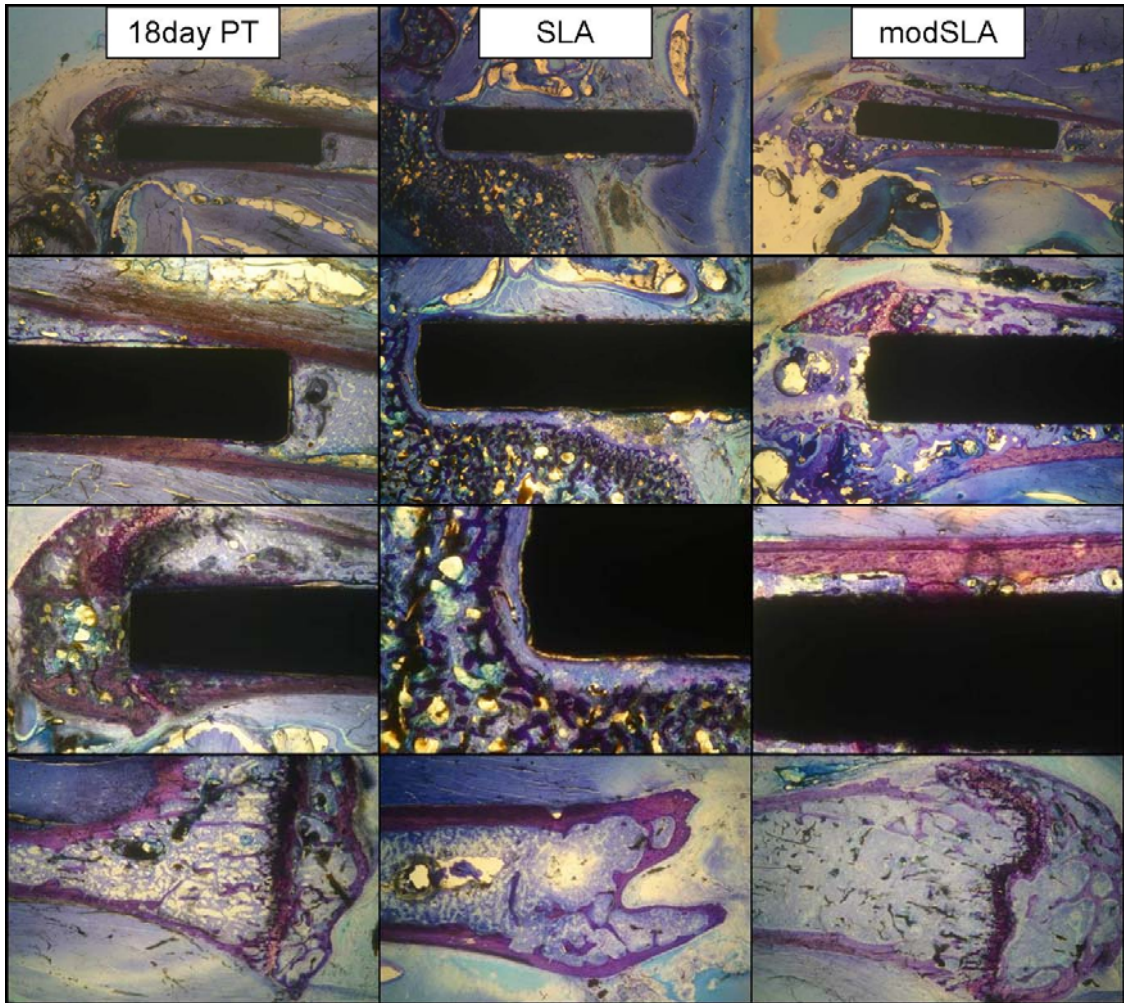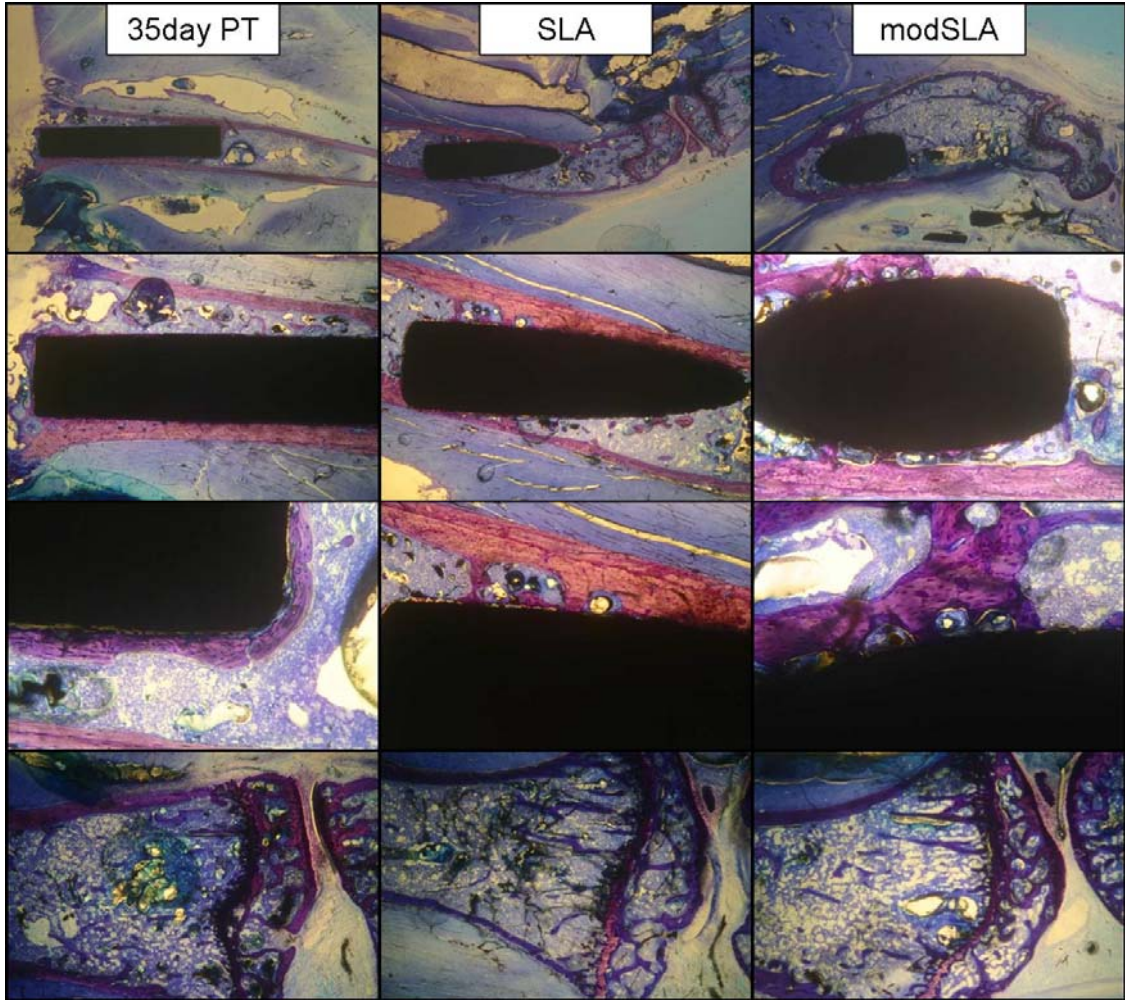
Discussion

This is a novel mouse femur intramedullary bone formation model to examine the effects of biomaterial surface properties on osseointegration. The success rate of this pilot study was 66%, which has improved from the pilot study (33%). Among the three failed implants, one of them completely missed the direction of the mouse femur and penetrated the condyle joint; the other two were slightly awry from the femur and broke the middle part of the bone. When we inserted the Ti rod, we had to conquer the resistance to push the implant because the size of the implant is similar to the internal diameter of the mouse femur. The resistance made it difficult to determine whether we had inserted the Ti rod to the narrowest section of the femur or we had broken the bone. One solution to increase the success rate is to produce smaller Ti rods for easier implantation. For smooth implants it is easy to produce Ti rods as small as 0.5 mm diameter. However, 0.9 mm is the current limit to manufacture the microstructured implants. The other way to increase surgery success is through more practice and dissections to better understand the anatomy of the mouse femur. It is especially important if the model is applied into vitamin D receptor or cyclooxygenase knock-out mice, because the bone size and quality in these knock-out mice are smaller and more brittle; and the success rate is expected to be even lower. To prevent the unnecessary pain of the mouse in which the implantation has failed, the animal should be examined by X-ray immediately after the surgery, and be euthanized if the bone is broken.

Rat [15-22] or rabbit [23, 24] marrow ablation models have been used to study effects of peri-implant bone formation. After the disruption of bone marrow, the intramedullary tissue undergoes a series of healing responses including coagulation initiation, primitive mesenchymal stem cell appearance, osteoblast proliferation, trabecular bone formation and bone resorption [25]. The new bone marrow structure is regenerated by about 28 days. The trabecular bone was formed by endosteal

82

osteoblast and osteoprogenitor cells that reside in hematopoietic tissue. This process is stimulated by the activation of endosteum and affected by many other factors. Ishizaka *et al.* found that the trabecular bone formation was enhanced as early as one week if the bone marrow was irrigated by saline before insertion of the implant. This is probably due to the removal of bone particles [17]. The long term effect of saline irrigation on bone-to-implant contact and implant mechanical integration is not consistent [17, 18]. In our study, mouse bone marrow was destroyed by testing the direction of the femur canal with a 22G needle before the placing the Ti rod. This is a similar process to the rat marrow ablation, and we observed extensive trabecular bone formation as in rat model. We did not irrigate the medullary canal in order not to complicate the surgical process.

In this study, we examined peri-implant bone formation at three time points to determine the best time point for future experiments. In the rat ablation model, bone formation was induced within 2 weeks and was followed by remodeling [15, 26]. Barber *et al.* found that the total bone quantity in the medullary canal at 4 and 8 weeks after Ti implantation was less compared to them at 2 weeks [15]. There was no difference between bone-to-implant percentage. In this pilot study we examined bone formation around 2 weeks (9 and 18 days) to determine the dynamic change of bone formation and bone resorption. Our results showed that at 9 days after implantation there was already extensive trabecular bone formation in mouse femur medullary canal, and by 18 days, the resorption removed most of the bone in the marrow chamber. Therefore, an earlier time point will be helpful to determine the rate of bone formation in response to different Ti surface treatments. Previous study showed that when Ti implants with SLA or modSLA surfaces were implanted into miniature pigs maxilla, bone apposition was faster around the modSLA surface [10]. Higher bone-to-implant contacts were observed around modSLA compared to SLA surfaces at 2 and 4 weeks after implantation. There was no difference between the groups at 8 weeks. In our study, we found bone marrow

was restored and stable bone formation established by 5 weeks.

We did not perform quantitative bone-to-implant measurements in the pilot study, because only one sample per group was included and some of them were failed. In future study, 6 animals will be used in each group, and quantitative histomorphometric analyses are necessary to evaluate bone volume and bone-to-implant contact. Moreover, mechanical testing will be tried to evaluate the strength of osseointegration. The mechanical analysis, together with histomorphometry, provides more comprehensive information on peri-implant bone formation.

This new mouse model affords important advantages to evaluate peri-implant bone formation in genetically modified mice and to isolate factors that influence osseointegration. As a pilot study, there is only one animal per group without generating statistically quantitative results. This study provides useful information for guiding future experiments. We conclude that an extra one third of the animals are needed for this model to ensure enough sample size for the experiments, and the appropriate time points to observe bone formation and bone remodeling are 1 and 2 weeks.

References

1. Shalabi MM, Gortemaker A, Van't Hof MA, Jansen JA, Creugers NH. Implant surface roughness and bone healing: a systematic review. J.Dent.Res. 2006; 85: 496-500.
2. Wennerberg A, Ektessabi A, Albrektsson T, Johansson C, Andersson B. A 1-year follow-up of implants of differing surface roughness placed in rabbit bone. Int.J.Oral Maxillofac.Implants. 1997; 12: 486-494.
3. Wennerberg A, Albrektsson T. Suggested guidelines for the topographic evaluation of implant surfaces. Int J Oral Maxillofac Implants 2000; 15: 331-344.
4. Khang W, Feldman S, Hawley CE, Gunsolley J. A multi-center study comparing dual acid-etched and machined-surfaced implants in various bone qualities. J.Periodontol. 2001; 72: 1384-1390.
5. Roccuzzo M, Bunino M, Prioglio F, Bianchi SD. Early loading of sandblasted and acid-etched (SLA) implants: a prospective split-mouth comparative study. Clin Oral Implants Res 2001; 12: 572-578.
6. Cochran DL, Buser D, ten Bruggenkate CM, Weingart D, Taylor TM, Bernard JP, Peters F, Simpson JP. The use of reduced healing times on ITI implants with a

sandblasted and acid-etched (SLA) surface: early results from clinical trials on ITI SLA implants. Clin.Oral Implants.Res 2002; 13: 144-153.

7. Bornstein MM, Lussi A, Schmid B, Belser UC, Buser D. Early loading of nonsubmerged titanium implants with a sandblasted and acid-etched (SLA) surface: 3-year results of a prospective study in partially edentulous patients. Int J Oral Maxillofac Implants 2003; 18: 659-666.

8. Rupp F, Scheideler L, Olshanska N, de Wild M, Wieland M, Geis-Gerstorfer J. Enhancing surface free energy and hydrophilicity through chemical modification of microstructured titanium implant surfaces. J.Biomed.Mater Res.A 2006; 76: 323-334.

9. Zhao G, Schwartz Z, Wieland M, Rupp F, Geis-Gerstorfer J, Cochran DL, Boyan BD. High surface energy enhances cell response to titanium substrate microstructure. J.Biomed.Mater Res.A 2005; 74: 49-58.

10. Buser D, Broggini N, Wieland M, Schenk RK, Denzer AJ, Cochran DL, Hoffmann B, Lussi A, Steinemann SG. Enhanced Bone Apposition to a Chemically Modified SLA Titanium Surface. J Dent.Res 2004; 83: 529-533.

11. Sendax VI, Baier RE. Improved integration potential for calcium-phosphate-coated implants after glow-discharge and water-storage. Dent Clin North Am 1992; 36: 221-224; discussion 225.

12. Boyan BD, Lohmann CH, Sisk M, Liu Y, Sylvia VL, Cochran DL, Dean DD, Schwartz Z. Both cyclooxygenase-1 and cyclooxygenase-2 mediate osteoblast response to titanium surface roughness. J.Biomed.Mater.Res. 2001; 55: 350-359.

13. Goodman S, Ma T, Trindade M, Ikenoue T, Matsuura I, Wong N, Fox N, Genovese M, Regula D, Smith RL. COX-2 selective NSAID decreases bone ingrowth in vivo. J.Orthop.Res. 2002; 20: 1164-1169.

14. Kato S, Takeyama K, Kitanaka S, Murayama A, Sekine K, Yoshizawa T. In vivo function of VDR in gene expression-VDR knock-out mice. J Steroid Biochem Mol Biol 1999; 69: 247-251.

15. Barber TA, Ho JE, De Ranieri A, Virdi AS, Sumner DR, Healy KE. Peri-implant bone formation and implant integration strength of peptide-modified p(AAM-co-EG/AAC) interpenetrating polymer network-coated titanium implants. J Biomed Mater Res A 2007; 80: 306-320.

16. Ferris DM, Moodie GD, Dimond PM, Gioranni CW, Ehrlich MG, Valentini RF. RGD-coated titanium implants stimulate increased bone formation in vivo. Biomaterials 1999; 20: 2323-2331.

17. Ishizaka M, Tanizawa T, Sofue M, Dohmae Y, Endo N, Takahashi HE. Bone particles disturb new bone formation on the interface of the titanium implant after reaming of the marrow cavity. Bone 1996; 19: 589-594.

18. De Ranieri A, Virdi AS, Kuroda S, Healy KE, Hallab NJ, Sumner DR. Saline irrigation does not affect bone formation or fixation strength of hydroxyapatite/tricalcium phosphate-coated implants in a rat model. J Biomed Mater Res B Appl Biomater 2005; 74: 712-717.

19. Pabbruwe MB, Standard OC, Sorrell CC, Howlett CR. Effect of silicon doping on bone formation within alumina porous domains. J Biomed Mater Res A 2004; 71: 250-257.

20. O'Toole GC, Salih E, Gallagher C, FitzPatrick D, O'Higgins N, O'Rourke SK. Bone sialoprotein-coated femoral implants are osteoinductive but mechanically compromised. J Orthop Res 2004; 22: 641-646.

21. Liao H, Mutvei H, Hammarstrom L, Wurtz T, Li J. Tissue responses to nacreous implants in rat femur: an in situ hybridization and histochemical study. Biomaterials 2002; 23: 2693-2701.

22. Schmidmaier G, Wildemann B, Schwabe P, Stange R, Hoffmann J, Sudkamp NP, Haas NP, Raschke M. A new electrochemically graded hydroxyapatite coating for osteosynthetic implants promotes implant osteointegration in a rat model. J Biomed Mater Res 2002; 63: 168-172.

23. Stewart M, Welter JF, Goldberg VM. Effect of hydroxyapatite/tricalcium-phosphate coating on osseointegration of plasma-sprayed titanium alloy implants. J Biomed Mater Res A 2004; 69: 1-10.

24. Kawamura H, Ito A, Muramatsu T, Miyakawa S, Ochiai N, Tateishi T. Long-term implantation of zinc-releasing calcium phosphate ceramics in rabbit femora. J Biomed Mater Res A 2003; 65: 468-474.

25. Amsel S, Maniatis A, Tavassoli M, Crosby WH. The significance of intramedullary cancellous bone formation in the repair of bone marrow tissue. Anat Rec 1969; 164: 101-111.

26. Kuroda S, Virdi AS, Li P, Healy KE, Sumner DR. A low-temperature biomimetic calcium phosphate surface enhances early implant fixation in a rat model. J Biomed Mater Res A 2004; 70: 66-73.

CHAPTER 5. SEX DIMORPHISM IN THE RESPONSE OF RAT OSTEOBLASTS TO ESTROGEN AND 1,25(OH)₂D₃ WHEN GROWN ON TITANIUM SURFACES

Introduction

Successful osseointegration of bone growth around an implant is dependent on implant surface, bone quality and systemic environment. To investigate surface effects on osteoblast, titanium (Ti) is a widely used model surface because of its good biocompatibility and clinical relevance. It is well known that rough Ti surfaces induce higher bone-to-implant contact and stronger mechanical integration in vivo, resulting in better osseointegration [1-3] . This result is supported by in vitro findings that rough surfaces enhance osteoblast differentiation, matrix deposition and growth factor productions [4-6] .

Numerous techniques have been applied on modification of surface textures, producing from nano to micrometer scale structures, to explore the optimum conditions for cell surface interaction. Among them, sand-blasting and acid etching (SLA) is a widely used method to create a complex topography on Ti. Sand-blasted (SL) Ti surfaces are composed of 30 - 100 μm diameter irregular cavities. This size is similar to osteoclast resorbed pits, which initiates bone remodeling and stimulates osteoblast activity [7]. It has been shown that pretreatment with osteoclasts on bone wafers promoted osteoblast differentiation. Acid etching (A) exerts a sub-micrometer roughness (700 – 800nm) on flat Ti. In combination with sand-blasting, the SLA has an arithmetic average of center line height (R_a) about 3-4 μm. Previous studies showed that osteoblasts are sensitive to both micrometer and sub-micrometer scale roughness [8, 9]. The combination of these structures has a synergistic effect in promoting osteoblast differentiation phenotype. Besides the parameter of roughness, the shape of surface microtopography is also very critical to osteoblast response.

Surface topography also influences cell responses to local regulatory factors and systemic hormones. The osteoblasts grown on rough surfaces create an osteogenic micro-environment by producing more cytokines and growth factors; and these local factors regulate osteoblasts through autocrine or paracrine pathways [10]. Surface roughness plays a role in the response of osteoblast-like cells to bone morphogenetic protein-2 (BMP-2) [11]. Responses of osteoblast-like MG63 cells to $1\alpha,25(OH)_2D_3$ are enhanced on rougher surfaces [12]. For some parameters, the effects of surface roughness and $1\alpha,25(OH)_2D_3$ are synergistic. The effects of $1\alpha,25(OH)_2D_3$ are also dependent on the state of maturation of the cell in the osteoblast lineage. More mature cells exhibit reduced response to $1\alpha,25(OH)_2D_3$ but are still affected by surface roughness [13].

The prevalence of many orthopaedic diseases, such as osteoporosis, osteoarthritis, spinal disorders and osteoporosis, are higher in women. The differences are related to intrinsic sexual differences at the cellular or molecular level [14]. In postmenopausal women, estrogen deficiency causes decreased osteoblast activity and increased osteoclastic resorption. The unbalanced bone turnover rates lead to osteoporosis, and potentially diminish bone formation around implants. *In vivo* studies show that in estrogen deficient animals, osseointegration around implants was impaired, represented by less bone mass, smaller contact area between bone and the implant [15, 16], and decreased pull-out strength of implants [17]. Previous study reported that 17β-estradiol (E2) regulates female human osteoblast responses to surface structure synergistically. Although estrogen is also necessary for bone strength in males, the mechanism of the estrogen effect is different from that on female osteoblasts. Therefore, it is important to understand how estrogen regulates male and female osteoblasts, especially the responses to implant surfaces.

The purpose of this study was to examine the role of sexual dimorphism in the responses of male and female osteoblasts to estrogen on microstructured surfaces. To further investigate the mechanism of estrogen effects, bovine serum albumin conjugated estradiol (E2-BSA) was used to examine the role of membrane estrogen receptor. During characterization of primary rat calvarial osteoblasts, we surprisingly found that male rat osteoblasts exhibit higher alkaline phosphatase activity and stronger responses to $1\alpha,25(OH)_2D_3$ compared to female cells, indicating sex specific differences between male and female osteoblasts in response to bone regulating hormones. Our results also showed that rat osteoblasts are sensitive to surface topography, as we and others observed with other cells. Estrogen increased female osteoblast differentiation while it had no effects on male cells. The effects of estrogen probably proceeded partially via membrane estrogen receptors.

Materials and Methods

Preparation and Characterization of Ti Disks

Ti disks were prepared from 1 mm thick sheets of grade 2 unalloyed Ti (ASTM F67 "Unalloyed titanium for surgical implant applications") and supplied by Institut Straumann AG (Walderburg, Switzerland). The disks were punched to be 15 mm in diameter so as to fit into the well of a 24-well tissue culture plate. Disks were degreased by washing in acetone, processing through 2% ammonium fluoride / 2% hydrofluoric acid / 10% nitric acid solution at 55°C for 30 s to produce pretreatment Ti disks (PT). Acid etched (A) surfaces were treated with HCl/H_2SO_4. SL surfaces were sandblasted with 0.25-0.50 mm corundum grits at 5 bar until the surface became a uniform gray. SLA surfaces were produced by the combination processes of sandblasting and acid etching as SL and A surface. Prior to cell culture, all the substrata were washed in ultrasonic cleaner and sterilized in an oxygen plasma cleaner (PDC-32G, Harrick

89

Plasma, Ithaca, NY). Surface characterizations were reported previously [5, 18] . The R_a of PT, A, SL and SLA surfaces are 0.04±0.00, 0.83±0.05, 2.48±0.09 and 3.22±0.88 µm, respectively.

<u>Rat Osteoblast Cultures</u>

Osteoblasts were isolated from frontal and parietal (calvaria) bones of 6-week old male and female Sprague-Dawley rats (200-225g) using enzymatic isolation. Briefly, rat bones were cleaned by removing periosteum and other soft tissues, and cut in 1-2 mm pieces. The bone chips were washed 3 times in Hank's balanced salt solution (HBSS) containing 3% penicillin-streptomycin. After washing, bone chips were digested with an enzymatic cocktail of 1.6mg/ml collagenase IA / 5.4mg/ml Dispase in HBSS for 1 hour at 37°C. The first round of digestion was discarded to avoid fibroblast contamination. The bone chips were digested three more times using the same method; each digested media was collected and quenched with full media (1% penicillin-streptomycin/ 10% fetal bovine serum/ DMEM). For each batch of cells, rat bones were dissected from 8 rats.

Osteoblastic phenotype was confirmed by examining cell responses to different concentrations of $1\alpha,25(OH)_2D_3$. Validated rat osteoblasts were plated at 10,000 cells/cm^2 density on tissue culture plastic or surfaces. Media were exchanged at 24 hours and then every 48 hours until the cells reached confluence on plastic. To examine cell response to osteotropic hormone $1\alpha,25(OH)_2D_3$, cells were treated with vehicle, 1nM or 10nM $1\alpha,25(OH)_2D_3$ for 24 h. In order to study cell response to estrogen, they were treated with vehicle, 10nM 17β-estradiol or same concentration of bovine serum albumin conjugated 17β-estradiol.

<u>Analysis of Cell Response</u>

Cell number was determined in all cultures 24 hours after cells on tissue culture plastic reached confluence. Cells were released from the surfaces by two sequential incubations in 0.25% trypsin for 10 min at 37°C, in order to assure that any remaining

cells were removed from rough TiO_2 surfaces. Released cells were counted using an automatic cell counter (Z1 cell and particle counter, Beckman Coulter, Fullerton, CA). Fewer than 1,000 cells were attached to the plastic surface underlying the Ti disks; therefore, these cells were not separated from total cells released from the disks, nor were they subtracted from the final cell numbers.

We used two determinants of osteoblast differentiation: alkaline phosphatase specific activity [orthophosphoric monoester phosphohydrolase, alkaline; E.C. 3.1.3.1] of cell lysates, and osteocalcin content of the conditioned media. Alkaline phosphatase is an early marker of differentiation and reaches its highest levels as mineralization is initiated. Osteocalcin is a late marker of differentiation and increases as mineral is deposited. Cell lysates were collected by centrifuging the cells after counting. Enzyme activity was assayed by measuring the release of *p*-nitrophenol from *p*-nitrophenylphosphate at pH 10.2 and results were normalized to protein content of the cell lysates [19]. The levels of osteocalcin in the conditioned media were measured using a commercially available radioimmunoassay kit (Human Osteocalcin RIA Kit, Biomedical Technologies, Stoughton, MA) and normalized to cell number, as described previously [12].

The conditioned media were also assayed for growth factors and cytokines. Osteoprotegerin (OPG) was measured using enzyme-linked immunosorbent assay (ELISA) kit (DY805 Osteoprotegerin DuoSet, R&D System, Minneapolis, MN) [20]. PGE_2 was assessed using a commercially available competitive binding radioimmunoassay kit (NEK020A Prostaglandin E_2 RIA kit, Perkin Elmer, Wellesley, MA). Active TGF-β1 was measured prior to acidification of the conditioned media, using an ELISA kit specific for human TGF-β1 (G7591 TGF-β1 E_{max} Immunoassay System, Promega Corp., Madison, WI). Total TGF-β1 was measured after acidifying the media and latent TGF-β1 was defined as total TGF-β1 minus active TGF-β1 [12].

91

<u>Statistical Analysis</u>

The data presented here are from one of two separate experiments. Both experiments yielded comparable observations. For any given experiment, each data point represents the mean ± standard error of six individual cultures. Data were first analyzed by analysis of variance; when statistical differences were detected, the Student's *t*-test for multiple comparisons using Bonferroni's modification was used. *P*-values < 0.05 were considered to be significant.

Results

To confirm osteoblastic phenotype of isolated rat calvarial cells, we examined cell responses to osteotropic hormone $1\alpha,25(OH)_2D_3$ for 24 h after reaching confluence on TCPS. Both male and female rat cells exhibit decreased cell growth and express higher alkaline phosphatase activity and osteocalcin level in response to $1\alpha,25(OH)_2D_3$ (Fig. 5-1). With treatment of 1nM $1\alpha,25(OH)_2D_3$, male rat calvarial cell number decreased 28%, while female cell number decreased 20%. In the presence of higher $1\alpha,25(OH)_2D_3$ concentration, cell number decreased 56% and 26% compared to control in male and female cell, respectively. Alkaline phosphatase activities increased in response to 10nM $1\alpha,25(OH)_2D_3$, represented by 80% and 74% increase in male and female cells, respectively. Osteocalcin levels, the most specific osteoblast differentiation maker, also increased when cells were treated with $1\alpha,25(OH)_2D_3$. Osteocalcin level doubled in male cells, while increased by 30% in female cells. The rat calvarial cells were also cultured in osteogenic media for four weeks, and formed multilayer nodules in the culture under light microscope. The results together confirmed the osteoblastic characteristic of our isolated rat calvarial cells.

The above results also indicate an interesting finding that the alkaline phosphatase activity of male osteoblasts was higher than that of female cells, and male

osteoblasts responded to $1\alpha,25(OH)_2D_3$ in a dose dependent manner and more extensively. To confirm whether this sexual dimorphism is a random or general property of osteoblasts, we harvested two new batches of rat osteoblasts to repeat the experiments. Moreover, we also examined the effects of substratum roughness on osteoblast response to $1\alpha,25(OH)_2D_3$.

Cell number of male rat osteoblasts on smooth PT was similar to that on tissue culture polystyrene (TCPS). On A and SLA, cell numbers were lower compared to TCPS (Fig. 5-2). Although the cell number on SL was slightly smaller than TCPS, there was no statistical difference between them. $1\alpha,25(OH)_2D_3$ treatment did not change cell numbers on surfaces. Similar effects were observed for female osteoblasts; cell numbers on A and SLA were lower than those on TCPS. Compared to A, there was a 25% decrease in cell number on SLA.

Alkaline phosphatase activities of male osteoblasts were sensitive to the surface. ANOVA analysis shows $p < 0.05$ between all groups, but Bonferroni tests did not demonstrate significant difference between each two surfaces (Fig. 5-3A). $1\alpha,25(OH)_2D_3$ treatment increased enzyme activity, especially the higher concentration $1\alpha,25(OH)_2D_3$, to which the alkaline phosphatase increased 70-100% compared to controls (Table 5-1). In female osteoblasts, neither surface nor hormone effects were observed with regard to enzyme activities (Table 5-1, Fig. 5-3B). This is probably due to relatively high variance in enzyme activities. Comparison between male and female cells showed that enzyme activities of male osteoblasts were 1-2 fold higher than those of female cells (Fig. 5-3C). The differences were larger on $1\alpha,25(OH)_2D_3$ treated groups, indicating a higher response of the hormone in male cells.

Table 5-1. Percentage increases of alkaline phosphatase treated with $1\alpha,25(OH)_2D_3$.

% increase		TCPS	PT	A	SL	SLA
Male	1nM 1,25	42	67	31	47	50
	10nM 1,25	78	106	76	73	95
Female	1nM 1,25	37	27	9	16	20
	10nM 1,25	42	27	30	29	42

Osteocalcin is the most specific osteoblast differentiation marker. There was no difference between osteocalcin levels in control cultures on TCPS, PT, A and SL (Fig. 5-4). Only on SLA, male osteoblasts released more osteocalcin. Male osteoblasts responded to $1\alpha,25(OH)_2D_3$ in an apparent dose dependent manner. 1nM $1\alpha,25(OH)_2D_3$ increased osteocalcin levels by 40-75%, while 10nM $1\alpha,25(OH)_2D_3$ treatment increased osteocalcin by 120-200% (Table 5-2). All cells on Ti substrata were more sensitive to $1\alpha,25(OH)_2D_3$ compared to TCPS. Female osteoblasts showed a similar surface effect; there was a higher osteocalcin level in the conditioned media on SLA surfaces. In contrast to male cells, the female osteoblasts responded to $1\alpha,25(OH)_2D_3$ in a much less extensive way. Even the higher concentration of $1\alpha,25(OH)_2D_3$ treatment did not increase osteocalcin level above 50% (Table 5-2).

94

Table 5-2. Percentage increase of osteocalcin levels treated with $1\alpha,25(OH)_2D_3$.

% increase		TCPS	PT	A	SL	SLA
Male	1nM 1,25	46	75	55	48	62
	10nM 1,25	120	203	195	150	197
Female	1nM 1,25	20	17	9	13	17
	10nM 1,25	42	39	32	38	46

The osteoblasts created an osteogenic microenvironment through autocrine or paracrine pathways to regulate bone formation. Therefore, besides differentiation markers, we also tested local factors produced by osteoblasts. Osteoprotegerin (OPG) is an osteoblast-generated protein that functions in modifying osteoclast maturation. The results showed that male osteoblasts on SLA released the greatest amount of OPG, followed by cells on A surfaces (Fig. 5-5). 10nM $1\alpha,25(OH)_2D_3$ enhanced OPG levels on all surfaces, but 1nM $1\alpha,25(OH)_2D_3$ had no effect (Table 5-3). Female osteoblasts produced similar levels of OPG to males, and showed comparable pattern of responses to substratum surface and $1\alpha,25(OH)_2D_3$ treatment.

Table 5-3. Percentage increases of osteoprotegerin treated with $1\alpha,25(OH)_2D_3$.

% increase		TCPS	PT	A	SL	SLA
Male	1nM 1,25	12	36	31	68	23
	10nM 1,25	80	105	124	137	101
Female	1nM 1,25	33	53	34	87	24
	10nM 1,25	72	85	55	146	41

TGF-β1 is an important growth factor that regulates osteoblast differentiation and osteoclast activity. While TGF-β1 is released into the media, most TGF-β1 combined with TGFβ binding protein and embedded into the matrix in latent form. Our results showed that both male and female osteoblasts released more TGF-β1 into the media on A and SLA surfaces, and in response to $1\alpha,25(OH)_2D_3$ (Fig. 5-6). The active TGF-β1 levels were similar between male and female cells; however, female latent TGF-β1 levels were 1-2 fold higher than those in the culture of male cells (Fig. 5-7).
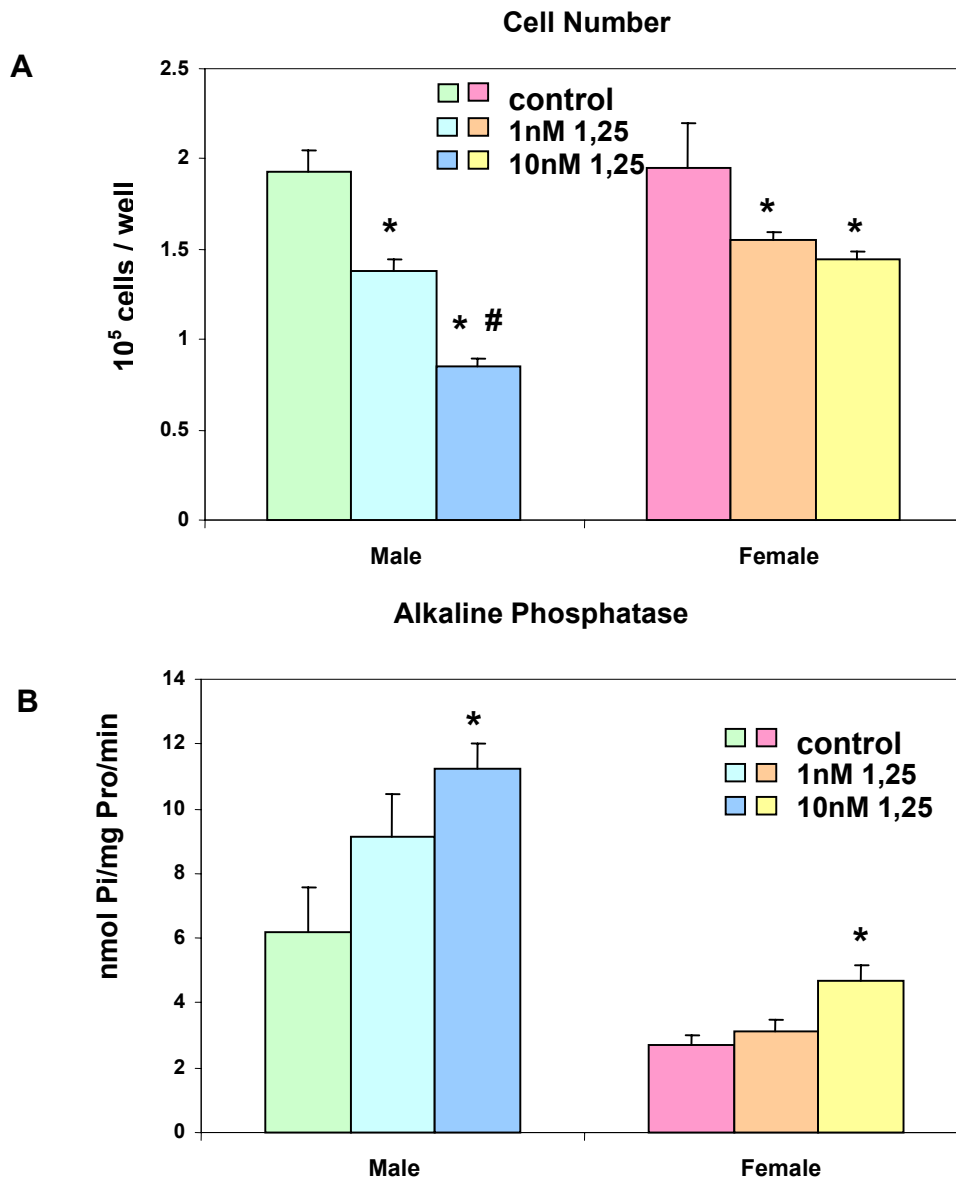
Cell Number

Alkaline Phosphatase

Figure 5-1. Characterization of rat calvarial osteoblast phenotype. Isolated male and female rat osteoblast cells were cultured on tissue culture treated polystyrene (TCPS). $1\alpha,25(OH)_2D_3$ (1 nM or 10 nM) or vehicle (control) was added at confluence and cells were incubated for an additional 24 hours. (A) Cell number was determined 24-hours after cells reached confluence on TCPS surfaces. (B) Alkaline phosphatase specific activity was measured in isolated cell lysates. (C) Osteocalcin levels were measured in conditioned media of confluent cultures. Values are means $\pm$ SEM of six independent cultures. Data are from one of two separate experiments, both with comparable results. Data were analyzed by ANOVA and significant differences between groups determined using the Bonferroni modification of Student's t-test. *$p<0.05$, v. control; #$p<0.05$, v. 1 nM $1\alpha,25(OH)_2D_3$.

Figure 5-1 Continued.

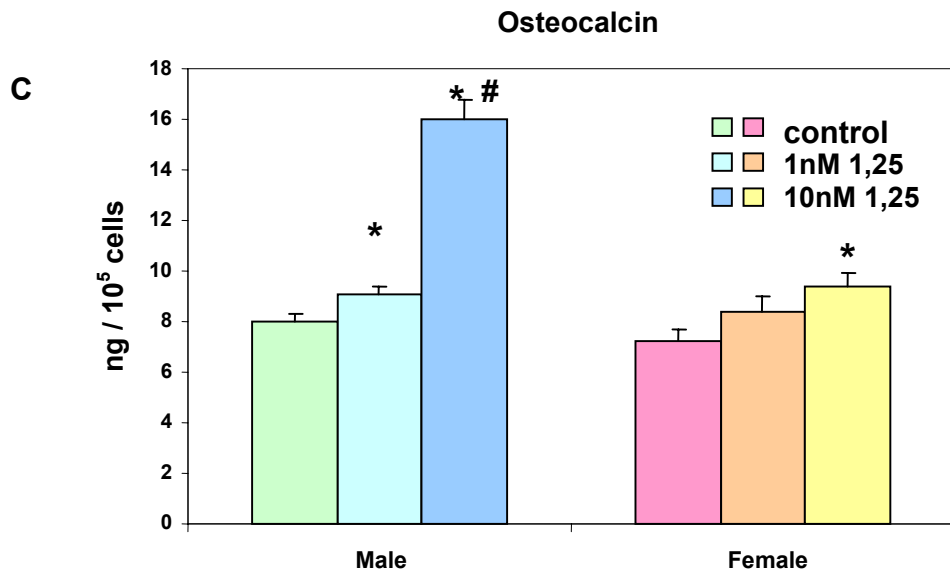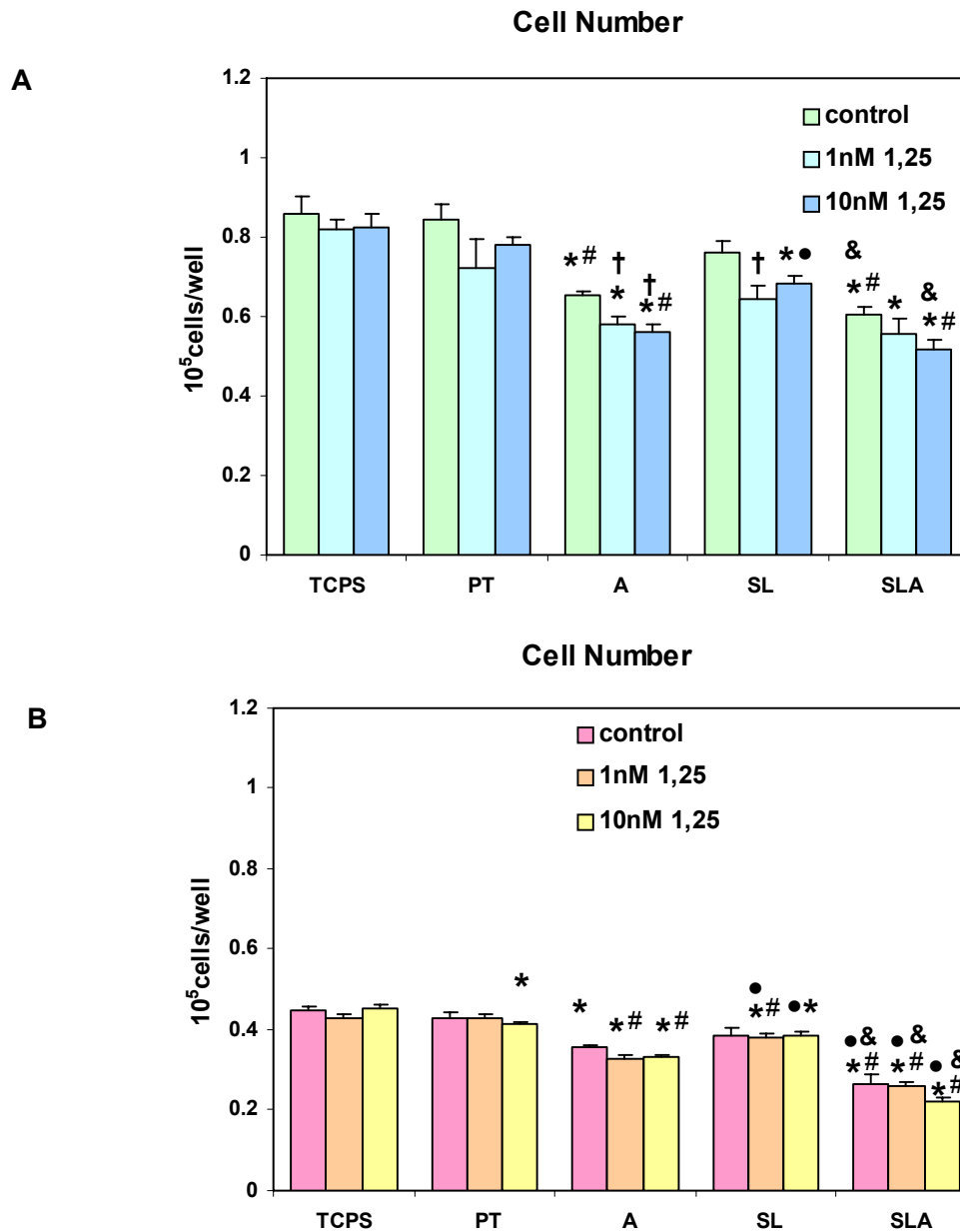**Cell Number**

Cell Number

Figure 5-2. Effect of surface microstructure on cell number of rat calvarial osteoblasts regulated by $1\alpha,25(OH)_2D_3$. Male (A) and female (B) rat calvarial osteoblasts were cultured on tissue culture plastic (TCPS), chemically polished Ti (PT), acid etched Ti (A), sand blasted Ti (SL) and sand blasted-acid etched Ti (SLA). $1\alpha,25(OH)_2D_3$ (1 nM or 10 nM) or vehicle (control) was added at confluence and cell numbers were determined 24 h after treatment. Values are means $\pm$ SEM of six independent cultures. Data are from one of two separate experiments, both with comparable results. Data were analyzed by ANOVA and significant differences between groups determined using the Bonferroni modification of Student's t-test. * $p<0.05$, Ti surfaces v. TCPS; # $p<0.05$, vs. PT; • $p<0.05$, v. A; & $p<0.05$, vs. SL; † $p<0.05$, $1\alpha,25(OH)_2D_3$ vs. control.

Alkaline Phosphatase

Alkaline Phosphatase
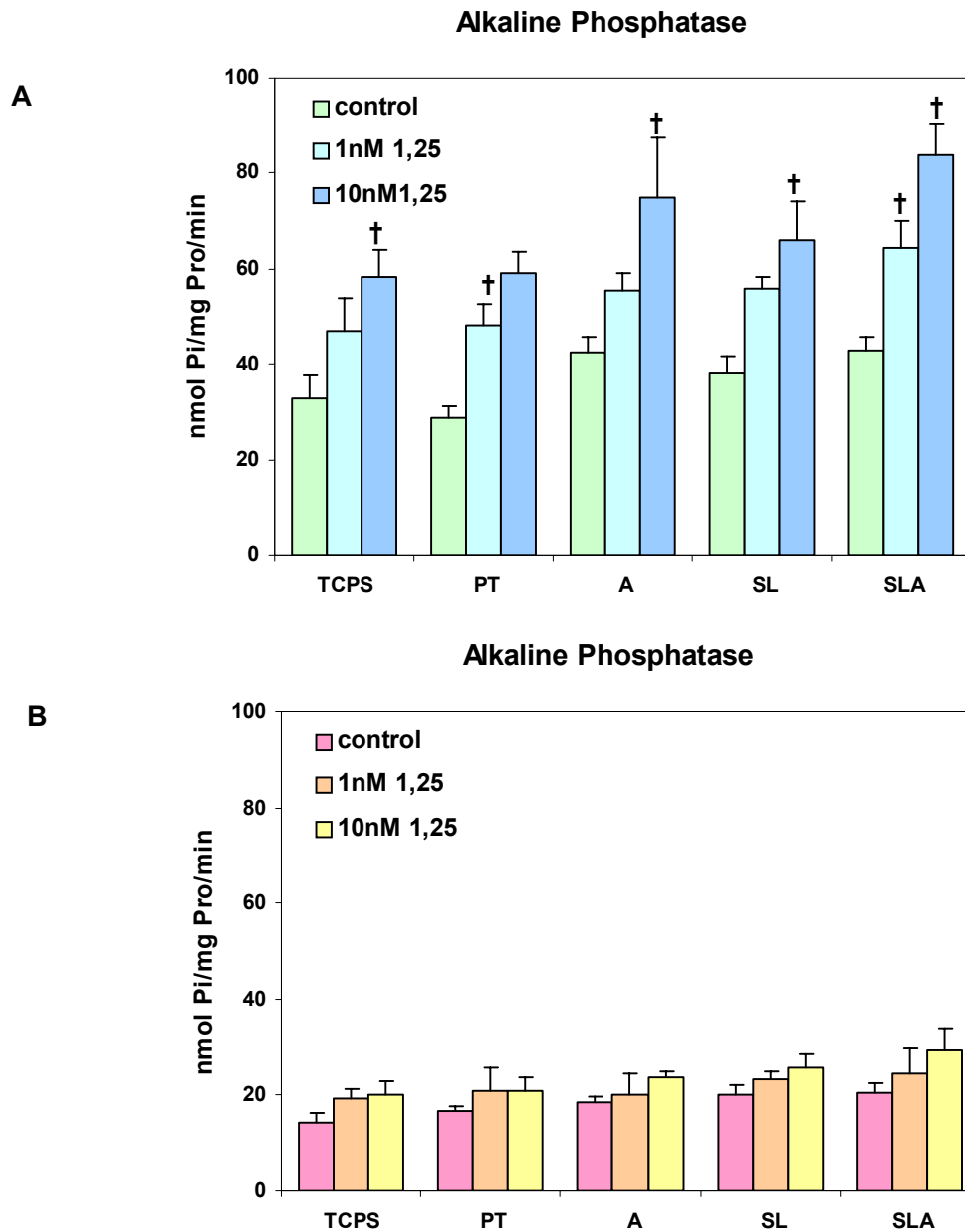

Figure 5-3. Effect of surface microstructure on alkaline phosphatase of rat calvarial osteoblasts regulated by $1\alpha,25(OH)_2D_3$. Male (A) and female (B) rat calvarial osteoblasts were cultured on tissue culture plastic (TCPS), chemically polished Ti (PT), acid etched Ti (A), sand blasted Ti (SL) and sand blasted-acid etched Ti (SLA). $1\alpha,25(OH)_2D_3$ (1 nM or 10 nM) or vehicle (control) was added at confluence and alkaline phosphatase activities in cell lysates were determined 24 h after treatment. Values are means $\pm$ SEM of six independent cultures. (C) Fold increase of _male_ alkaline phosphatase compared _to female_ cells. Data are from one of two separate experiments, both with comparable results. Data were analyzed by ANOVA and significant differences between groups determined using the Bonferroni modification of Student's t-test. $\dagger p<0.05$, $1\alpha,25(OH)_2D_3$ vs. control.

C

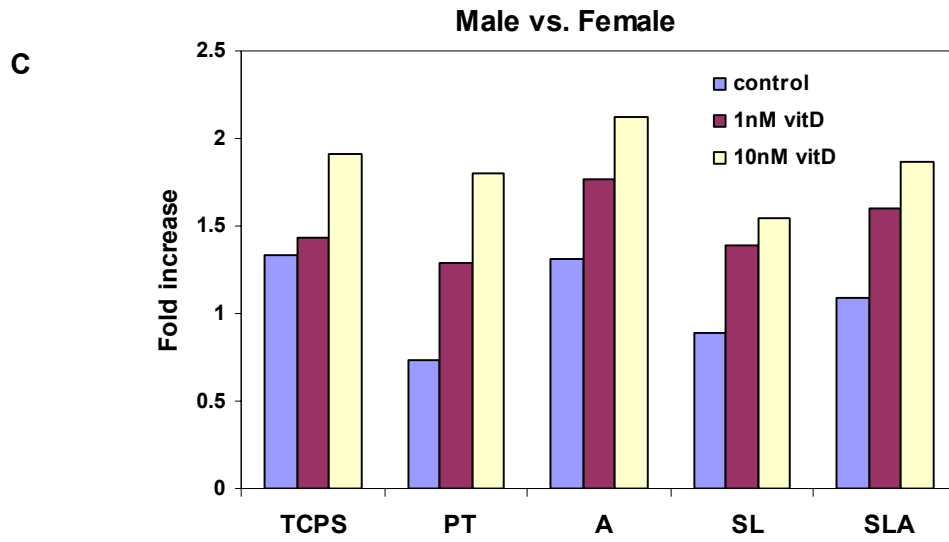Figure 5-3 Continued.

Osteocalcin

A

ng / 10⁵ cells

□ control
□ 1nM 1,25
□ 10nM 1,25

30

20

10

0

TCPS   PT   A   SL   SLA

Osteocalcin

B

ng / 10⁵ cells

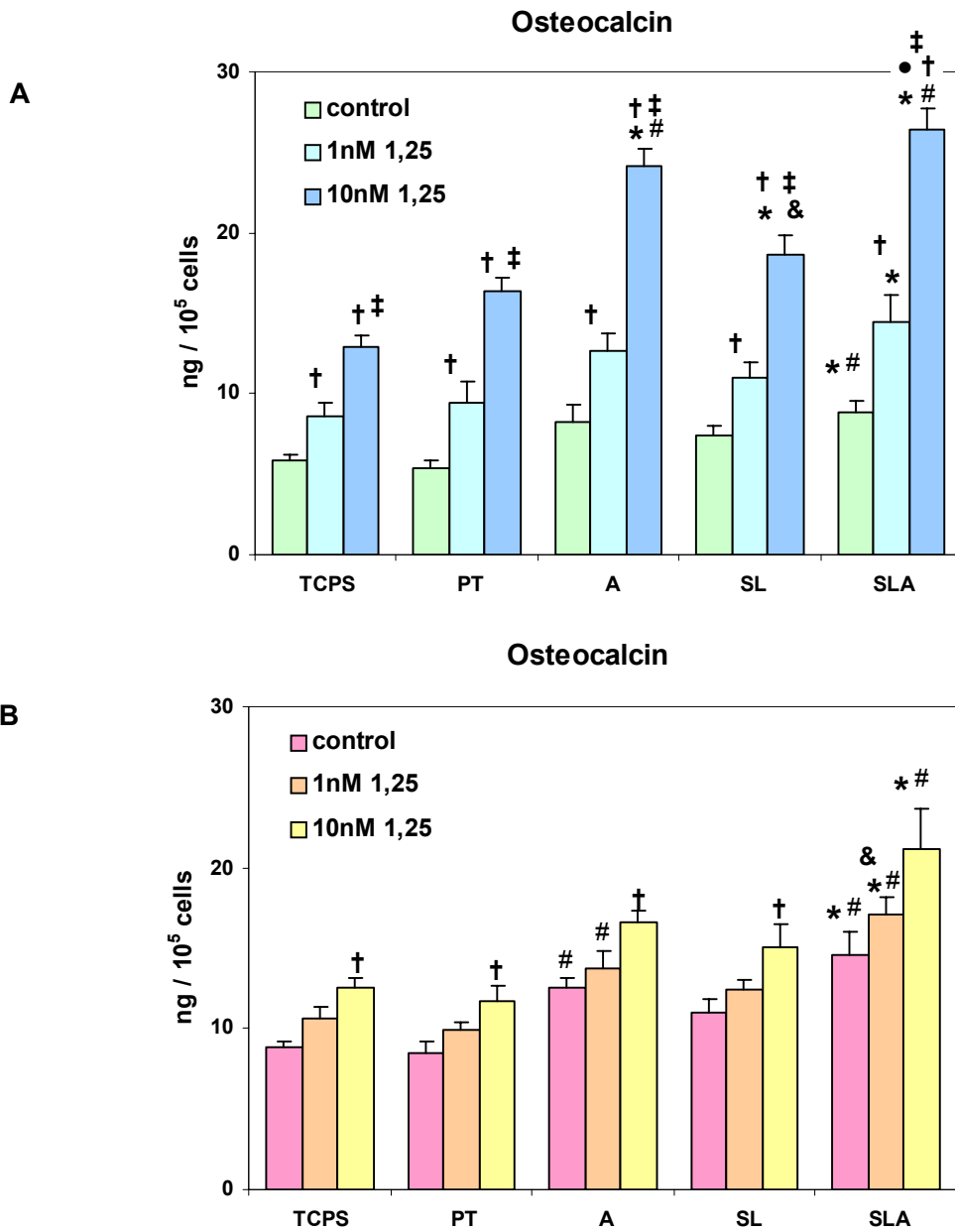□ control
□ 1nM 1,25
□ 10nM 1,25

30

20

10

0

TCPS   PT   A   SL   SLA

Figure 5-4. Effect of surface microstructure on osteocalcin levels of rat calvarial osteoblasts regulated by $1\alpha,25(OH)_2D_3$. Male (A) and female (B) rat calvarial osteoblasts were cultured on tissue culture plastic (TCPS), chemically polished Ti (PT), acid etched Ti (A), sand blasted Ti (SL) and sand blasted-acid etched Ti (SLA). $1\alpha,25(OH)_2D_3$ (1 nM or 10 nM) or vehicle (control) was added at confluence and osteocalcin levels in conditioned media were determined 24 h after treatment. Values are means $\pm$ SEM of six independent cultures. Data are from one of two separate experiments, both with comparable results. Data were analyzed by ANOVA and significant differences between groups determined using the Bonferroni modification of Student's t-test. * $p<0.05$, Ti surfaces v. TCPS; # $p<0.05$, vs. PT; • $p<0.05$, v. A; & $p<0.05$, vs. SL; †$p<0.05$, $1\alpha,25(OH)_2D_3$ vs. control, ‡ vs. 1 nM $1\alpha,25(OH)_2D_3$.

Osteoprotegerin

Osteoprotegerin
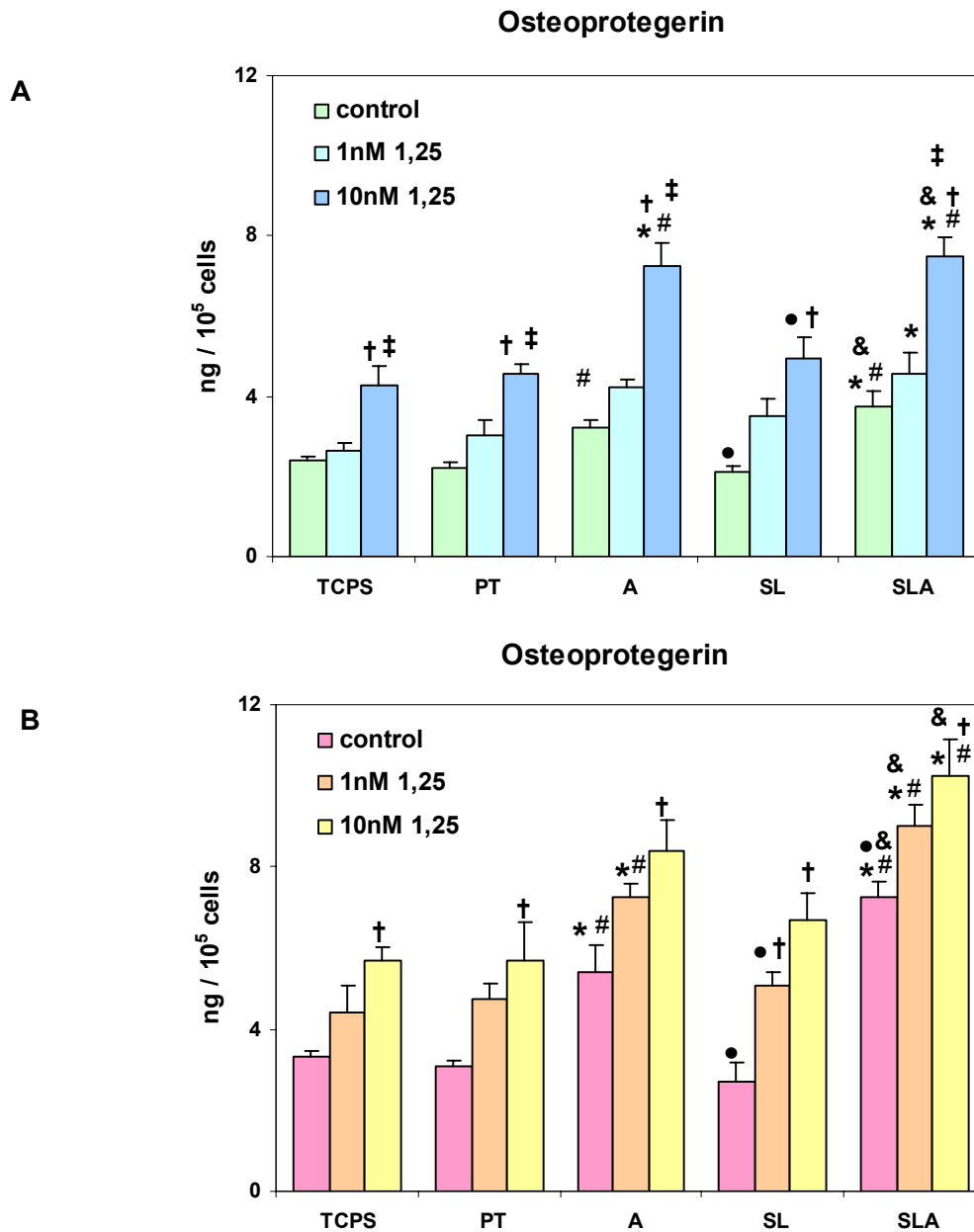

Figure 5-5. Effect of surface microstructure on osteoprotegerin levels of rat calvarial osteoblasts regulated by $1\alpha,25(OH)_2D_3$. Male (A) and female (B) rat calvarial osteoblasts were cultured on tissue culture plastic (TCPS), chemically polished Ti (PT), acid etched Ti (A), sand blasted Ti (SL) and sand blasted-acid etched Ti (SLA). $1\alpha,25(OH)_2D_3$ (1 nM or 10 nM) or vehicle (control) was added at confluence and osteoprotegerin levels in conditioned media were determined 24 h after treatment. Values are means $\pm$ SEM of six independent cultures. Data are from one of two separate experiments, both with comparable results. Data were analyzed by ANOVA and significant differences between groups determined using the Bonferroni modification of Student's t-test. * $p<0.05$, Ti surfaces v. TCPS; # $p<0.05$, vs. PT; • $p<0.05$, v. A; & $p<0.05$, vs. SL; †$p<0.05$, $1\alpha,25(OH)_2D_3$ vs. control, ‡ vs. 1 nM $1\alpha,25(OH)_2D_3$.

Figure 5-6. Effect of surface microstructure on active TGF-β1 levels of rat calvarial osteoblasts regulated by 1α,25(OH)$_2$D$_3$. Male (A) and female (B) rat calvarial osteoblasts were cultured on tissue culture plastic (TCPS), chemically polished Ti (PT), acid etched Ti (A), sand blasted Ti (SL) and sand blasted-acid etched Ti (SLA). 1α,25(OH)$_2$D$_3$ (1 nM or 10 nM) or vehicle (control) was added at confluence and active TGF-β1 levels in conditioned media were determined 24 h after treatment. Values are means $\pm$ SEM of six independent cultures. Data are from one of two separate experiments, both with comparable results. Data were analyzed by ANOVA and significant differences between groups determined using the Bonferroni modification of Student's t-test. * $p<0.05$, Ti surfaces v. TCPS; # $p<0.05$, vs. PT; • $p<0.05$, v. A; & $p<0.05$, vs. SL; †$p<0.05$, 1α,25(OH)$_2$D$_3$ vs. control, ‡ vs. 1 nM 1α,25(OH)$_2$D$_3$.

Latent TGF-β1

Latent TGF-β1
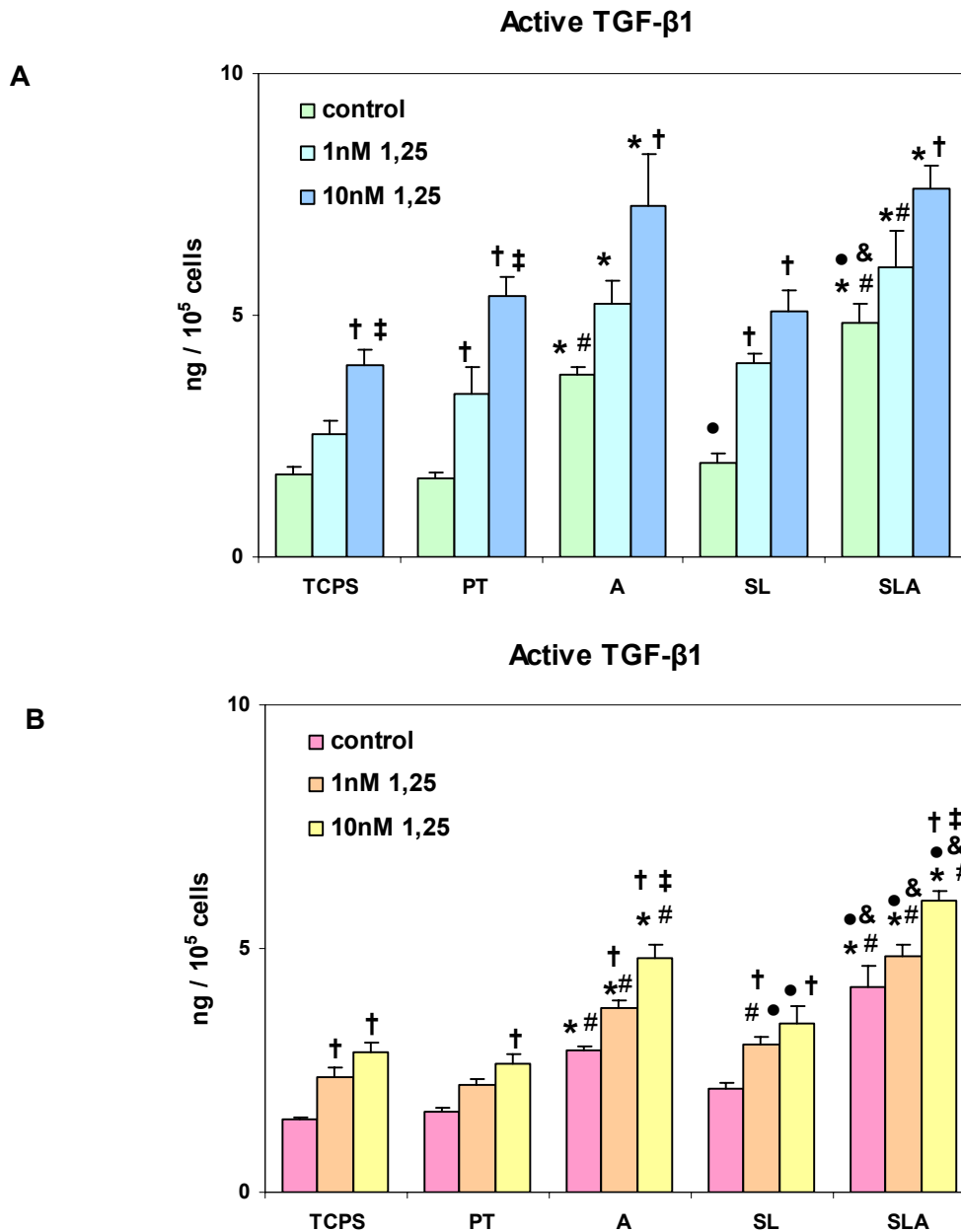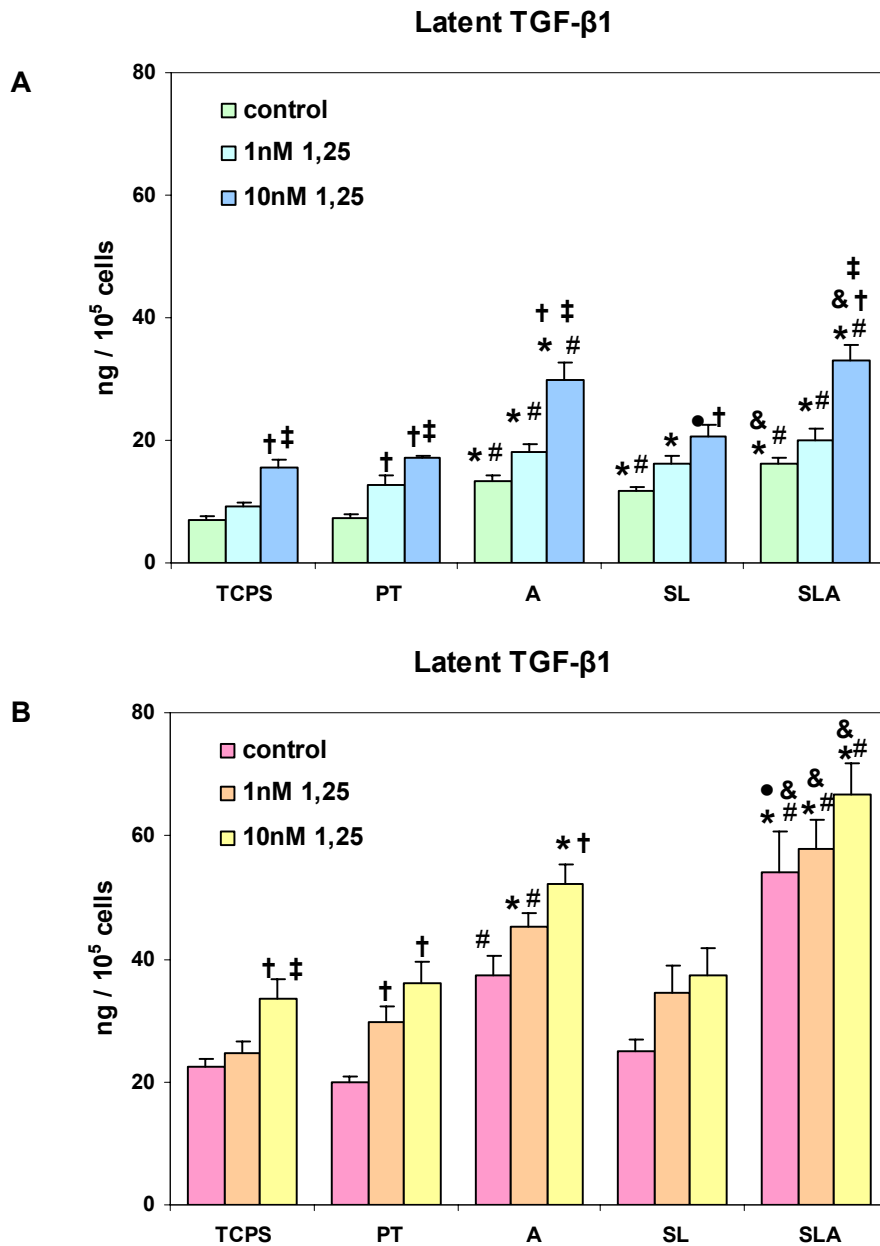

Figure 5-7. Effect of surface microstructure on latent TGF-β1 levels of rat calvarial osteoblasts regulated by $1\alpha,25(OH)_2D_3$. Male (A) and female (B) rat calvarial osteoblasts were cultured on tissue culture plastic (TCPS), chemically polished Ti (PT), acid etched Ti (A), sand blasted Ti (SL) and sand blasted-acid etched Ti (SLA). $1\alpha,25(OH)_2D_3$ (1 nM or 10 nM) or vehicle (control) was added at confluence and latent TGF-β1 levels in conditioned media were determined 24 h after treatment. Values are means $\pm$ SEM of six independent cultures. (C) Fold increase of <u>female</u> latent TGF-β1 compared <u>to male</u> cells. Data are from one of two separate experiments, both with comparable results. Data were analyzed by ANOVA and significant differences between groups determined using the Bonferroni modification of Student's t-test. * $p<0.05$, Ti surfaces v. TCPS; # $p<0.05$, vs. PT; • $p<0.05$, v. A; & $p<0.05$, vs. SL; †$p<0.05$, $1\alpha,25(OH)_2D_3$ vs. control, ‡ vs. 1 nM $1\alpha,25(OH)_2D_3$.
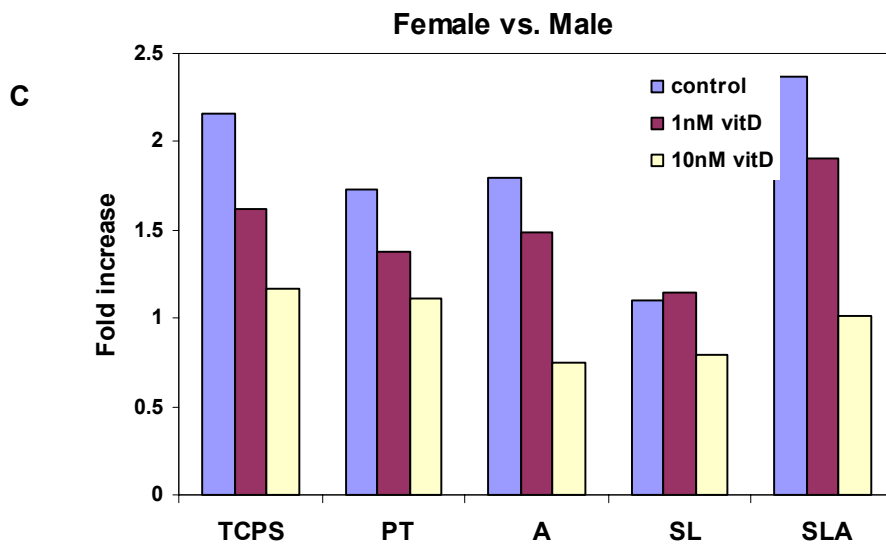
Figure 5-7 Continued.

The above results demonstrated explicit effects of SLA in modulating both male and female osteoblast differentiation and local factor production. Therefore, in the following experiment to examine whether effects of estradiol were sexually dimorphic, we only included TCPS, PT and SLA surfaces. E2-BSA is a big molecule that can not penetrate cell plasma membranes. Therefore, E2-BSA is only able to bind membrane estrogen receptors, but not receptors inside of the cell to activate the traditional nuclear receptor pathway.

As shown previously, both male and female cell numbers cultured on rough SLA surfaces were lower than those on TCPS and smooth PT surfaces (Fig. 5-8). E2 or E2-BSA treatment had no effects on male osteoblasts. 10 nM E2 treatment of cultures on TCPS decreased female rat cell number by 27%.

Alkaline phosphatase activities in both male and female isolated rat osteoblasts were lower in cultures grown on SLA surfaces (Fig. 5-9). E2 and E2-BSA increased the enzyme activity of female osteoblasts on SLA, but no effects were observed in male cells or female cells on smooth surfaces.

Osteoblasts on microstructured SLA surfaces produced 70-130% more osteocalcin than on TCPS and smooth PT surfaces (Fig. 5-10). Addition of E2 or E2-BSA had no effects on male cells. In contrast, E2 affected female rat osteoblast differentiation status represented by increasing osteocalcin approximately 50% on all surfaces. Female cell responses to the E2 or E2-BSA were similar on all surfaces.

Surface microtopography modulates osteoblasts through creating an osteogenic microenvironment. PGE_2 and TGF-β1 levels responded in a similar manner as osteocalcin (Fig. 5-11,12,13). Rat osteoblasts grown on SLA surfaces produced 2-3 fold higher PGE_2, and active and latent TGF-β1. E2 and E2-BSA increased these local factors in female osteoblasts by 40-60%, but did not have any statistically significant effects on male rat osteoblasts.

Figure 5-8. Effect of surface microstructure on cell number of rat calvarial osteoblasts regulated by 17β-estradiol (E2) or BSA conjugated estradiol (E2-BSA). Male (A) and female (B) rat calvarial osteoblasts were cultured on tissue culture plastic (TCPS), chemically polished Ti (PT), and sand blasted-acid etched Ti (SLA). 10 nM E2, 10 nM E2-BSA or vehicle (control) was added at confluence and cell numbers were determined 24 h after treatment. Values are means ± SEM of six independent cultures. Data are from one of two separate experiments, both with comparable results. Data were analyzed by ANOVA and significant differences between groups determined using the Bonferroni modification of Student's t-test. * $p < 0.05$, Ti surfaces v. TCPS; # $p < 0.05$, vs. PT; †$p < 0.05$, E2 or E2-BSA vs. control.

www.manaraa.com

Alkaline Phosphatase
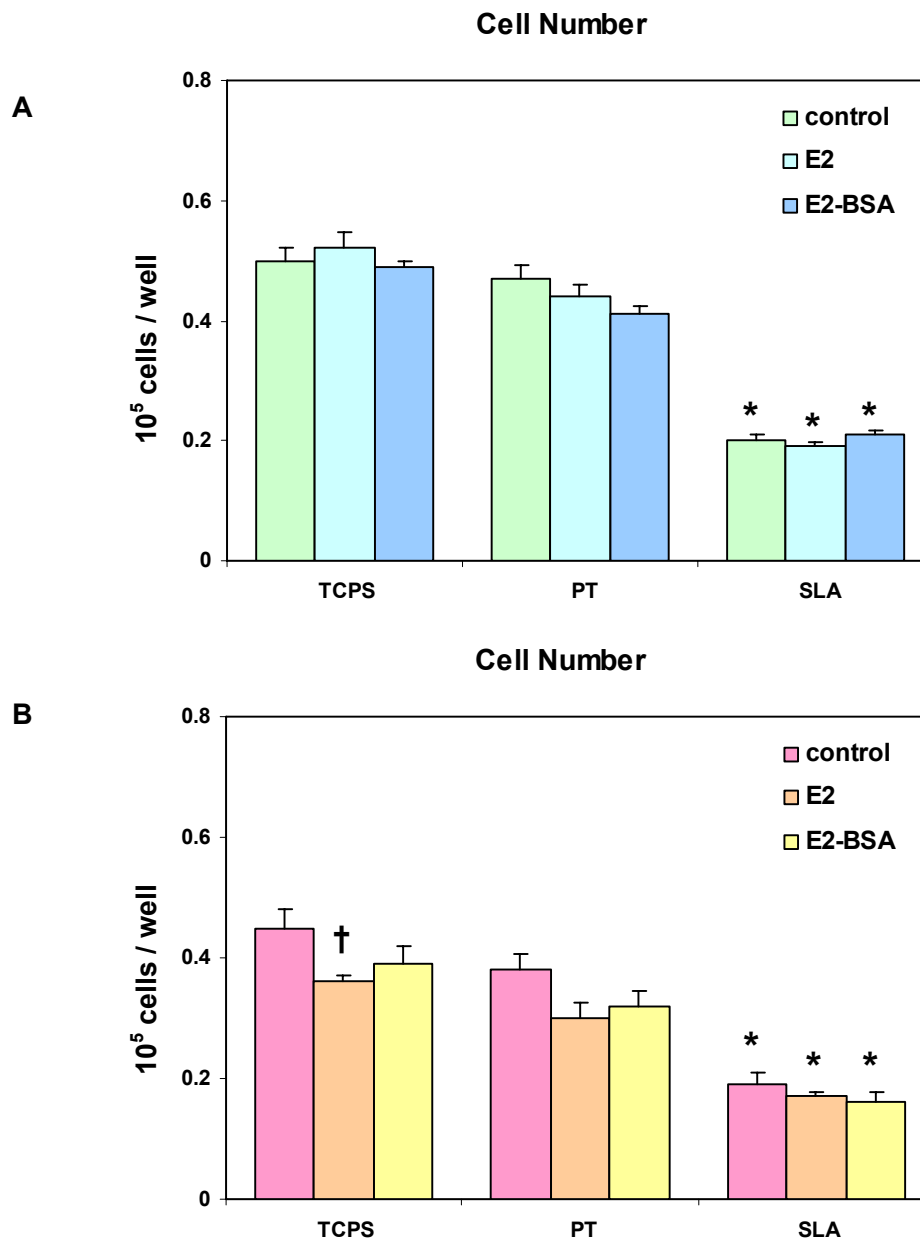
A

Alkaline Phosphatase

B

Figure 5-9. Effect of surface microstructure on alkaline phosphatase of rat calvarial osteoblasts regulated by 17β-estradiol (E2) or BSA conjugated estradiol (E2-BSA). Male (A) and female (B) rat calvarial osteoblasts were cultured on tissue culture plastic (TCPS), chemically polished Ti (PT), and sand blasted-acid etched Ti (SLA). 10 nM E2, 10 nM E2-BSA or vehicle (control) was added at confluence and alkaline phosphatase activities in cell lysates were determined 24 h after treatment. Values are means ± SEM of six independent cultures. Data are from one of two separate experiments, both with comparable results. Data were analyzed by ANOVA and significant differences between groups determined using the Bonferroni modification of Student's t-test. * $p<0.05$, Ti surfaces v. TCPS; # $p<0.05$, vs. PT; †$p<0.05$, E2 or E2-BSA vs. cntrol.

Osteocalcin

Osteocalcin

Figure 5-10.   Effect of surface microstructure on osteocalcin levels of rat calvarial osteoblasts regulated by 17β-estradiol (E2) or BSA conjugated estradiol (E2-BSA). Male (A) and female (B) rat calvarial osteoblasts were cultured on tissue culture plastic (TCPS), chemically polished Ti (PT), and sand blasted-acid etched Ti (SLA). 10 nM E2, 10 nM E2-BSA or vehicle (control) was added at confluence and osteocalcin levels in the conditioned media were determined 24 h after treatment. Values are means ± SEM of six independent cultures. Data are from one of two separate experiments, both with comparable results. Data were analyzed by ANOVA and significant differences between groups determined using the Bonferroni modification of Student's t-test. * p<0.05, Ti surfaces v. TCPS; # p<0.05, vs. PT; †p<0.05, E2 or E2-BSA vs. control.
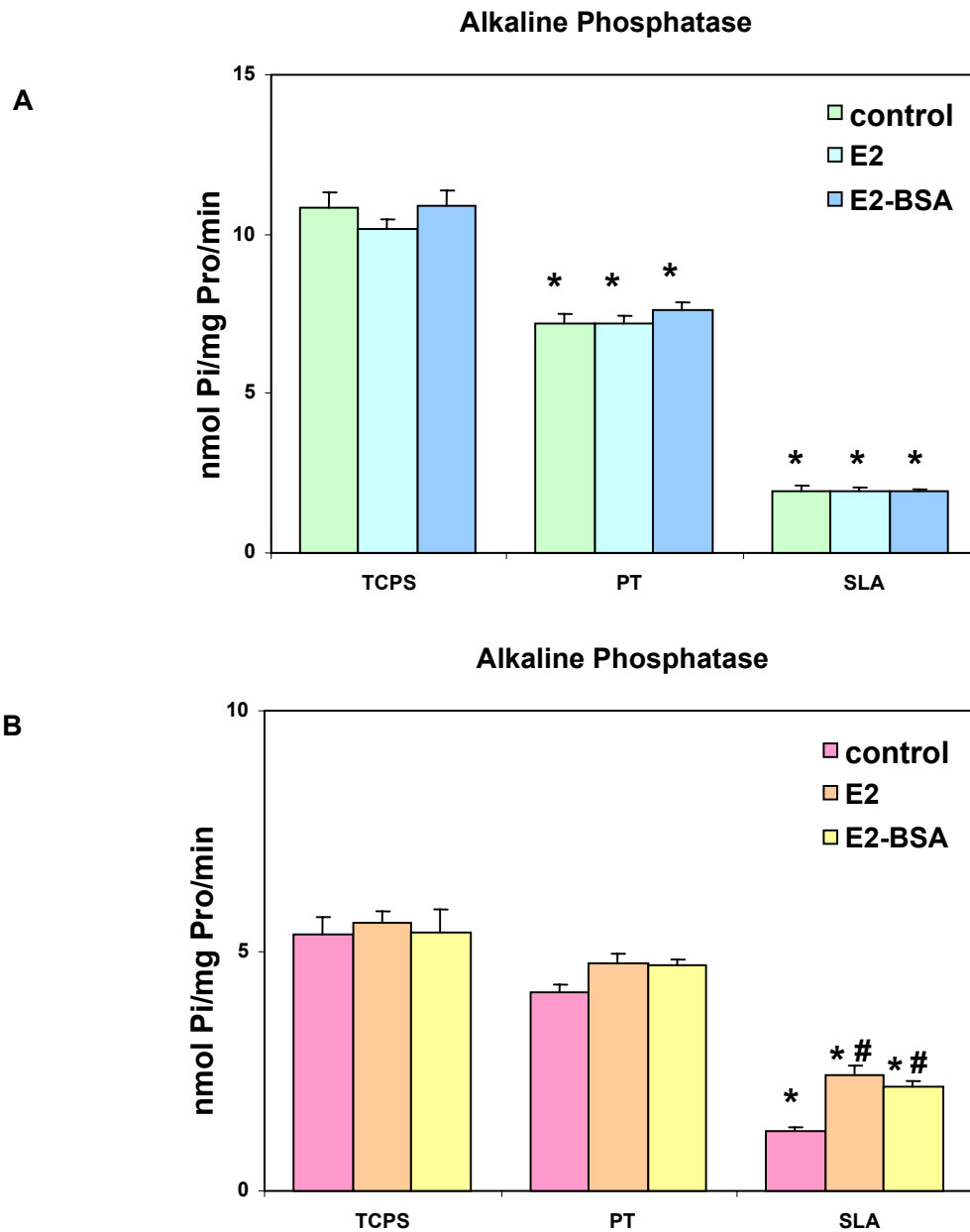
Figure 5-11. Effect of surface microstructure on PGE_2 levels of rat calvarial osteoblasts regulated by 17 β-estradiol (E2) or BSA conjugated estradiol (E2-BSA). Male (A) and female (B) rat calvarial osteoblasts were cultured on tissue culture plastic (TCPS), chemically polished Ti (PT), and sand blasted-acid etched Ti (SLA). 10 nM E2, 10 nM E2-BSA or vehicle (control) was added at confluence and PGE_2 levels in the conditioned media were determined 24 h after treatment. Values are means $\pm$ SEM of six independent cultures. Data are from one of two separate experiments, both with comparable results. Data were analyzed by ANOVA and significant differences between groups determined using the Bonferroni modification of Student's t-test. * $p < 0.05$, Ti surfaces v. TCPS; # $p < 0.05$, vs. PT; †$p < 0.05$, E2 or E2-BSA vs. control.
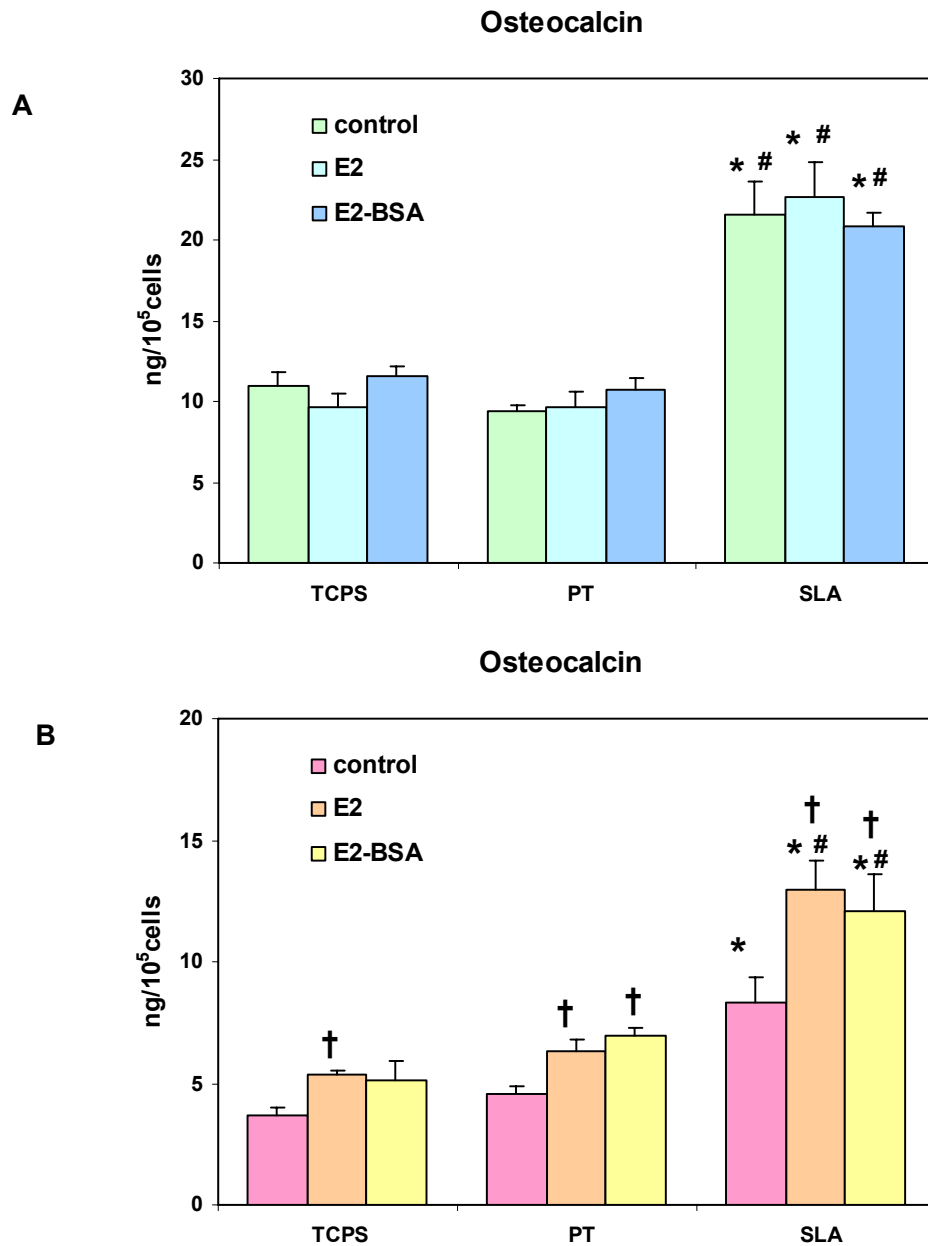
Active TGF-β1
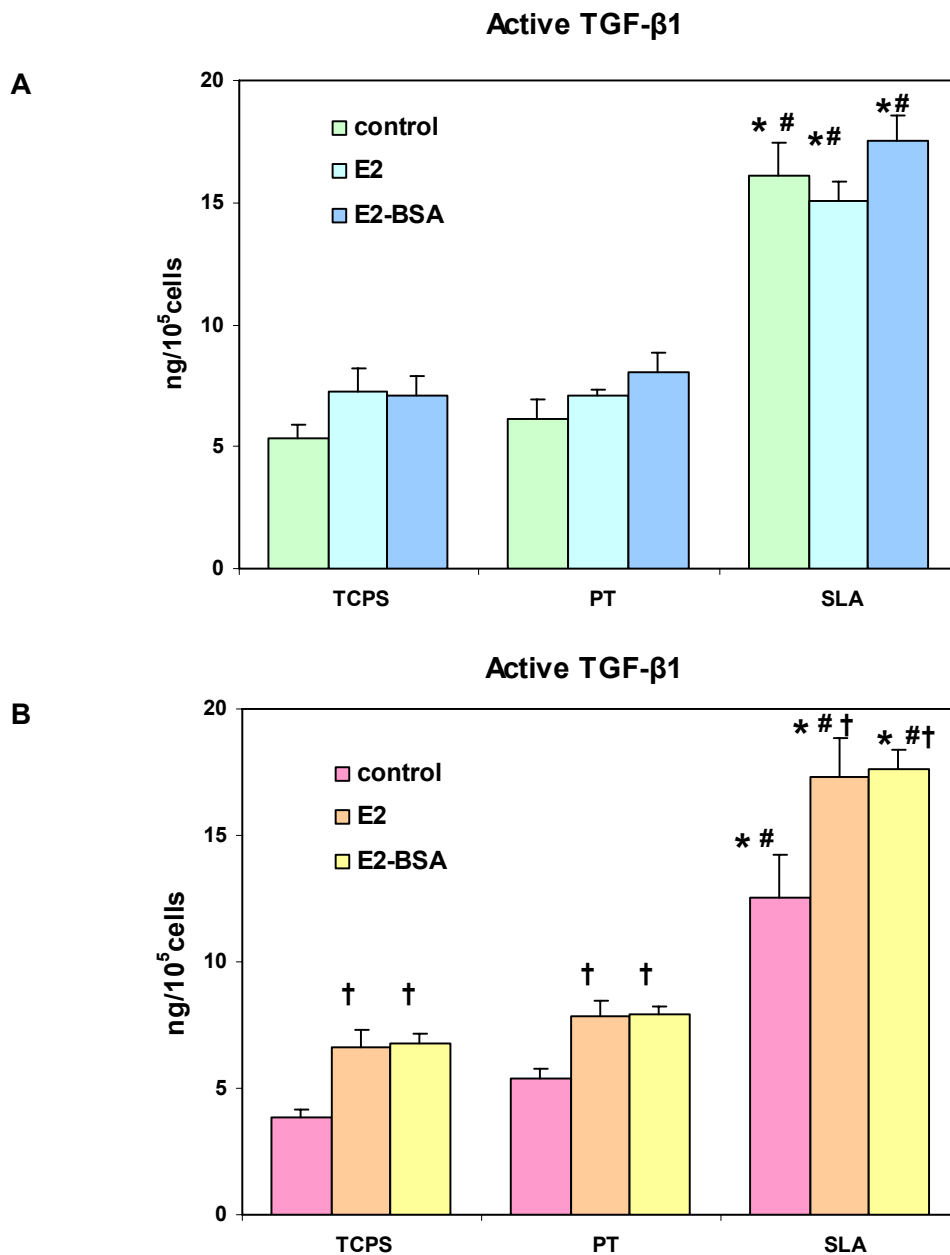
Active TGF-β1

Figure 5-12. Effect of surface microstructure on active TGF-β1 levels of rat calvarial osteoblasts regulated by 17β-estradiol (E2) or BSA conjugated estradiol (E2-BSA). Male (A) and female (B) rat calvarial osteoblasts were cultured on tissue culture plastic (TCPS), chemically polished Ti (PT), and sand blasted-acid etched Ti (SLA). 10 nM E2, 10 nM E2-BSA or vehicle (control) was added at confluence and active TGF-β1 levels in the conditioned media were determined 24 h after treatment. Values are means $\pm$ SEM of six independent cultures. Data are from one of two separate experiments, both with comparable results. Data were analyzed by ANOVA and significant differences between groups determined using the Bonferroni modification of Student's t-test. * $p<0.05$, Ti surfaces v. TCPS; # $p<0.05$, vs. PT; †$p<0.05$, E2 or E2-BSA vs. control.
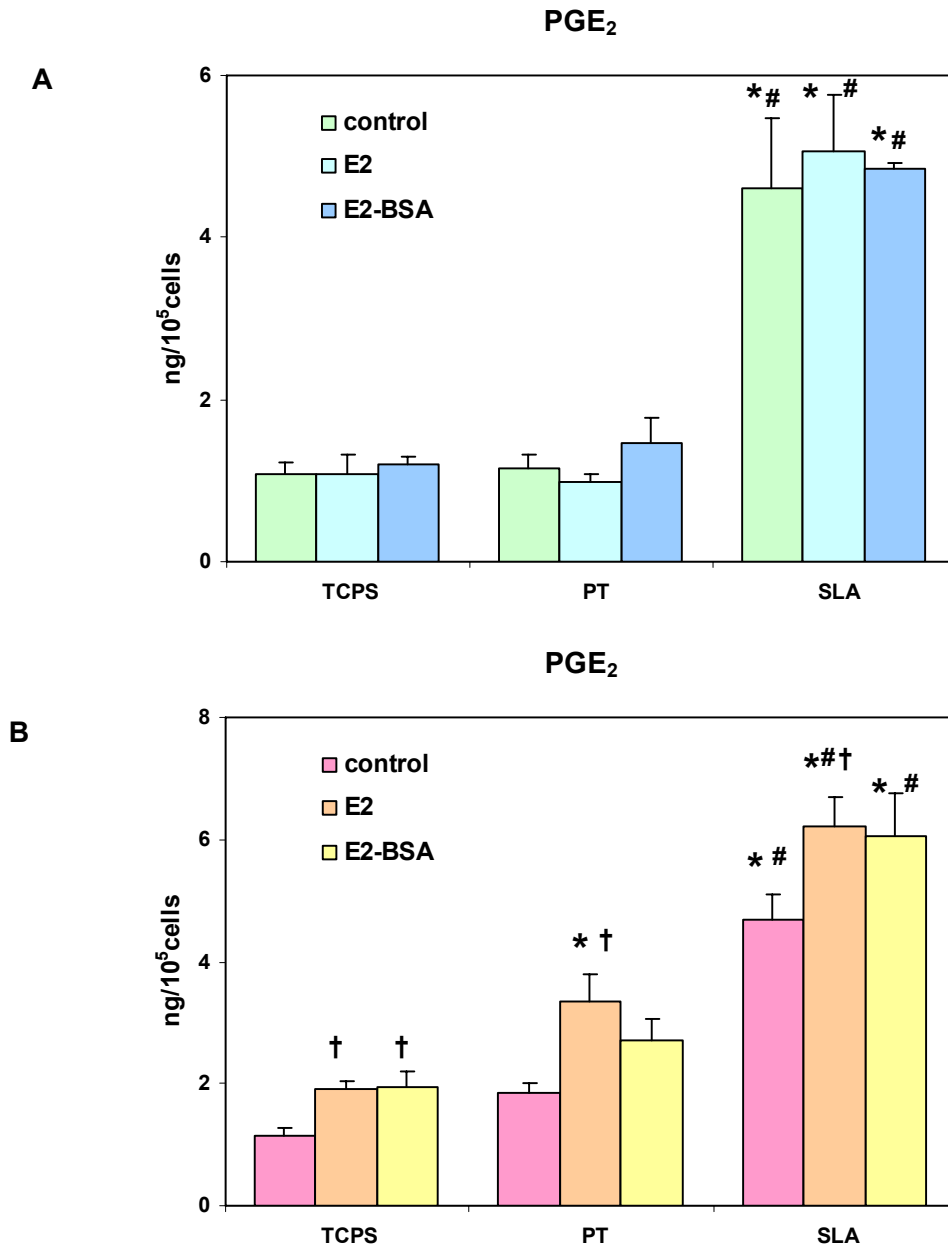
Figure 5-13. Effect of surface microstructure on latent TGF-β1 levels of rat calvarial osteoblasts regulated by 17β-estradiol (E2) or BSA conjugated estradiol (E2-BSA). Male (A) and female (B) rat calvarial osteoblasts were cultured on tissue culture plastic (TCPS), chemically polished Ti (PT), and sand blasted-acid etched Ti (SLA). 10 nM E2, 10 nM E2-BSA or vehicle (control) was added at confluence and latent TGF-β1 levels in the conditioned media were determined 24 h after treatment. Values are means $\pm$ SEM of six independent cultures. Data are from one of two separate experiments, both with comparable results. Data were analyzed by ANOVA and significant differences between groups determined using the Bonferroni modification of Student's t-test. * $p < 0.05$, Ti surfaces v. TCPS; # $p < 0.05$, vs. PT; † $p < 0.05$, E2 or E2-BSA vs. control.
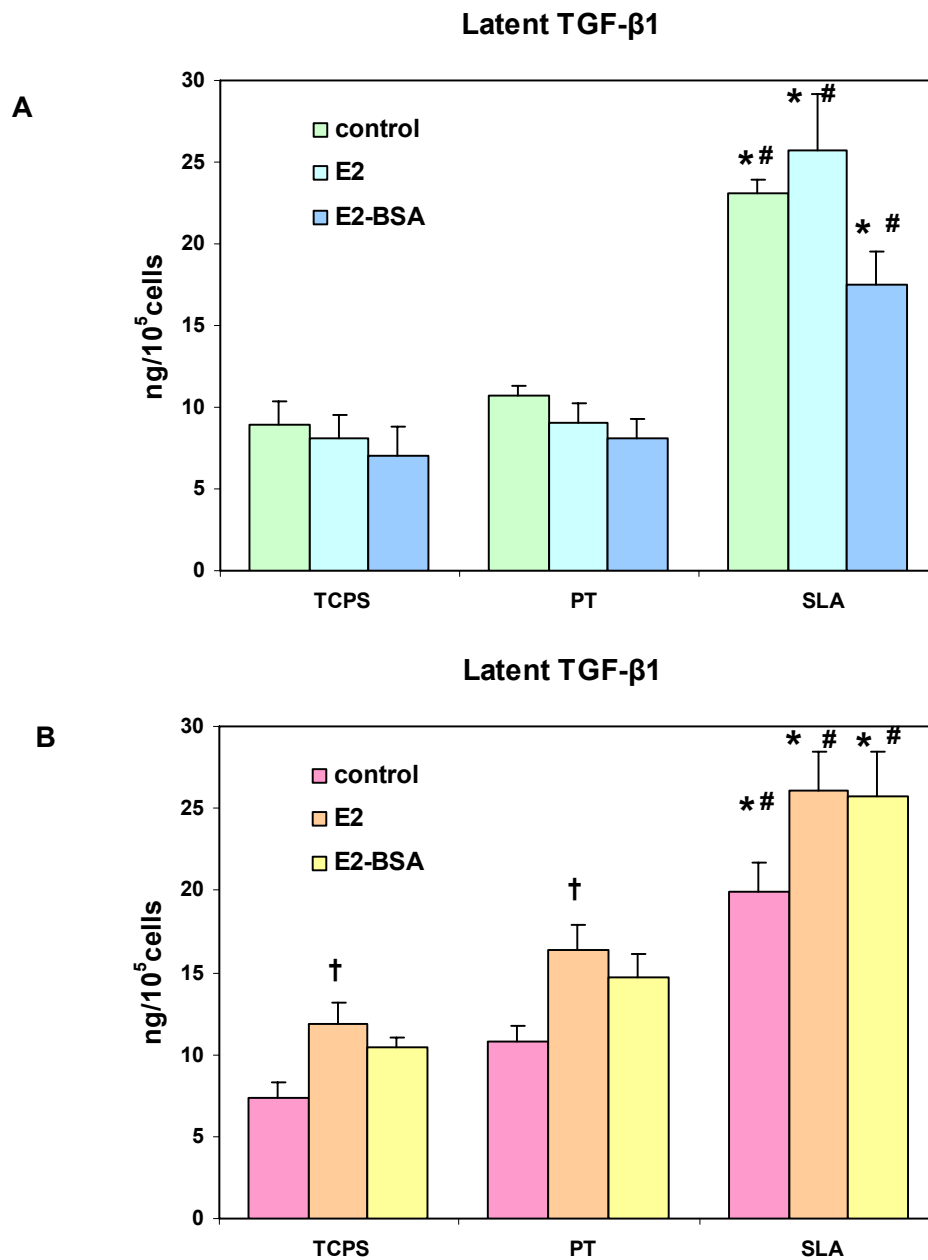
Discussion

In this study, rat osteoblasts were enzymatically isolated from calvarial bone and osteoblastic traits were confirmed by showing increased cell differentiation in response to $1\alpha,25(OH)_2D_3$. Both male and female rat osteoblasts exhibited decreased cell number, increased cell differentiation and local factor production when grown on rough Ti surfaces, as do human osteoblasts, indicating that osteoblast responses to surface microtopography are not species specific.

Treatment of cells with $1\alpha,25(OH)_2D_3$ stimulated rat osteoblast differentiation and local factor production. Osteocalcin levels were synergistically enhanced on microrough SLA surface with $1\alpha,25(OH)_2D_3$ treatment. These observations are similar to those in MG63 cells and fetal rat cavarial cells [5, 13], which are known to be relatively immature osteoblasts. More mature osteoblast-like cells, such as OCT-1 or osteocyte-like MLO-4 cells, did not respond to $1\alpha,25(OH)_2D_3$ or even exhibited decreased local factor production. Gerstenfeld et al. previously reported that immature osteoblasts are stimulated by $1\alpha,25(OH)_2D_3$, whereas mature osteoblasts are inhibited by $1\alpha,25(OH)_2D_3$ [21]. Taken together, results suggested that our enzymatically isolated osteoblasts from 6-week rat calvarial skeleton are relatively immature pre-osteoblasts.

The sexual dimorphism phenomenon in human bone is well known. Men's skeletons are 10% larger than women, have longer limbs, and higher proportions of bone and muscle. During aging, the amount of bone resorbed from the inner surface of the cortical bone is similar in male and female, but the amount of bone formed at the outer side is greater in males, resulting in more loss of trabecular bone quality and quantity in female [22].

Our results suggest that non sex hormones may also exert different effects on male and female bone cells. In this study, we observed a higher baseline of alkaline phosphatase activity and more sensitive response to $1\alpha,25(OH)_2D_3$ in male osteoblasts.

114

Previous study reported that surface roughness increased human osteoblast-like cell response to $1\alpha,25(OH)_2D_3$ [12]; but the study was only performed on male cell lines. In this study, male or female cells were collected from 8 rats. The rats of the same sex were euthanized at the same day and cells were harvested together. Male and female cells were collected at a week apart. To eliminate the concern that differences between male and female cell behavior are artifacts of different tissue culture conditions, we strictly controlled culture conditions, including using same seeding density, culture media, isolation procedures, processes to sterilize the Ti surfaces and performing biochemical analysis at the same time. Therefore, the results indicate there are inherent sexual dimorphic phenotypes of osteoblasts and different responses to $1\alpha,25(OH)_2D_3$. The mechanism of this phenomenon is not clear. It is possible to be related to different $1\alpha,25(OH)_2D_3$ receptor expression in male and female cells. Rats reach sexually mature at 6-weeks of age, corresponding to puberty in human beings. It is also important to determine whether the sexual dimorphism we observed are because of different maturation status in male and females.

Estrogen plays a major role in regulating bone remodeling in females, including inhibition of the activation of bone remodeling units, suppressing bone resorption and stimulating bone formation. Deficiency of estrogen causes in an imbalance between bone resorption and bone formation and results a net loss of bone [23]. In the last decade, an estrogen effect on male skeleton was also established, although not as extensive as in females. Males with deficiency of estrogen receptors or aromatase had defects in skeletal phenotypes [24-26]. During aging female bone loss is due to an increased rate of bone resorption. In contrast male bone loss is the results of less bone formation [27]. There is also sex-related difference of osteocyte lacunar density in human vertebral cancellous bone [28]. Sexual dimorphism may be attributed to

115

differences in estrogen receptor isoform expression [29]. An alternate explanation is the different aromatase activities that convert testosterone into 17β-estradiol [30].

Previous study showed that estrogen effects on female human osteoblasts are synergistic with surface microtopography [31]. 17β-estradiol had no effect on osteoblast markers or growth factors on TCPS or smooth PT surface, but caused dose dependent increases on rough SLA surfaces. In this study, we did not observe synergistic effects between estrogen and surface structure. 17β-estradiol increased cell differentiation to the same extent on all surfaces, including TCPS.

Both promotive [32, 33] and inhibitory [34] effects of estrogen on osteoblast proliferation have been reported. Osteoblast differentiation, matrix formation and mineralization are dependent on osteoblast maturation and estrogen receptor isoform expression [35]. The effect of 17β-estradiol on osteoblastic prostaglandin biosynthesis is also controversial. Studies in fetal mouse showed that estrogen inhibited parathyroid stimulated prostaglandin production [36]. Ovariectomized rats had higher PGE_2 release, and *in vivo* injection of estrogen inhibited PGE_2 levels [37]. Other studies indicated opposite effects of estrogen. Secreto et al. found that in the presence of multiple osteotropic cytokines such as TGF-β and tumor necrosis factor-α, both male and female human osteoblasts responded to 17β-estradiol with increased levels of PGE_2 [31]. We previously reported that female human osteoblasts on microrough Ti also responded to 17β-estradiol with enhanced PGE_2 [38]. The different results among these studies reflect the complicated mechanism of estrogen, and the results should be interpreted with consideration of cell species, adult or fetal cell culture, differentiation stage and estrogen receptor expression. Moreover, the presence of phenol red in regular media acts as a weak estrogen [39], and may interfere with the experimental treatment. Therefore, phenol red free and serum free media will be ideal to exclude the interference of other unknown factors.

116

The traditional signaling pathway of estrogen is through its nuclear receptor, which binds estrogen with high affinity and associates with estrogen response elements in the promoter regions of target genes. Recently, membrane estrogen receptors have also been shown to play an important role in regulating cell growth non-genomic actions of estrogen [40]. This alternate mechanism is characterized by rapid activation of cytosolic signaling pathway, and insensitivity to transcriptional inhibitors. No distinct membrane associated estrogen receptor isoform has been identified. Instead, it is generally accepted that membrane localized estrogen receptors are the same as and in equilibrium with cellular receptors. E2-BSA only binds to membrane estrogen receptors because it is too large to penetrate plasma membrane and bind to the nuclear receptor. The results show that both 17β-estradiol and E2-BSA increases female osteoblast differentiation and local factor production to a similar level, suggesting that in surface dependent osteoblasts, estrogen functions mainly through the membrane receptor. In this study, we measured differentiation markers and local factors produced by cells and accumulated in the media for 24 h. It is not sure whether these molecules were most released in the early stage of treatment as a rapid response, or they are continuously accumulated in the media. To solve this problem, further studies should be performed to examine rapid response of osteoblasts to E2-BSA.

The results of this study revealed the physiological difference in male and female osteoblasts and sexual dimorphism in the response to bone regulating hormones. Currently, most preclinical studies of therapeutic interventions are performed in only male or only female animal models. Further investigations on sex specific differences should be performed to better understand cellular responses to biomaterials.

References

1. Goldberg VM, Jinno T. The bone-implant interface: a dynamic surface. J Long Term Eff Med Implants 1999; 9: 11-21.

2. Buser D, Schenk RK, Steinemann S, Fiorellini JP, Fox CH, Stich H. Influence of surface characteristics on bone integration of titanium implants. A histomorphometric study in miniature pigs. J.Biomed.Mater.Res. 1991; 25: 889-902.

3. Wennerberg A, Albrektsson T, Andersson B, Krol JJ. A histomorphometric and removal torque study of screw-shaped titanium implants with three different surface topographies. Clin.Oral Implants.Res. 1995; 6: 24-30.

4. Brunette DM, Ratkay J, Chehroudi B, Davies JE. Behaviour of osteoblasts on micromachined surfaces. In: The Bone-Biomaterial Interface. Toronto, Ontario: University of Toronto Press; 1991: 170-180.

5. Martin JY, Schwartz Z, Hummert TW, Schraub DM, Simpson J, Lankford J, Dean DD, Cochran DL, Boyan BD. Effect of Titanium Surface-Roughness on Proliferation, Differentiation, and Protein-Synthesis of Human Osteoblast-Like Cells (Mg63). J.Biomed.Mater.Res. 1995; 29: 389-401.

6. Deligianni DD, Katsala N, Ladas S, Sotiropoulou D, Amedee J, Missirlis YF. Effect of surface roughness of the titanium alloy Ti-6Al-4V on human bone marrow cell response and on protein adsorption. Biomaterials 2001; 22: 1241-1251.

7. Boyan BD, Schwartz Z, Lohmann CH, Sylvia VL, Cochran DL, Dean DD, Puzas JE. Pretreatment of bone with osteoclasts affects phenotypic expression of osteoblast-like cells. J Orthop.Res 2003; 21: 638-647.

8. Zinger O, Zhao G, Schwartz Z, Simpson J, Wieland M, Landolt D, Boyan B. Differential regulation of osteoblasts by substrate microstructural features. Biomaterials 2005; 26: 1837-1847.

9. Zhao G, Zinger O, Schwartz Z, Wieland M, Landolt D, Boyan BD. Osteoblast-like cells are sensitive to submicron-scale surface structure. Clin.Oral Implants Res. 2006; 17: 258-264.

10. Boyan BD, Lossdorfer S, Wang L, Zhao G, Lohmann CH, Cochran DL, Schwartz Z. Osteoblasts generate an osteogenic microenvironment when grown on surfaces with rough microtopographies. Eur.Cell Mater. 2003; 6: 22-27.

11. Ong JL, Carnes DL, Cardenas HL, Cavin R. Surface roughness of titanium on bone morphogenetic protein-2 treated osteoblast cells in vitro. Implant.Dent. 1997; 6: 19-24.

12. Boyan BD, Batzer R, Kieswetter K, Liu Y, Cochran DL, Szmuckler-Moncler S, Dean DD, Schwartz Z. Titanium surface roughness alters responsiveness of MG63 osteoblast-like cells to 1 alpha,25-(OH)(2)D-3. J.Biomed.Mater.Res. 1998; 39: 77-85.

13. Lohmann CH, Bonewald LF, Sisk MA, Sylvia VL, Cochran DL, Dean DD, Boyan BD, Schwartz Z. Maturation state determines the response of osteogenic cells to surface roughness and 1,25-dihydroxyvitamin D-3. Journal of Bone and Mineral Research 2000; 15: 1169-1180.

14. Tosi LL, Boyan BD, Boskey AL. Does sex matter in musculoskeletal health? The influence of sex and gender on musculoskeletal health. J Bone Joint Surg Am 2005; 87: 1631-1647.

15. Pan J, Shirota T, Ohno K, Michi K. Effect of ovariectomy on bone remodeling adjacent to hydroxyapatite-coated implants in the tibia of mature rats. J.Oral Maxillofac.Surg. 2000; 58: 877-882.

16. Yamazaki M, Shirota T, Tokugawa Y, Motohashi M, Ohno K, Michi K, Yamaguchi A. Bone reactions to titanium screw implants in ovariectomized animals. Oral Surg.Oral Med.Oral Pathol.Oral Radiol.Endod. 1999; 87: 411-418.

17. Martin RB, Paul HA, Bargar WL, Dannucci GA, Sharkey NA. Effects of estrogen deficiency on the growth of tissue into porous titanium implants. J.Bone Joint Surg.Am. 1988; 70: 540-547.

18. Rupp F, Scheideler L, Olshanska N, de Wild M, Wieland M, Geis-Gerstorfer J. Enhancing surface free energy and hydrophilicity through chemical modification of microstructured titanium implant surfaces. J.Biomed.Mater Res.A 2006; 76: 323-334.

19. Bretaudiere JP, Spillman T, Bergmeyer HU. Alkaline phosphatases. In: Methods of Enzymatic Analysis. Weinheim, Germany: Verlag Chemica; 1984: 75-92.

20. Lossdorfer S, Schwartz Z, Wang L, Lohmann CH, Turner JD, Wieland M, Cochran DL, Boyan BD. Microrough implant surface topographies increase osteogenesis by reducing osteoclast formation and activity. J Biomed Mater Res 2004; 70A: 361-369.

21. Gerstenfeld LC, Zurakowski D, Schaffer JL, Nichols DP, Toma CD, Broess M, Bruder SP, Caplan AI. Variable hormone responsiveness of osteoblast populations isolated at different stages of embryogenesis and its relationship to the osteogenic lineage. Endocrinology 1996; 137: 3957-3968.

22. Seeman E. Clinical review 137: Sexual dimorphism in skeletal size, density, and strength. J Clin Endocrinol Metab 2001; 86: 4576-4584.

23. Syed F, Khosla S. Mechanisms of sex steroid effects on bone. Biochem Biophys Res Commun 2005; 328: 688-696.

24. Smith EP, Boyd J, Frank GR, Takahashi H, Cohen RM, Specker B, Williams TC, Lubahn DB, Korach KS. Estrogen resistance caused by a mutation in the estrogen-receptor gene in a man. N Engl J Med 1994; 331: 1056-1061.

25. Morishima A, Grumbach MM, Simpson ER, Fisher C, Qin K. Aromatase deficiency in male and female siblings caused by a novel mutation and the physiological role of estrogens. J Clin Endocrinol Metab 1995; 80: 3689-3698.

26. Carani C, Qin K, Simoni M, Faustini-Fustini M, Serpente S, Boyd J, Korach KS, Simpson ER. Effect of testosterone and estradiol in a man with aromatase deficiency. N Engl J Med 1997; 337: 91-95.

27. Aaron JE, Makins NB, Sagreiya K. The microanatomy of trabecular bone loss in normal aging men and women. Clin Orthop Relat Res 1987: 260-271.

28. Vashishth D, Gibson GJ, Fyhrie DP. Sexual dimorphism and age dependence of osteocyte lacunar density for human vertebral cancellous bone. Anat Rec A Discov Mol Cell Evol Biol 2005; 282: 157-162.

29. Batra GS, Hainey L, Freemont AJ, Andrew G, Saunders PT, Hoyland JA, Braidman IP. Evidence for cell-specific changes with age in expression of oestrogen receptor (ER) alpha and beta in bone fractures from men and women. J Pathol 2003; 200: 65-73.

30. Oz OK, Zerwekh JE, Fisher C, Graves K, Nanu L, Millsaps R, Simpson ER. Bone has a sexually dimorphic response to aromatase deficiency. J.Bone Miner.Res. 2000; 15: 507-514.

31. Lohmann CH, Tandy EM, Sylvia VL, Hell-Vocke AK, Cochran DL, Dean DD, Boyan BD, Schwartz Z. Response of normal female human osteoblasts (NHOst)

to 17 beta-estradiol is modulated by implant surface morphology. J.Biomed.Mater.Res. 2002; 62: 204-213.

32. Ernst M, Heath JK, Rodan GA. Estradiol effects on proliferation, messenger ribonucleic acid for collagen and insulin-like growth factor-I, and parathyroid hormone-stimulated adenylate cyclase activity in osteoblastic cells from calvariae and long bones. Endocrinology 1989; 125: 825-833.

33. Slootweg MC, Swolin D, Netelenbos JC, Isaksson OG, Ohlsson C. Estrogen enhances growth hormone receptor expression and growth hormone action in rat osteosarcoma cells and human osteoblast-like cells. J Endocrinol 1997; 155: 159-164.

34. Waters KM, Rickard DJ, Riggs BL, Khosla S, Katzenellenbogen JA, Katzenellenbogen BS, Moore J, Spelsberg TC. Estrogen regulation of human osteoblast function is determined by the stage of differentiation and the estrogen receptor isoform. J Cell Biochem 2001; 83: 448-462.

35. Pilbeam CC, Klein-Nulend J, Raisz LG. Inhibition by 17 beta-estradiol of PTH stimulated resorption and prostaglandin production in cultured neonatal mouse calvariae. Biochem.Biophys.Res.Commun. 1989; 163: 1319-1324.

36. Feyen JH, Raisz LG. Prostaglandin production by calvariae from sham operated and oophorectomized rats: effect of 17 beta-estradiol in vivo. Endocrinology 1987; 121: 819-821.

37. Secreto FJ, Grover A, Pacurari M, Rice MB, Kantorow M, Bidwai AP, Blaha JD, Keeting PE. Estrogen potentiates the combined effects of transforming growth factor-beta and tumor necrosis factor-alpha on adult human osteoblast-like cell prostaglandin E2 biosynthesis. Calcif.Tissue Int. 2003; 73: 565-574.

38. Monroe DG, Spelsberg TC. A case for estrogen receptors on cell membranes and nongenomic actions of estrogen. Calcif.Tissue Int. 2003; 72: 183-184.

39. Berthois Y, Katzenellenbogen JA, Katzenellenbogen BS. Phenol red in tissue culture media is a weak estrogen: implications concerning the study of estrogen-responsive cells in culture. Proc.Natl.Acad.Sci.U.S.A 1986; 83: 2496-2500.

40. Kousteni S, Bellido T, Plotkin LI, O'Brien CA, Bodenner DL, Han L, Han K, DiGregorio GB, Katzenellenbogen JA, Katzenellenbogen BS, Roberson PK, Weinstein RS, Jilka RL, Manolagas SC. Nongenotropic, sex-nonspecific signaling through the estrogen or androgen receptors: dissociation from transcriptional activity. Cell 2001; 104: 719-730.

CHAPTER 6. DISCUSSION

In Vitro Cell Culture Model

Various modification methods on biomaterial surfaces have been investigated with the intention of achieving a desired host tissue response to implants. Conventional biomaterial research has been based on trial and error optimization instead of intentional design to favor selective cell and tissue behavior. For example, the current dental implants' macroscopic and microscopic features, such as threaded screws and sandblasting/etching structures, were developed with material and mechanical considerations to strengthen interlocking with the bone. Although these commercially available substrata were not invented with the purpose of optimizing cell biology, they serve as good model surfaces for laboratory investigations to understand *in vitro* cell responses to different surface properties, and provide a convenient research system to compare *in vitro* tissue culture results with clinical applications. The understanding of fundamental cell-substratum interaction will provide positive feedback on the biomaterial surface design with more biological considerations. Although *in vitro* culture systems for cell-surface interaction are widely adopted, they have intrinsic limitations as discussed below.

(1) The cells used for *in vitro* studies are derived from a variety of host species, anatomical locations and maturation statuses, making it difficult to compare results from research using different cells. Specifically, in orthopaedic biomaterial research, the commonly studied cells are osteoprogenitor cells, osteoclasts, stem cells and fibroblasts. These cells are not the first cells in contact with the surface *in vivo*. Instead, they are recruited to a surface that has been modified by inflammatory cells.

(2) The cells used for *in vitro* studies can be divided into two major types: transformed or primary isolated cells. The transformed cells grow fast and yield

121

relatively consistent phenotype after many passages. However, the mutated genotype calls attention to the comparison between transformed and normal cells. Cell attachment, migration, proliferation, differentiation and sensitivity to growth factors are changed in malignant cell lines. Fresh normal isolated cells are supposed to more closely represent the reality of *in vivo* response. However, they are composed of a heterogeneous cell population, and their properties are highly dependent on isolation techniques. The phenotype of isolated normal cells may change extensively under tissue culture conditions. In some cases the cells may even lose their differentiated phenotype. More variations are observed in studies using primary cells compared to transformed cell lines. Therefore, cell responses to certain biomaterial surface feature sshould be generalized in the consideration of various cell types. In this dissertation, we demonstrated osteogenic effects of microstructured Ti surface by using a human osteosarcoma cell line and primary rat calvarial osteoblasts. The results are consistent with other studies on normal human osteoblasts and bone marrow stem cells [1, 2], indicating the general property of surface structure on improving osteoblast differentiation. Further studies are undergoing to examine the effects of surface structure and surface chemical composition on male and female human normal osteoblasts.

(3) The cleaning, sterilization and storage of substrata could significantly change surface chemistry, further affecting cell responses. The substrata used in the lab may not present the same surface chemistry as clinical implants. A variety of methods are applied in different labs and make it difficult to compare the results. Surface chemistry is usually measured by XPS, EDX or other equipments, which stimulate the surface atoms and measure the energy of excited particles under the extremely high vacuum. Although we do not know the exact surface that perceived by the cells, it is necessary to understand the surface chemistry that is most close to the reality. One limitation of this

122

dissertation is that the characterization of surface chemistry was performed before sterilization. In these studies, the substrata were steam autoclaved (as in Chap. 2) or glow discharged (as in Chap. 3 & 5) before cell seeding. It is known that these surface treatments alter surface chemical composition and may further affect cell responses [3, 4]. Therefore, the sterilization processes may bring extra differences based on different surface structure and chemical composition.

To avoid this limitation, in future experiments we will store the acid etched (A) and sandblasted/acid etched (SLA) samples in concealed packages and clean the surface by gamma irradiation, as modA and modSLA. The gamma irradiated surfaces will be well characterized. Before cell culture, the disks will be used directly after being taken from the irradiated package to prevent extra change in surface chemistry. It should be noted that the storage time will also have influence on surface chemistry, because Ti atoms will keep reacting with oxygen in the atmosphere or the particles from the package material will deposit on the substratum. The ideal characterization of surface chemistry is to measure every disk before use; but it is temporarily not practicable in the lab.

(4) *In vitro* cells are usually cultured in the presence of 10% bovine serum. Serum is separated from the whole blood from which blood cells and fibrinogen are removed. When orthopaedic implants are inserted *in vivo*, the biomaterial surfaces are covered with whole blood immediately and the coagulation cascade is activated to form a fibrin-based clot. The recruited osteoprogenitor cells respond to this fibrin modified surface. The components of the serum have large variability among different manufacturers or batches. Therefore, it is necessary to control the lot of serum for predictable and repetitive results. Fibronectin and vitronectin are the main adhesion proteins in the serum that adsorb on biomaterial surfaces and mediate cell attachment. Surface properties do not affect the initial amount and type of the proteins that arrive at

123

the surface. These are controlled by the concentration and flux in accordance with physical-chemical principles. The conformation of the proteins is determined by the surface properties; and the relative change of conformation determines whether the protein is retained on the surface or being replaced by other proteins. The protein-surface interactions are stabilized by electrochemical forces between the molecules, including van der Waal's force, dehydration force and hydrogen bond, all of which are associated with surface properties. Albumin, immunoglobulin, vinculin and fibronectin are presented in the adsorbed conditioning film in serum-supplemented cell culture media, while fibrinogen is the main protein when in contact with blood. Despite the differences of protein adsorption, Baier and colleagues pointed out that the similar substratum surface properties lead to similar biomass responses to synthetic materials, with regard to retention and spreading versus retraction and delamination, in the media as diverse as blood, saliva and seawater.

Although there are many limitations in the cell culture system, it is still a powerful tool to simplify the complicated *in vivo* situation. By strictly controlling the culture system and changing one specific condition, we are able to study the cell response to that specific factor for understanding cell physiology. In this dissertation, we noticed that the cell shape is associated with protein expressions in response to surface structure and surface chemistry. Cells on microstructured and modified Ti surface exhibit round morphology with increased expression of differentiation markers, growth factor and cytokine. In the next section, I will discuss the previous research about this phenomenon and previously proposed theories.

Cell Shape and Surface Properties

Cell shape is found to be coupled with DNA synthesis, apoptosis, gene expression, differentiation and enzyme production. Folkman et al. found that bovine

124

endothelial cells were flat (51 μm diameter x 3 μm height) on tissue culture plastic and proliferation rate was high; while same cells on hydrophilic polymer coated surfaces were round (9 μm diameter x 20 μm height) with a low proliferation rate [5]. The results suggested that higher proliferation is associated with flat morphology. This phenomenon is also confirmed by other studies [6, 7]. Round cell shape may also correlate with terminal differentiation or apoptosis. Human epidermal keratinocytes cultured on a small adhesive areas were round and expressed more terminal differentiation markers. Opposite cell behaviors were observed on larger adhesive area for flat cells [6]. Human and bovine endothelial cells were found to exhibit more apoptosis on small adhesive islets and had round morphology [7]. Cell shape is also associated with enzymatic reactions. Axelson found significant reduction of reactive oxygen species from inflammatory bursts in well-spread monocyte-derived macrophages on plasma-treated substratum, and in contrast, with large reactive oxygen species formation in less-spread cells on standard-cleaned substrata [8].

In these studies, cell shapes were altered by changing surface chemical composition to control the adhesive surface area. The experiments were not designed to distinguish whether cell shape *causes* cell response or cell shape and other behaviors are *associated* phenomena in response to other factors together. To solve this problem, Ingber and colleagues developed a delicate experimental model for modifying cell shape without changing surface properties [9]. RGD coated magnetic micro-beads were added into the culture media after the cells were seeded on the substratum, so that the bead only bound to the surface receptor integrin that was located on the free surface of cell plasma membrane in contact with the media. By maneuvering the movement of the micro-bead through magnetic force, cell shape was changed accordingly. The system was applied to examine cell adhesion force and the effects of mechanical force; and it

125

also has the potential to explore the effects of cell shape on proliferation, differentiation or gene expression.

It should be noted that cell shape and growth or gene expression are not always coupled, especially for the transformed cells. The malignant cells could proliferate even in suspension without anchoring to the substratum. Moreover, cell shape alone cannot induce enough response in many cell types. For example, rabbit fibroblasts were induced to express matrix degrading enzymes, when treated with a cytoskeleton inhibitor to form a round shape. In contrast, chondrocytes, which already present round morphologies, still need growth factor stimulation to produce this protein. Other types of cells may not produce this enzyme either due to a change of cell shape or to growth factor treatment [10]. In this dissertation, we observed different responses of MG63 cell to SLA and modSLA substrata, but the cell morphology on these two surfaces are indistinguishable. Although cell shape may not be a predictor for proliferation, differentiation and other responses, the study of cell shape in certain models will provide important information on the mechanism by which cytoskeleton regulates cell behavior.

Surface structure and surface chemistry affect cell morphology. Rat osteoblasts respond to Grade 1 and Grade 4 commercially pure Ti with different cell shape, collagen expression and calcium secretion [11]. Epithelial cells, fibroblasts and osteoblasts flatten down and spread out extensively on smooth Ti compared to micro-structured surfaces [12, 13]. Fibroblasts cultured on micro-grooved Ti (V-shape groove with 6 μm width and 3 μm height) displayed elongated morphology and were 1.5 fold taller than cells on smooth Ti [14]. The flattened cell shape on a smooth surface is different from fibroblast morphology *in vivo* or on a collagen-based matrix; in contrast, the cell morphology on rough surfaces is closer to that seen *in vivo* [15]. When the osteoblast-like cells were cultured in serum free media, there was no difference between cell morphology on smooth or rough surfaces [16]. The cells packed and piled up as if to

126

increase cell-cell interactions and to share limited matrix proteins. This result indicates that the effects of surface roughness on cell morphology is mediated by protein adsorption.

Cell attachment and adhesion to adsorbed extracellular proteins are mediated through integrins, which cluster together to form focal adhesions. On smooth surfaces, cells are able to form large focal adhesions with the length up to 6 μm. In contrast, cells on microstructured surfaces cannot assemble continuous focal adhesions because of irregular surface structure features. From our scanning electron microscopic pictures, we noticed that the osteoblasts did not align with the sub-micrometer scale roughness completely. Therefore, the focal adhesions may be interrupted by a roughened surface. The different distributions and structures of focal adhesions may contribute to roughness dependent cell responses.

Several theories have been proposed previously to explain the intrinsic relationship of cell shape with cell function. Harris has developed an elastic silicon substratum model and established the important role of traction force in regulating cell behavior [17]. Baier has proposed the relationship between membrane strain and cell responses. During the initial 4 hours of cell seeding, the peripheral area of osteoblasts symmetrically spreads out. When cells were cultured from 8 hours until reaching confluence, the cell morphologies were asymmetric. Therefore, the change of cell symmetry may cause plasma membrane deformation and induce membrane stain, which exert effects on cellular metabolic activity or active synthesis.

These membrane strain effects may also explain shear force induced osteoblast differentiation [18]. Ingber proposed a "cellular tensegrity theory" to explain the mechanism of cellular responses to mechanical environments. Tensegrity is an architectural term to describe the structures that are stabilized by continuous, integrated tension forces. In this model, the tensile forces that are exerted by extracellular matrix

127

and microtubules are balanced by contractile microfilaments (such as actin and myosin) and intermediate filaments. Change of cell shape transduces mechanical force to cytoskeleton structural deformation to minimize energy status and induces the alteration in nuclear matrix. For example, the spatial rearrangement between DNA sequence and protein-RNA scaffold may switch cell growth and gene expression [19]. Ben-Ze'ev concluded that soluble peptide ligands stimulate cell shape change by reorganizing cytoskeleton. The cell shape and contact are regulated by plasma membrane associated cytoskeleton rearrangement. The intracellular cytoskeleton filaments control the localization of regulatory molecules that transduce signal pathways. An example is that actin-binding protein may associate with phosphoinositide and then activate a second messenger system [20].

These theories emphasize the important role of contractile force exerted by actin in maintaining cell shape and regulating cell function. However, passive spreading and contraction alone cannot explain the phenomenon of haptotaxis. Haptotaxis is the cell's ability to move toward the direction of higher adhesive area [21]. When fibroblasts were cultured on a gradient of adhesive substrata, the cells crawled toward the surface with highest adhesive coating. If the cells keep a contractile posture, the cells will not migrate out. Therefore, it is reasonable to assume that the cells also actively form cellular extensions to explore their environment. The active formation of cellular extensions is supported by the facts that filopodia are formed not only at the bottom of the cells, but also at the top the cells. The extended lamellipodia or filopodia may be randomly protruded from the cell body and attach to the substratum. The contractile force inside the cells retract the extensions that attach on the surface with lower adhesive area, but leave the attachment with higher adhesion. The dynamic balance between retraction force and active formation of cell extensions allow the cells to adapt to the surface property and migrate along adhesion gradient. The filopodia and lamellipodia are filled

128

with organized actin filaments. The actin arrangements are dependent on many other enzymes and signaling molecules, indicating the process is an active formation that consumes energy.

Future Directions

In this dissertation, we found that Ti surface structure and surface chemical composition regulate osteoblast cell shape and differentiation phenotype. On microstructured and more hydrophilic Ti surface, osteoblasts exhibit round cell shape, spread out slower, secrete more differentiation markers and produce an osteogenic microenvironment through a paracrine or autocrine pathway. More studies should be performed to further understand the mechanism of this phenomenon. Here summarized are the main future directions.

(1) As mentioned above, the surface needs to be well characterized for studying cell responses. To compare cell responses to one specific surface feature, the other surface properties should be controlled to be exactly the same. The surface structure, chemical composition, surface charge and hydrophilicity should be measured on the substrata on which the cells are cultured, without further interference of cleaning or sterilization process. Therefore, the A and SLA surfaces in the future experiments will be sterilized by the same gamma irradiation sterilization as for modified surfaces. The surface properties will be characterized after gamma irradiation to present the real surface that is perceived by the cells.

(2) Serum-supplement culture media contain various proteins that are adsorbed on the substratum and mediate cell attachment and growth. The exact type and amount of the proteins in the serum are unknown. To overcome this limitation, future experiments should be performed in serum-free media. One or several specific types of proteins will be added into the media. Both initial and dynamic change of protein

www.manaraa.com

adsorption will be determined to understand the effects of surface properties on protein adsorption. Then cell growth and differentiation in response to these specific proteins will be studied to reveal the related interactions among cells, proteins and surface properties.

(3) Integrins are the main cell membrane receptors that mediate cell attachment to extracellular matrix. To understand cell-substratum interaction, it is necessary to investigate the role of integrins in mediating cell responses. Previous studies in our lab have showed that on microstructured Ti surfaces, MG63 cells express more integrin α2 and β1, while the expression of α5 does not change [22]. Inhibition of integrin β1 expression by small interference RNA also blocks cell responses to surface structure [23]. The results suggest that integrin plays an important role in transferring the surface structure signal to cell response. To confirm the efficiency of inhibition of integrin β1 expression at the protein level, more studies are being performed to examine the protein expression of β1, β3, α2 and α5 in β1 silenced cells. Cell adhesion assays are also being performed to determine the effects of integrin β1 in regulating MG63 attachment on tissue culture plastic.

An interesting question is to evaluate the adhesion force of MG63 cells on microstructured and hydrophilic surfaces, and to correlate adhesion force with cell shape and behavior. A hypothesis to explain round morphology and differentiated phenotype of MG63 cells on microstructured and hydrophilic surface is that modified surface structure and chemical composition disrupt the continuous cell attachment as on the smooth surfaces. With limited attachment, the cells are forced to form round morphology and rearrange cytoskeletons to modify gene expression. To test the hypothesis, cell attachment could be evaluated by measuring adhesion strength and focal adhesion formation. Adhesion strength can be measured by centrifuge assay if the substrata can be glued on the tissue culture plate. Focal adhesion size and distribution

will be observed by immunofluorescence labeling of major focal adhesion proteins; and the activity of focal adhesion enzymes like focal adhesion kinase can be measured to understand the intrinsic signaling pathway. Because of the roughness, most parts of the cells on microstructured surface are usually out of the focus plane, resulting in shorter and irregular focal adhesions. To obtain a complete picture of cell shape, confocal microscope can be applied to reconstruct the three dimensional cell morphology with labeled adhesion sites.

(4) The cytoskeleton is the key linker that relates cell morphology with function. Most previous studies have investigated the effects of the cytoskeleton in fibroblasts, epithelial cells or smooth muscle cells because the cytoskeleton is important for the function of these cells, such as migration or exerting mechanical force. The cytoskeleton is also critical to osteoblasts, because osteoblasts need migrate to the location of resorption pit to form new bone and osteocytes are sensitive to environmental mechanical stimulations. Few studies have been performed the effects of the cytoskeleton in osteoblasts. To examine the hypothesis that the cytoskeleton is associated with cell function on microstructured and hydrophilic Ti, we propose to evaluate cell behavior on these surfaces in the presence of cytoskeleton disruption or polymerization. For example, if the cell morphology on modSLA is dependent on reorganized actin filaments in response to surface structure and chemical composition, then the disruption of actin polymerization is expected to block surface effects.

(5) To observe the dynamic balance of active filopodia formation and passive contraction, it is necessary to observe real time cell contact and spread at the initial time period after seeding. For rough and opaque substrata, it is not possible to directly observe the change of cell shape via light microscopy. An alternative way is to develop a transparent polymeric surface that present the same structure, so that the change of cell morphology will be monitored in culture. Polymeric replicas of SLA surface have

131

been investigated before [24]. It is still difficult to control surface structure as well as metallic Ti, because the polymeric surface structures flatten in contact with the culture media. The polymer surface presents a relatively round bump structure instead of the sharp peak as on SLA. More research needs to be performed to chose the best materials that replicate SLA surface structures.

(6) It is known that osteoblasts are not the first cells that appear on the implant surface. When implants are inserted, hematoma forms around the implant surface and inflammatory cells are attracted to the insertion place; then stem cells and osteoprogenitor cells are recruited to the implantation site and differentiate into osteoblast. Therefore, further studies of the effects of surface properties on stem cell differentiation will help better correlate *in vitro* cell culture results with *in vivo* bone responses.

References

1. Lohmann CH, Tandy EM, Sylvia VL, Hell-Vocke AK, Cochran DL, Dean DD, Boyan BD, Schwartz Z. Response of normal female human osteoblasts (NHOst) to 17 beta-estradiol is modulated by implant surface morphology. J.Biomed.Mater.Res. 2002; 62: 204-213.
2. Kawahara H, Soeda Y, Niwa K, Takahashi M, Kawahara D, Araki N. In vitro study on bone formation and surface topography from the standpoint of biomechanics. J Mater Sci Mater Med 2004; 15: 1297-1307.
3. Vezeau PJ, Koorbusch GF, Draughn RA, Keller JC. Effects of multiple sterilization on surface characteristics and in vitro biologic responses to titanium. J Oral Maxillofac.Surg. 1996; 54: 738-746.
4. Sendax VI, Baier RE. Improved integration potential for calcium-phosphate-coated implants after glow-discharge and water-storage. Dent Clin North Am 1992; 36: 221-224; discussion 225.
5. Folkman J, Moscona A. Role of cell shape in growth control. Nature 1978; 273: 345-349.
6. Watt FM, Jordan PW, O'Neill CH. Cell shape controls terminal differentiation of human epidermal keratinocytes. Proc Natl Acad Sci U S A 1988; 85: 5576-5580.
7. Chen CS, Mrksich M, Huang S, Whitesides GM, Ingber DE. Geometric control of cell life and death. Science 1997; 276: 1425-1428.

8. Axelson EA. Differential influences of small particles and surface-modified polystyrene substrata on the shapes and reactivities of human monocytes. New York: State University of New York at Buffalo; 2000. M.S. Thesis.

9. Alenghat FJ, Fabry B, Tsai KY, Goldmann WH, Ingber DE. Analysis of cell mechanics in single vinculin-deficient cells using a magnetic tweezer. Biochem Biophys Res Commun 2000; 277: 93-99.

10. Werb Z, Hembry RM, Murphy G, Aggeler J. Commitment to expression of the metalloendopeptidases, collagenase and stromelysin: relationship of inducing events to changes in cytoskeletal architecture. J Cell Biol 1986; 102: 697-702.

11. Ahmad M, Gawronski D, Blum J, Goldberg J, Gronowicz G. Differential response of human osteoblast-like cells to commercially pure (cp) titanium grades 1 and 4. J Biomed Mater Res 1999; 46: 121-131.

12. Chou L, Firth JD, Uitto VJ, Brunette DM. Effects of titanium substratum and grooved surface topography on metalloproteinase-2 expression in human fibroblasts. J Biomed Mater Res 1998; 39: 437-445.

13. Martin JY, Schwartz Z, Hummert TW, Schraub DM, Simpson J, Lankford J, Dean DD, Cochran DL, Boyan BD. Effect of Titanium Surface-Roughness on Proliferation, Differentiation, and Protein-Synthesis of Human Osteoblast-Like Cells (Mg63). J.Biomed.Mater.Res. 1995; 29: 389-401.

14. Chou L, Firth JD, Uitto VJ, Brunette DM. Substratum surface topography alters cell shape and regulates fibronectin mRNA level, mRNA stability, secretion and assembly in human fibroblasts. J Cell Sci 1995; 108 (Pt 4): 1563-1573.

15. Brunette DM. Principles of cell behavior on titanium surface and their application to implanted devices. In: Brunette DM, Tengvall P, Textor M, Thomsen P (eds.), Titanium in Medicine. Berlin: Springer; 2001: 485-512.

16. Degasne I, Basle MF, Demais V, Hure G, Lesourd M, Grolleau B, Mercier L, Chappard D. Effects of roughness, fibronectin and vitronectin on attachment, spreading, and proliferation of human osteoblast-like cells (Saos-2) on titanium surfaces. Calcif Tissue Int 1999; 64: 499-507.

17. Harris AK, Wild P, Stopak D. Silicone rubber substrata: a new wrinkle in the study of cell locomotion. Science 1980; 208: 177-179.

18. Bannister SR, Lohmann CH, Liu Y, Sylvia VL, Cochran DL, Dean DD, Boyan BD, Schwartz Z. Shear force modulates osteoblast response to surface roughness. J Biomed Mater Res 2002; 60: 167-174.

19. Ingber DE. The origin of cellular life. Bioessays 2000; 22: 1160-1170.

20. Ben-Ze'ev A. Animal cell shape changes and gene expression. Bioessays 1991; 13: 207-212.

21. Carter SB. Haptotaxis and the mechanism of cell motility. Nature 1967; 213: 256-260.

22. Raz P, Lohmann CH, Turner J, Wang L, Poythress N, Blanchard C, Boyan BD, Schwartz Z. 1alpha,25(OH)2D3 regulation of integrin expression is substrate dependent. J Biomed Mater Res A 2004; 71A: 217-225.

23. Wang L, Zhao G, Olivares-Navarrete R, Bell BF, Wieland M, Cochran DL, Schwartz Z, Boyan BD. Integrin beta1 silencing in osteoblasts alters substrate-dependent responses to 1,25-dihydroxy vitamin D3. Biomaterials 2006; 27: 3716-3725.
24. Wieland M, Chehroudi B, Textor M, Brunette DM. Use of Ti-coated replicas to investigate the effects on fibroblast shape of surfaces with varying roughness and constant chemical composition. J.Biomed.Mater Res. 2002; 60: 434-444.